Copyright

by

Jon H. Kilgore, P. E.

1997

TRANSFER AND DEVELOPMENT LENGTH OF DEBONDED 0.6 INCH (15MM) DIAMETER PRESTRESSING STRAND IN AASHTO TYPE I CONCRETE BEAMS

BY

JON HANSEN KILGORE, BSCE

THESIS

Presented to the Faculty of the Graduate School
of The University of Texas at Austin
in Partial Fulfillment
of the Requirements
for the Degree of

MASTER OF SCIENCE IN ENGINEERING

THE UNIVERSITY OF TEXAS AT AUSTIN

DECEMBER 1997

DEDICATION

To
Dawn, Ariel and Mariah

ACKNOWLEDGMENTS

I would like to express my gratitude to the Texas Department of Transportation for providing this program, without which this thesis would not have been possible. Their willingness to promote and support research in the field of transportation, which covers a broad spectrum of disciplines, is a great service to the people of Texas in which we serve.

I am grateful to my family to which I dedicate this work, I appreciate the support and patience throughout this study which took many long hours away from home.

My thanks to Dr. Burns for his patience, encouragement and always being able to put things in a positive perspective. I appreciate the review and comments provided by Dr. Kreger.

There were many hours involved in setting up each test at Ferguson Structural Engineering Laboratory and I appreciated the effort of everyone involved and enjoyed spending the time with Usnik Tuladar, John Grove, Heather Jobson, Kevin Skyrmes, and Sherman White. Thanks to Robbie Barnes for the scheduling and organization involved in preparation for testing.

ABSTRACT

TRANSFER AND DEVELOPMENT LENGTH OF DEBONDED 0.6 INCH (15MM) DIAMETER PRESTRESSING STRAND IN AASHTO TYPE I CONCRETE BEAMS

by

Jon Hansen Kilgore, M.S.E.

The University of Texas at Austin, 1997

Supervisor: Ned H. Burns

The objective of this project is to determine the anchorage length required for 0.6 inch (15 mm) prestressing strand as used in prestressed AASHTO Type I concrete beams. The focus of the report is the effect debonding has on the transfer and development lengths of this large diameter seven wire strand with a bright surface condition placed in concrete beams having varying concrete strengths. The strands are placed on a 2 inch grid as is common in the precast/prestress industry which is an effective method of placing the large prestressing force that can be achieved with this larger diameter strand at a greater eccentricity.

Tests such as pull out and end slip at transfer (pull in) are performed and evaluated as methods to determine the quality of bonding characteristics of 0.6 inch prestressing strand. Results of this study are compared with equations used in design by the American Concrete Institute and the American Association of State Highway and Transportation Officials and those developed by other researchers.

TABLE OF CONTENTS

LIST OF TABLES

LIST OF FIGURES

CHAPTER 1
INTRODUCTION

1.1 Background

Prestressed pretensioned concrete beams are the most common and economical type of superstructure designed for Texas highway bridge structures today. With the development of high strength concrete, longer span lengths can be reached which require a larger prestressing force. Use of 0.6 inch diameter seven wire prestressing strand at a 2 inch grid spacing is a very efficient way of providing this force at a greater eccentricity. This strand has a 40% greater area than the ½ inch diameter strand commonly used, which is also useful in reducing the number of strands required in normal strength concrete, yielding an economic benefit. Previous research has indicated that the required development length permitted by current governing codes, the American Concrete Institute (ACI)[1] and the American Association of State Highway and Transportation Officials (AASHTO)[2], might not be adequate for 0.6 inch diameter strands. It is a reasonable question to raise considering the large increase in capacity with only a 20% greater perimeter than the ½" diameter strand to provide anchorage in a pretensioned beam.

In the design of a simple span concrete highway beam, due to prestressing forces and eccentricities required at mid span of a structure, it is necessary to reduce the prestress force at the ends of a member to prevent exceeding the allowable tension in the top concrete fiber and compression in the bottom concrete fiber. This is accomplished by draping or debonding of the strands. Debonding strands is common and has the advantage of not requiring a

tremendous hold-down force, which could be a safety hazard to plant employees if mechanical devices used to apply the force failed. There is a limited amount of research available investigating the bonding capacity of debonded strands to ensure that they will provide adequate anchorage in highway girders. Based on available research, the ACI and AASHTO codes require that the current expression for development length be doubled if concrete tension is allowed in the service load design of a beam[3,18].

To better understand the bonding behavior of 0.6 inch diameter seven wire prestressing strands, this along with other research has been initiated by the Federal Highway Administration (FHWA) and the Texas Department of Transportation (TxDOT).

1.2 Overview of Testing

This thesis covers one series of tests in a project investigating the development length of 0.6 inch diameter prestressing strand at a two inch grid spacing in a Type I AASHTO beam. All test beams in this study were fabricated at a prestressing plant with sudden release of the strand by torch cutting. The effects of various levels of debonding as opposed to fully bonded strand, concrete strength, surface condition of the strand, and additional mild reinforcement at the beam ends to arrest shear cracks are being considered.

The focus of the following investigation is on beams with fifty percent of the strands debonded in a staggered pattern. The surface condition of the prestressing steel is bright or smooth to represent strand placed in the beam soon after being received from the steel mill, which can produce longer transfer and

development lengths. Variables influencing transfer and development lengths that are being tested consist of additional mild reinforcing in the web at the end of a member, to arrest shear cracks, and the effect of concrete strength.

1.3 Objectives

Early research indicated that debonding has a negative effect on the development length of prestressing strand [3] which brought about the requirement that calculated development length be doubled when it is used. Since then a few other studies have been conducted but a broad data base does not exist to establish new guidelines. One objective of this project is to provide additional data and better define the behavior of 0.6 inch prestressing strand when used in a debonded application.

Concrete strength has an effect on transfer and development length, but it is not well defined and does not correlate well between studies. This investigation includes three groups of concrete strength including high performance concrete (HPC) on which few tests in this area have been performed. The general trend is that with increased concrete strength, the transfer and development lengths are reduced. This effect is examined.

In an attempt to mitigate possible bond failure of prestressing strand, additional mild reinforcement is placed in the web, as previously mentioned, to arrest shear cracks. In one end of a pair of test beams (one in four tests within a concrete strength group) a horizontal "h" bar is placed in the web (see Chapter 4 for detail). Tests with an identical embedment length but without an "h" bar are compared to determine the effect the addition of this reinforcement has.

1.4 Scope

The scope of this project includes the fabrication of six AASHTO Type I concrete beams at a prestressing plant. The length of test beams was 54 feet. All beams had 8 bottom strands with two of those being debonded for 36 inches and two for 72 inches from the end of the beam, providing 50 percent debonding of the strands in a staggered pattern. The transfer length was measured from concrete strains at the centroid of prestressing strands before and after release of the prestressing force at the precasting yard. Strand pull in, the end slip at transfer, was also measured and later used to estimate transfer length.

At Ferguson Structural Engineering Laboratory (FSEL) a 60 inch wide by 6.5 inch thick slab was placed on the beam to act compositely during load testing. Tests were setup with varying embedment lengths. These tests were used to determine if the beam could develop its full capacity before significant slip of the strands occurred. For a given concrete strength, four such tests were performed, providing twelve tests on the six beams fabricated.

An analysis was performed on each test loading to compare the predicted to actual behavior. This analysis was performed based on strain compatibility using mathematical models of the stress strain relationships of concrete and the prestressing strand. Moment curvature theory was used to predict load deflection response.

CHAPTER 2

ANCHORAGE IN PRETENSIONED BEAMS

2.1 Definitions

Transfer Length (L_t)

Strand placed in a prestressed beam must be anchored to lock in an effective portion of the jacking force. In a post-tensioned beam this is provided by a mechanical anchor which effectively applies a point load at the end of the beam. In pretensioned beams no such anchor exists; anchorage is provided by bond between the concrete and surface of the prestressing strand. Transfer of prestress is no longer similar to a point load applied at the end of the beam, but is distributed through bond to the concrete over some length. This length is referred to as the transfer length.

Development Length (L_d)

The transfer length provides anchorage of the effective prestressing force, but an additional length referred to as the flexural bond length (L_{fb}) is required to develop the force in the strand at ultimate load. This length is measured from the end of the transfer zone to a critical section being considered. The development length is the combination of the transfer and flexural bond lengths. An analogy to the pullout of a deformed reinforcement bar can be made. The length of bar embedded in the concrete necessary to develop its ultimate strength (f_u) is the development length. Figure 2.1 graphically shows the zones of transfer and development at the end of a beam[4].

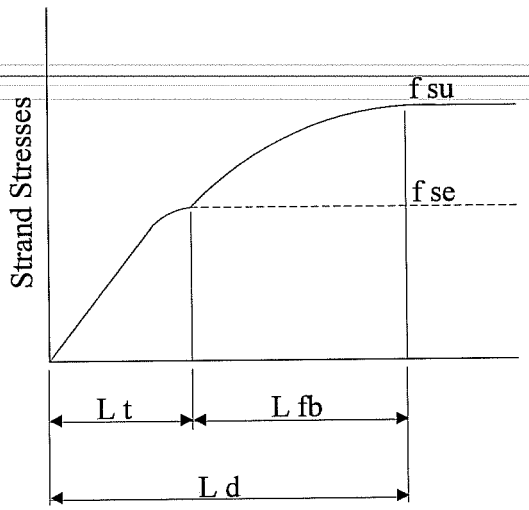

Figure 2.1 Zone of Anchorage In a Pretensioned Beam.

2.2 Mechanics of Bond in the Transfer and Development Zones

Bond stresses in the transfer zone are generally considered to be uniform. There are primarily two mechanisms that contribute to bond, Hoyer's effect and mechanical interlocking. The first, Hoyer's effect, is also referred to as wedge action. When jacking forces are applied to the prestressing strand a reduction in strand diameter occurs caused by Poisson's ratio. After the strand is released when concrete has reached the required initial strength (f'_{ci}), its diameter attempts to expand to its original dimension, but is restrained by surrounding concrete at the end of the beam. Since the effective prestress force is transferred to the concrete through bond, the stress increases in the strand as the distance from the end of the beam increases. At the end of the transfer zone bond stresses are zero, and the strand retains an effective prestress.

The second mechanism is due to mechanical interlocking caused by the helical twist of the outside wires in seven wire prestressing strand. The concrete cast around the strand is molded around the twisted wires that act in a similar manner to deformations on a reinforcing bar. As the strand tries to pull through the concrete, it tries to untwist through the mold created in the concrete which creates resistance to slip. Figure 2.2 demonstrates the contribution of each of these mechanisms to transfer of effective prestress force in the end region of a beam. As shown in the figure, the actual relationship of bond stress along the transfer length is roughly bilinear, being uniform over 95% of it's length[5]. This is usually taken to be uniform over the entire transfer length.

Adhesion of concrete to prestressing strand, which is rigid brittle behavior, also occurs in a prestressed beam. In the transfer and development regions of a prestressed beam, strains in the concrete relative to the strand are in the plastic range as demonstrated mathematically by Janney[6]. Therefore adhesion which acts in the elastic range, does not participate in transferring prestressing forces.

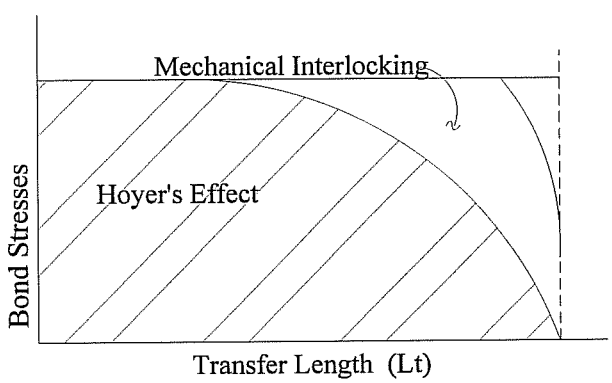

Figure 2.2 Transfer Bond Mechanisms (Reference 13)

The ACI and AASHTO codes use the following equation for design purposes in determining the transfer length:

$$L_t = \frac{f_{se}}{3} d_b$$

This is based on equilibrium between a uniform bond stress (U_t) of 400 psi applied to the circumference of the prestressing strand and the effective prestress applied to the area of the strand, taken as 72.5% of the nominal area. This is as it was recommended to ACI by Mattock[7] based on studies by Hanson and Kaar[8] and Kaar et al[9]. It was adopted into the AASHTO code in 1973. Transfer lengths calculated from this equation give an average value of measured transfer lengths. Actual measured transfer lengths have a large amount of variation and may be very much larger or smaller. Based on an effective prestress of 150 ksi, the equation reduces to $50d_b$. This assumption of effective prestress is dated, and current values are over 160 ksi.

The European code[10] states that actual lengths vary between 45 and 90 times the bar diameter. The Federal Highway Administration conducted a study of existing data and found a wide range of measured transfer lengths[11]. This is due to the large number of factors that effect the transfer length, including the following:

- Bar Diameter
- Initial Prestress (f_{si})
- Surface Condition

- Concrete Strength (f'_{ci})
- Release method (sudden vs. gradual)
- Consolidation of Concrete
- Cover and Spacing

This study will focus on clean or bright strands with 50% of the strands debonded in a staggered pattern. Three groups of concrete strength and the effect of additional reinforcement to control web cracking will be investigated.

Currently there are no acceptance criteria to assure the quality of bond. An attempt to do so has been suggested by the use of Pull Out Tests in a recent study[12]. In this test, strands are placed in a concrete block at a given embedment length and a tensile force is applied to determine the resistance that the strand can develop. This study was performed on 1/2 inch diameter prestressing strand but could easily be adopted to 0.6 inch diameter strand. The method appears to be an effective means to achieve a more consistent quality of bond between different prestressing strand manufacturers.

Development length, as mentioned before, consists of the transfer length combined with the flexural bond length. In the region of flexural bond the only mechanism that contributes to bond is mechanical interlocking[8]. At a crack location the bond stresses adjacent to the crack increase and form a bond wave. According to Hanson and Kaar[8] if that wave reaches the transfer zone, the strand diameter will decrease due to an increase in stress, causing a reduction in bond resistance and therefore slip will occur. This is discussed in depth in a comprehensive study by Russell and Burns[13] that emphasizes the importance of

the cracking moment on the development length. The ACI and AASHTO equation for development length is as follows:

$$L_d = \left(f_{su} - \frac{2}{3} f_{se} \right) d_b$$

This Equation can be rewritten with the terms for transfer and flexural bond length separated:

$$L_d = \frac{f_{se}}{3} d_b + \left(f_{su} - f_{se} \right) d_b$$

The flexural bond length was derived much as the transfer length, based on a uniform flexural bond stress (U_b) times the circumference set equal to the ultimate prestress less the effective prestress force (f_{su}-f_{se}). Figure 2.3 demonstrates the effect cracking has on stress in a prestressing strand within the development zone.

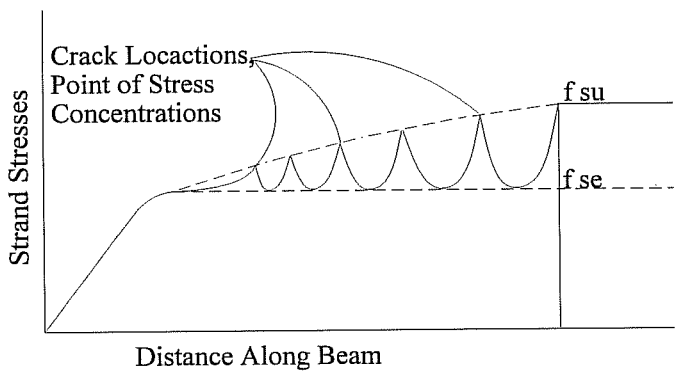

Figure 2.3 Strand Stress in Cracked Pretensioned Beams. (Reference 13)

Studies performed since the mid 1980's have produced varied results[14, 15, 16]. These reports are in part the reason that the Federal Highway Administration placed a moratorium in 1988 on the use of 0.6 inch diameter strand and increased

the development length provided by ACI and AASHTO by 1.6 times. This was partially lifted in 1996, allowing the use of 0.6 inch prestressing strand. There are a variety of reasons that results from past studies vary so widely, but the processes involved in manufacturing of prestressing strand differ from producer to producer. This leaves a strand surface condition from these different producers with bonding characteristics that vary as widely. The pull out tests previously mentioned could be a method to assure the quality of bond in strand from different manufacturers. Results from this and other studies[13] show that the current equation gives reasonable transfer and development lengths that are safe to use in design.

Table 2.1 presents transfer and development length equations from several sources. These are discussed in detail in Reference 30. Some of these expressions include effects such as concrete strength and other variables mentioned which are evaluated in Chapter 6 and are compared with the results of this study.

TABLE 2.1 Transfer and Development Length Equations

Author	Year	Transfer Length (L_t)	Development Length (L_d)
ACI 318[1] AASHTO[2] (1)	1963	$= \frac{f_{se}}{3} d_b$ $\approx 50 d_b$	$= L_t + (f_{su} - f_{se}) d_b$
Martin & Scott[24] (2)	1976	$= 80 d_b$	$f_{su} \le \frac{L_e}{80 d_b}\left(\frac{135}{d_b^{1/6}} + 31\right) \quad L_e \le 80 d_b$ $f_{su} \le \frac{135}{d_b^{1/6}} + \frac{0.39 L_e}{d_b} \quad L_e \ge 80 d_b$
Zia & Mostafa[25]	1977	$= 1.5 \frac{f_{si}}{f_{ci}} d_b - 4.6$	$= L_t + 1.25(f_{su} - f_{se}) d_b$
Cousins, Johnston, & Zia[5] (5)	1990	$= \frac{\left(U'_t \sqrt{f'_{ci}}\right)}{2B} + \frac{f_{se} A_{ps}}{\pi d_b U'_t \sqrt{f'_{ci}}}$	$= L_t + (f_{su} - f_{se}) \left(\frac{A_{ps} / (\pi d_b)}{U'_d \sqrt{f'_c}}\right)$
Russell & Burns[13] (4)	1993	$= \frac{f_{se}}{2} d_b$ $\approx 80 d_b$	*Fully Bonded*: $M_{cr} > L_t V_u$ *Debonded*: $\frac{L_b + L_t}{Span} \le \frac{1}{2}\left(1 - \sqrt{1 - \frac{M_{cr}}{M_u}}\right)$
Mitchell, Cook, Khan, & Tham[23]	1993	$= \frac{f_{si}}{3} d_b \sqrt{\frac{3}{f'_{ci}}}$	$= L_t + (f_{su} - f_{se}) d_b \sqrt{\frac{4.5}{f'_c}}$
Burdette, Deatherage, & Chew	1994	$= \frac{f_{si}}{3} d_b$	$= L_t + 1.50(f_{su} - f_{se}) d_b$
Buckner[11] (FHWA)	1994	$= \frac{1250 f_{si}}{E_c} d_b$ $\approx \frac{f_{si}}{3} d_b$	$= L_t + \lambda(f_{su} - f_{se}) d_b$ $\lambda = (0.6 + 40\varepsilon_{su}) or \left(0.72 + 0.102 \frac{\beta_1}{\omega_p}\right)$ $(1.0 \le \lambda \le 2.0)$

Notes for Table 2.1

Notation changed in some cases to provided consistency between equations.

Units of length and area are in inches.

Units of stress are in ksi except Cousins et. al.

(1) Second equation for L_t is from shear provisions of ACI 318 Section 11.4.

(2) Martin & Scott's L_d equation limits f_{ps} as a function of L_e.

(3) $B_{avg} = 300$ psi/in, $U'_t = 6.7$, and $U'_d = 1.32$ for strand without epoxy.

(4) Russell & Burns L_d criteria are based on preventing cracking in transfer zone.
L_b = length of debonding.

(5) Cousins et. al. units of stress are in psi

CHAPTER 3
DEBONDED STRANDS,
REVIEW OF RELATED RESEARCH

3.1 Introduction

Strands are commonly debonded in the production of prestressed highway girders. It is an effective and safe method to reduce the prestress force at the end regions of the beam where working stresses in the concrete can be exceeded. Draping strands is another option that requires a large hold down force. This force is applied by a mechanical hold down device which could cause serious injury to employees if it were to fail. The additional work and materials required to drape a strand give debonding an economic advantage as well.

Under the current ACI and AASHTO codes, if concrete tension is allowed in the design of pretensioned girders with debonded strands, then it is required to double the calculated development length. If no concrete tension is allowed under service loads, then this is no longer necessary. The amount of existing data on debonded strands is limited, and none pertaining to 0.6" diameter strand is available. The following is a discussion of the research on which the code has based these requirements.

3.2 Kaar and Magura (1965)[3]

This study included five AASHTO Type III half scale girders. The design and test results are summarized in Table 3.1. The first three girders were identical with varying lengths of debonded strand as noted in Table 3.1. They were fatigue loaded for five million cycles and performed well with no slip. Allowable tension in the concrete was at $3\sqrt{f'_c}$. Figure 3.1 is the setup for the static test performed on the five beams. The intent was to ensure that the moment diagram would "... be similar to that of a reasonable moment envelope for highway bridge girders."

TABLE 3.1
SUMMARY OF RESULTS
KAAR AND MAGURA (1965)

Beam	Debond %	Debond Length (in)	Le in	M test M calc.	Slip in	Failure Mode
1	0	-	2.5 Ld	0.98	none	Flexure
2	33	76	2.0 Ld	0.96	very small	Flexure
3	50	131	1.0 Ld	0.84	total failure	Bond
4	0	-	2.5 Ld	0.89	none	Horiz. Shear
5	33	76	2.0 Ld	1.01	none	Flexure

Strand		Test Beam	
Type:	250 ksi Stress Relieved	Type:	AASHTO Type III (half scale)
Diameter:	3/8 in	Span:	33 ft
Number:	12	Ld:	50 in
fsu:	277 ksi	(fsu-fse):	137 ksi
fse:	140 ksi	f'c:	7.0 to 9.3 ksi
		Slab:	39 in x 3 in

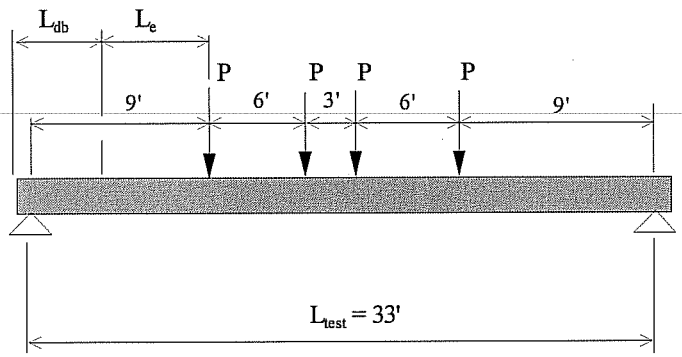

Figure 3.1 Test Setup Kaar and Magura (1965)

Test girder 1, which was fully bonded with an embedment length (L_e) of $2.5L_d$, had no slip under static loading to failure. Girder 2, which they considered partially blanketed since $L_e = 2.0L_d$, showed some very small slips while still essentially reaching calculated ultimate strength as shown in Table 3.1. Girder 3, considered fully blanketed, $L_e = L_d$, had a complete failure of the strands with the longest blanketed length. Based on previous studies[8], if a crack occurs in or near the transfer zone, a bond wave forms and slip will occur. Figures 3.2 and 3.3 are the moment diagrams for these two girders showing the ultimate and cracking moments along with the applied moment at failure. Failure was flexural for girder 2 and bond for girder 3. It is clear that the test moments just reached the cracking moment at the transfer zone of the longest set of debonded strands in test girder 2. In test girder 3 cracking was extensive in the region of debonding when the beam failed so failure was not unexpected.

Girders 4 and 5 were fully bonded and partially blanketed, respectfully, with the amount of shear reinforcement reduced from the first three beams.

Otherwise, they were identical to girders 1 and 2. Girder 4 failed in horizontal shear after reaching 89% of its calculated capacity. Girder 5 failed in flexure with no strand slip.

In this series of tests, beams performed well with a embedment length twice that required by the ACI and AASHTO codes, and failed completely with an embedment length of 1.0 L_d. As a result of this research, ACI and AASHTO allowed the use of debonded strands but required that L_d be doubled.

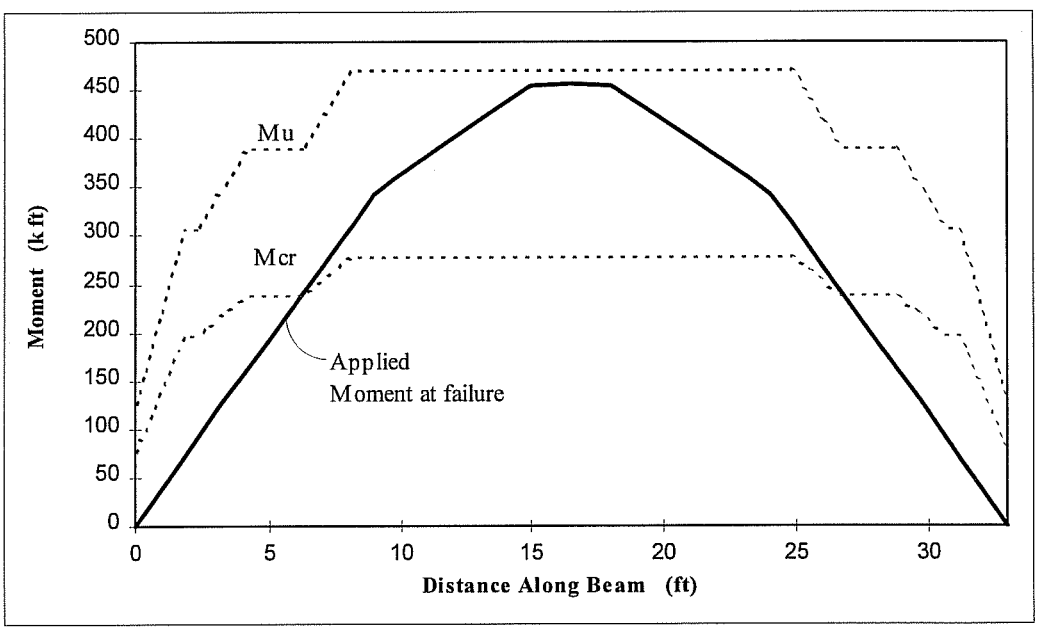

Figure 3.2 Test Girder 2, $L_e = 2.0\ L_d$
Kaar and Magura (1965)

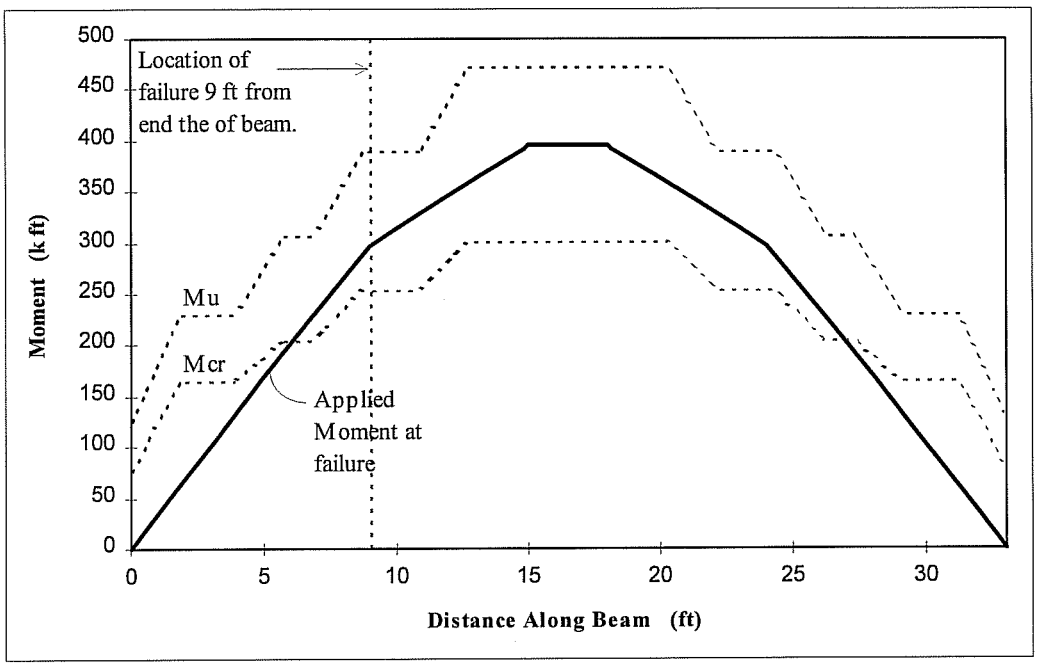

Figure 3.3 Test Girder 3, L_e =1.0 L_d

Kaar and Magura (1965)

3.3 Dane and Bruce (1975)[17]

The test beams in this study were separated into two sets which are summarized in Tables 3.2 and 3.2a. The first set is similar to the beams fabricated by Kaar and Magura, except with a decrease in the percentage of debonding to 17%. Debonding was concurrent as opposed to staggered, meaning that all debonding of strands ended at the same location. The second set were half scale AASHTO type II beams which had 22 strands with 18% of the strands debonded. A test span of 33 and 48 feet was used for the Type III and Type II beams, respectively. A two point loading was used, which was placed at third points as shown in Figure 3.4. Test beams G1 and G2 and G7, which had draped

strands, were pilot beams with which to compare the behavior of the debonded beams in each series.

TABLE 3.2

SUMMARY OF RESULTS

DANE AND BRUCE (1975)

Beam	Debond %	Debond Length (in)	Le in	M test / M calc.	Slip in	M (Test) / M (Pilot)
G1	Pilot	Draped	2.2 Ld	1.13	0.00	-
G2	Pilot	Draped	2.2 Ld	1.10	0.00	-
G3	17	116.5	0.34 Ld	1.04	1.44	0.97
G4	17	116.5	0.34 Ld	1.10	1.70	1.01
G5	17	116.5	0.34 Ld	1.06	0.88	0.98
G6	17	116.5	0.34 Ld	1.07	1.05	0.97

Strand			Test Beam		
Type:	250 ksi Stress	Relieved	Type:	AASHTO (half scale)	Type III
Diameter:	3/8 in		Span:	33 ft	
Number:	12		Ld:	64 in.	
fsu:	268 ksi		(fsu-fse):	108 ksi	
fse:	160 ksi		f'c:	6.1 to 6.8	ksi
			Slab:	39 in x 3 in	

TABLE 3.2a
SUMMARY OF RESULTS
DANE AND BRUCE (1975)

Beam	Debond %	Debond Length (in)	Le in	M test / M calc.	Slip in	M (Test) / M (Pilot)
G7	Pilot	Draped	3.3 Ld	1.02	0.000	-
G8	18	144	1.0 Ld	1.06	0.193	1.04
G9	18	144	1.0 Ld	1.00	0.234	0.98

Strand			Test Beam		
Type:	250 ksi Stress	Relieved	Type:	AASHTO Type II	(full scale)
Diameter:	7/16 in		Span:	48 ft	
Number:	22		Ld:	60 in.	
fsu:	268 ksi		(fsu-fse):	112 ksi	
fse:	156 ksi		f'c:	5.0 to	5.5 ksi
			Slab:	58 in x	5 in

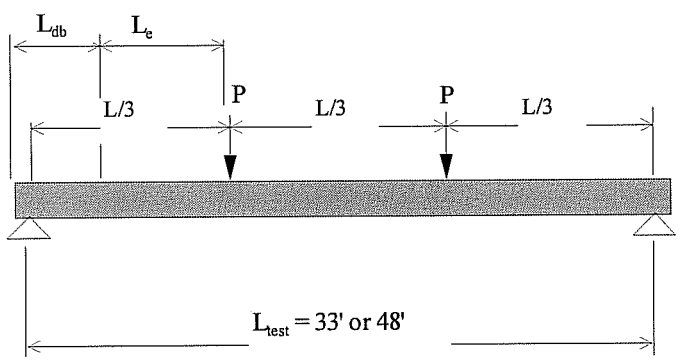

Figure 3.4 Test Setup Dane and Bruce (1975)

All beams experienced flexural failure with large deflections, although considerable slips occurred. The occurrence of large slips is not surprising considering that an embedment length equal to the transfer length was used in the

Type III girders. Figures 3.5 and 3.6 show the test moment compared to the resisting cracking and ultimate moments provided by the debonded strands. In girders G8 and G9 it can be seen that the cracking moment is reached in the transfer zone as the ultimate moment of the section is reached. The slips in these girders were small in magnitude compared to girders G3 through G6 in Figure 3.6. These tests further demonstrate the safety in debonded strands but they are narrow in scope and have relatively few debonded strands.

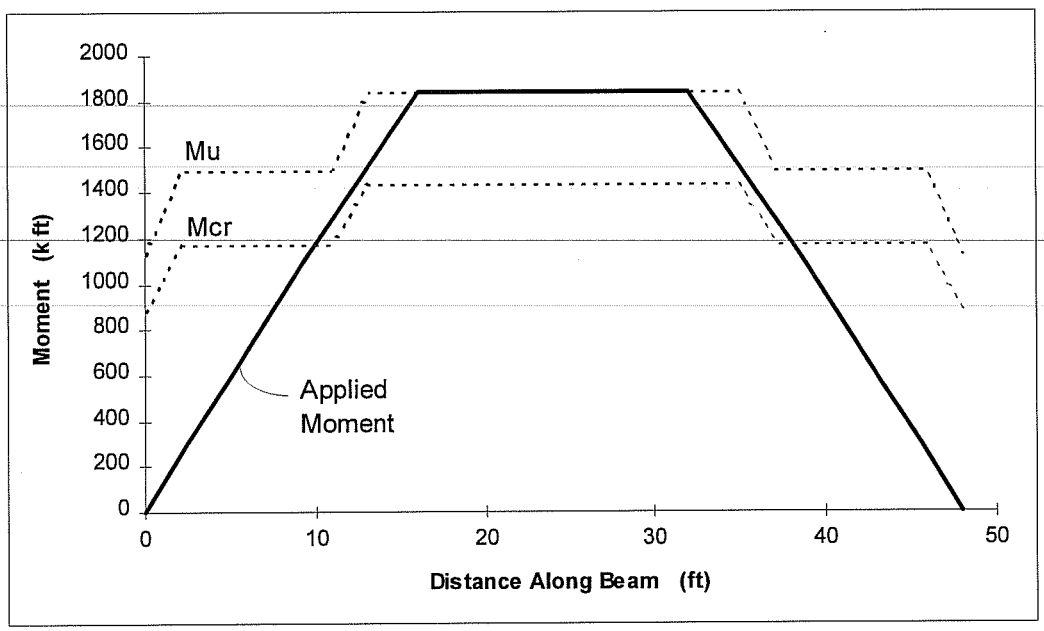

Figure 3.5 Test Girders G8 & G9, $L_e = 1.0\ L_d$

Bruce and Dane (1975)

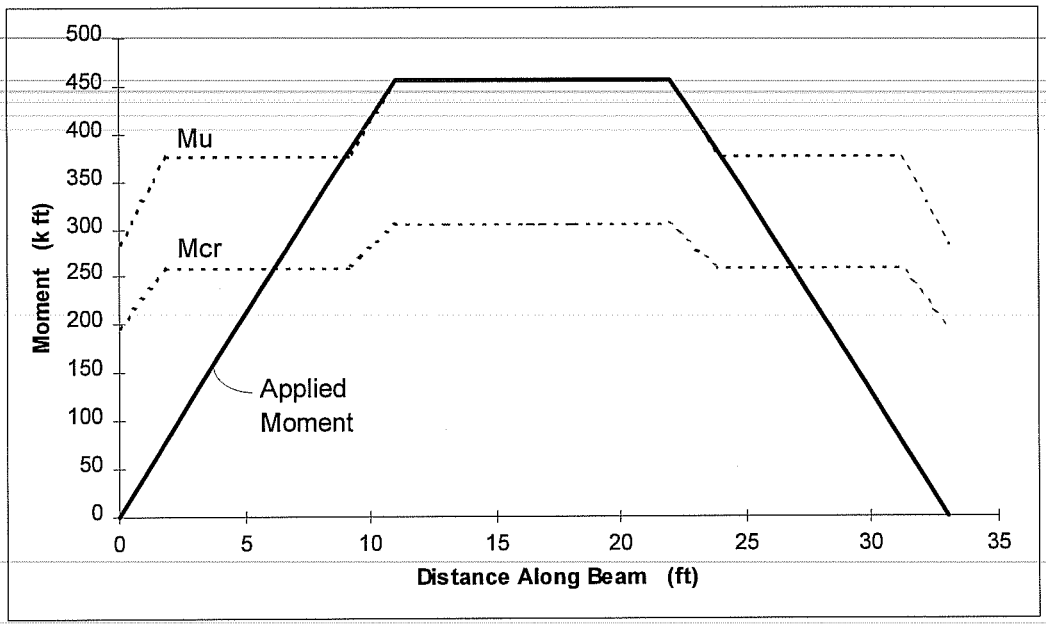

Figure 3.6 Test Girders G3 Through G6, L_e =0.34 L_d

Bruce and Dane (1975)

3.4 Rabbat, Kaar, Russell and Bruce (1979)[18]

The girders in this test are the same full scale AASHTO Type II girders used in tests performed by Dane and Bruce. The design and results are summarized in Table 3.3. These beams were first fatigue loaded under 5 million cycles. The first three beams listed in Table 3.3 (G11, G13 and G10) were designed to allow $6\sqrt{f'c}$ tension in the bottom of the beam. These beams failed under fatigue loading. Measured slips were very small, and little can be said about the anchorage since actual failure was due to fatigue.

The remaining three beams listed, which were designed with zero allowable tension in the bottom fiber of the beam, were tested statically to failure. Slip did occur, but the final failure mode was flexural with large deflections.

Once again, as in the Kaar and Magura study, an attempt to simulate the moment envelope for a highway girder was made when the loading arrangement was established as shown in Figure 3.7. Test moments are well above the resisting cracking moments in the debonded areas so that severe cracking occurred in the transfer zone before flexural failure occurred, as demonstrated by the moment diagram in Figure 3.8.

TABLE 3.3

SUMMARY OF RESULTS

RABBAT, KAAR, RUSSELL AND BRUCE (1979)

Beam	Debond %	Debond Length (in)	Le in	Allowable Tension	Slip in	Failure Mode
G11	18	198	1.0 L_d	$6\sqrt{f'_c}$	0.026	Fatigue
G13	18	132	2.0 L_d	$6\sqrt{f'_c}$	0.006	Fatigue
G10	-	Draped	4.0 L_d	$6\sqrt{f'_c}$	0.000	Fatigue
G14	18	198	1.0 L_d	0	0.570	Flexure
G12	18	198	1.0 L_d	0	0.510	Flexure
G10 A	-	Draped	4.0 L_d	0	0.000	Flexure

Strand			Test Beam	
Type:	250 ksi Stress	Relieved	Type:	AASHTO Type II (full scale)
Diameter:	7/16 in		Span:	49 ft
Number:	22		Ld:	66 in.
fsu:	264 ksi		(fsu-fse):	124 ksi
fse:	140 ksi		f'c:	5.9 to 7.6 ksi
			Slab:	58 in x 5 in

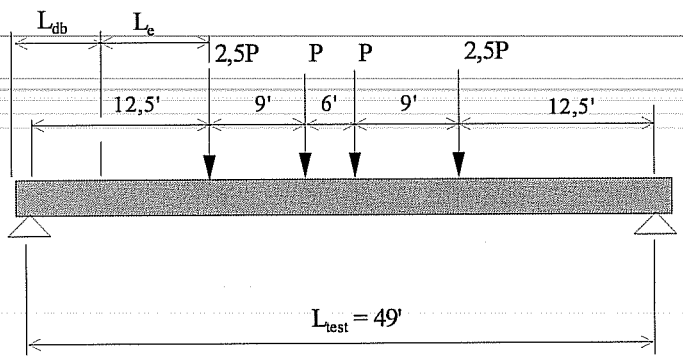

Figure 3.7 Test Setup Rabbat, Kaar, Russell and Bruce (1979)

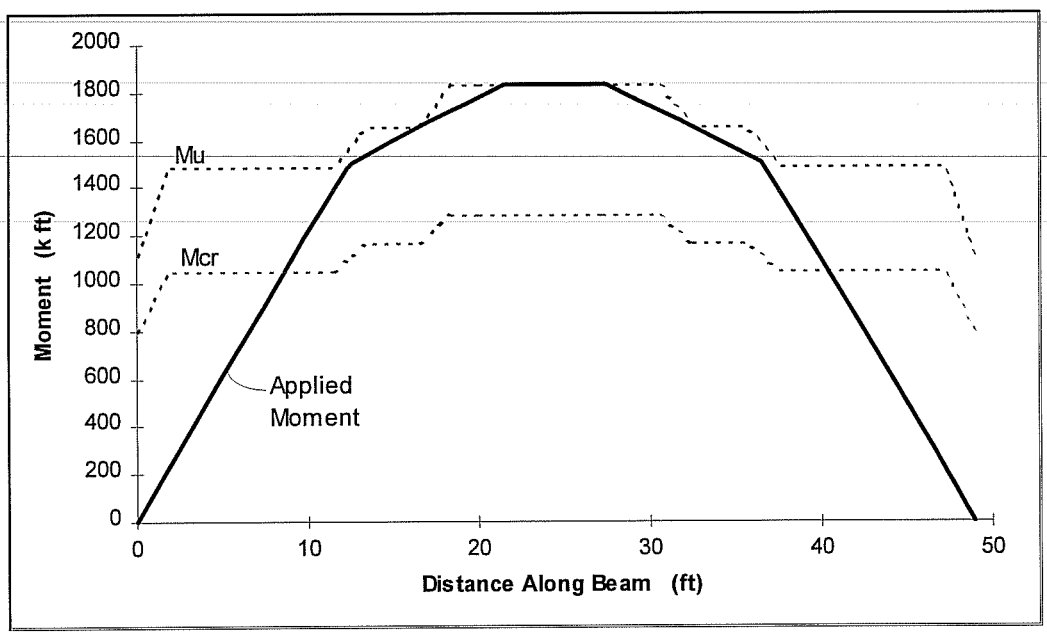

Figure 3.8 Test Girders G12 and G15, Le = 1.0 Ld

Rabbat, Kaar, Russell and Bruce (1979)

These tests demonstrated that debonding could be safely used in highway girders, and the ACI and AASHTO codes did not require doubling the calculated development length when no tension was allowed in design.

3.5 Russell and Burns (1993)[13]

Russell and Burns performed a comprehensive study to establish guidelines for transfer and development lengths of large diameter prestressing strand. A variety of test specimens was fabricated to test the effects of both static and fatigue loadings on pretensioned concrete beams. Covered herein are the tests that investigated the effects of debonding on structural behavior. The first six beams listed in Table 3.4 (Those listed above the heavy line across the table) were tested statically to determine the effect debonding has on structural behavior. Fifty percent of the strands were debonded, which is more than the 25% maximum allowed by the AASHTO Load and Resistance Factor Design (LRFD) Specification, Section 5.11.4.2. This section also stipulates that no more than 40% in any single row and no outside strands may be debonded.

The method of termination of debonded strands was varied as well, concurrent versus staggered. When debonding of all strand ends at a single location, it is referred to as ending concurrently and when termination of debonding material on different strand sets is distributed over several locations, it is referred to as staggered. Unless extensive damage occurred to a beam during testing, both beam ends were tested . The test setup used for these tests is shown in Figure 3.9.

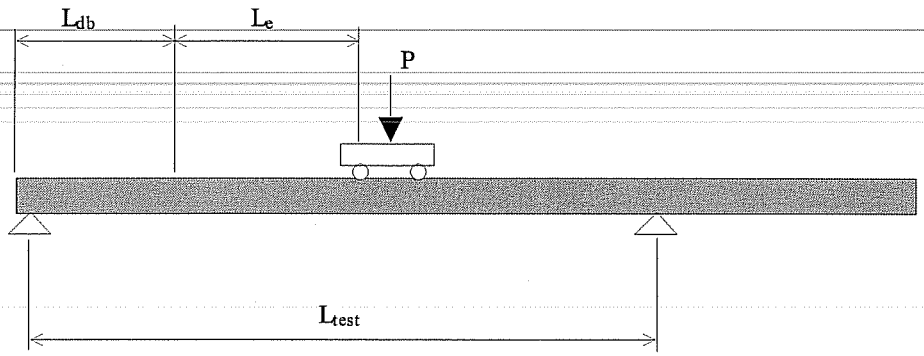

Figure 3.9 Test Setup Russell and Burns (1993)

The next five beams listed in Table 3.4 were tested under repeated loadings to determine the effects of fatigue. The first beam in this series had four fully bonded 0.6 inch diameter strands at a 2 inch grid spacing. The next four debonded beams, F1 through F4, were identical to beams 3 through 6 in the first series. They were loaded with fatigue loading which ranged from 25% to 100% of the service load, based on a tension stress in the bottom fiber of $6\sqrt{f'_c}$. Each specimen was precracked before testing which significantly increases the stress range that occurs in the prestressing strand. Once the beam had been subjected to repeated loadings, it was loaded statically to failure to determine what effect the fatigue loading had on behavior.

The final series of beams was Texas Department of Transportation (TxDOT) full scale standard Type C beams with a composite slab. The intent was to compare the behavior of a full scale highway girder to the performance of the previous test beams. A summary of these beams is found in Table 3.5. These

beams were subjected to fatigue and static loadings similar to the second series of test beams described above.

TABLE 3.4
SUMMARY OF RESULTS
RUSSELL AND BURNS (1993)

	Test	Debond %	Debond Length (in)	Le in	M test M calc.	Slip in	Failure Mode
a	DB850-1A	50	36 S	1.05 Ld	0.85	0.80	Bond/Shear
a	DB850-1B	50	36 S	1.05 Ld	0.95	0.70	Bond/Shear
a	DB850-2A	50	36 S	0.95 Ld	0.94	0.35	Bond/Shear
a	DB850-2B	50	36 C	1.10 Ld	0.96	0.40	Flexure
b	DB850-3A	50	78 S	1.00 Ld	0.98	0.54	Bond
b	DB850-3B	50	78 S	1.35 Ld	1.03	0.28	Flexure
b	DB850-4A	50	78 S	1.50 Ld	1.00	0.00	Flexure
b	DB850-4B	50	78 S	1.25 Ld	1.00	0.24	Flex w/Slip
b	DB850-5A	50	78 C	1.25 Ld	0.93	0.81	Bond
b	DB850-6A	50	78 C	1.88 Ld	0.97	0.11	Flex/Bond
@b	FA460-F4A	-	-	1.25Ld	0.99	0.00	Flexure
b	FA460-F4B	-	-	1.00Ld	0.98	0.01	Flexure
b	DB850-F1A	50	78 S	1.25Ld	0.93	0.20	Flex w/Slip
b	DB850-F1B	50	78 S	1.00Ld	0.94	0.53	Bond
b	DB850-F2A	50	78 S	1.00Ld	0.82	0.64	Bond
	DB850-F2B	50	78 S	1.38Ld	0.93	0.15	Flexure
	DB850-F3	50	78 C	1.50Ld	0.92	0.44	Bond
	DB850-F4	50	78 C	1.25Ld	0.87	0.33	Bond

Strand

Type:	270 ksi Low Relaxation
Diameter:	1/2 in
Number:	8
fsu:	283 ksi
fse:	162 ksi
Lt=	30 in (avg)
S:	Staggered Debonding
C:	Concurrent Debonding

Test Beam

Type:	d=	23.5 in
	A=	197 in2
	I=	12080 in4
Length:	27.5 ft	(a)
	40 ft	(b)
Ld:	80 in.	
(fsu-fse):	121 ksi	
f'c:	6.8 to	7.4 ksi
Slab:	N/A	

@ 4 - 0.6 dia strands, Ld=96"

TABLE 3.5
SUMMARY OF RESULTS
RUSSELL AND BURNS (1993)

Test	Debond %	Debond Length (in)	Le in	M test M calc.	Slip in	Failure Mode
FZ2450-3N	-	-	2.70 Ld	1.00	0.00	Flexure
FZ2450-3S	-	-	1.80 Ld	1.00	0.01	Flexure
DZ2450-1N	36	72 S	1.88 Ld	0.89	0.80	Horiz. Shear
DZ2450-1S	36	96 S	0.68 Ld	0.89	0.80	Horiz. Shear
DZ2450-2N	36	72 S	1.88 Ld	0.96	0.35	Flexure
DZ2450-2S	36	96 S	0.68 Ld	0.96	0.35	Flexure

Strand			Test Beam	
Type:	270 ksi Low Relaxation		Type:	TxDOT Type C
Diameter:	1/2 in		Span:	48 ft
Number:	22- bot & 2 top		Ld:	80 in.
fsu:	283 ksi		(fsu-fse):	121 ksi
fse:	162 ksi		f'c:	10,4 ksi
Lt=	30 in (avg.)		Slab:	72 in x 8.25 in
S:	Staggered Debonding			

Interpretation of the results for the various embedment lengths relied on a prediction model that the researchers established based on the cracking moment of a section. Figure 3.10 shows moments versus distance along the span for test DB850-3A with an embedment length equal to the current development length equation. The cracking moment for sections along the beam, which varies due to debonding, is calculated and compared to the moment from the applied load. It can be seen that the cracking moment in the last region of debonded strands is exceeded, thus cracking in the transfer zone occurred. As shown by other research,[6, 8] the result of cracking in the transfer zone is that strand slip will occur precipitating an initial bond failure and the possibility of complete bond failure as the load increases.

The researchers expressed required development length, L_d (Calculated), Figure 3.10, as a function of debond length (L_{db}), cracking moment (M_{cr}) and ultimate moment (M_u) as follows:

$$L_d = \frac{M_U}{M_{CR}} \bullet \left(L_{db} + L_t\right) - L_{db} .$$

In this equation, an attempt to quantify flexural bond stress is not made as in past studies, but instead control is applied to the cracking moment in the transfer zone.

The importance of the method of termination for debonding, concurrent versus staggered, is also demonstrated. Figure 3.11 shows the negative effect that concurrent debonding has on a pretensioned beam and the advantages gained by staggering debonding. The clear advantage is shown as the prestress force is maintained at an acceptable level with the distribution provided by staggered debonding. Staggered debonding prevents adverse behavior from reduced shear and cracking moment capacity. The cracking moment capacity for this case is exceeded slightly by the applied moment at ultimate as shown by the solid line in Figure 3.11.

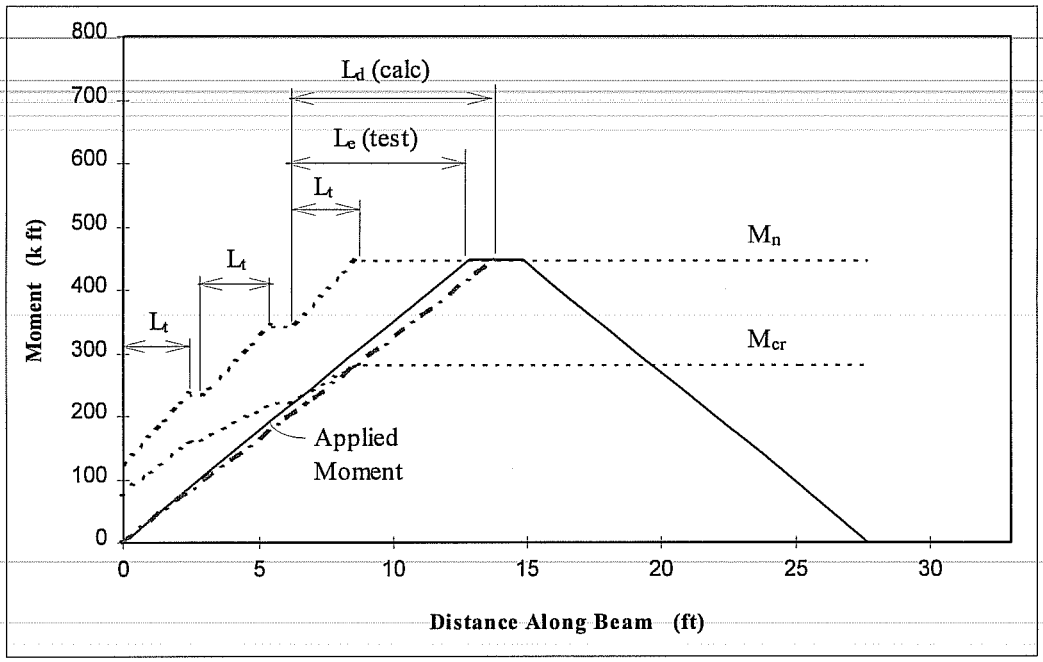

Figure 3.10 Test DB850-3A, L_e=1.0 L_d

Russell and Burns (1993)

Inadequate shear capacity due to debonding or lack of proper reinforcement proved to be a critical concern. While strands that slipped due to flexural cracking were able to develop significant stress, and in some cases provide the nominal flexural capacity, the same proved catastrophic with shear cracking. Once a crack due to shear passed through the transfer region of a strand, slips that occurred were sudden and violent, and total loss of capacity occurred. In tests performed on full size girders, horizontal shear reinforcement ("h" bars) were provided in addition to vertical shear reinforcement. This was effective in controlling the propagation of shear cracks through the transfer zone and preventing catastrophic failure from strand slip.

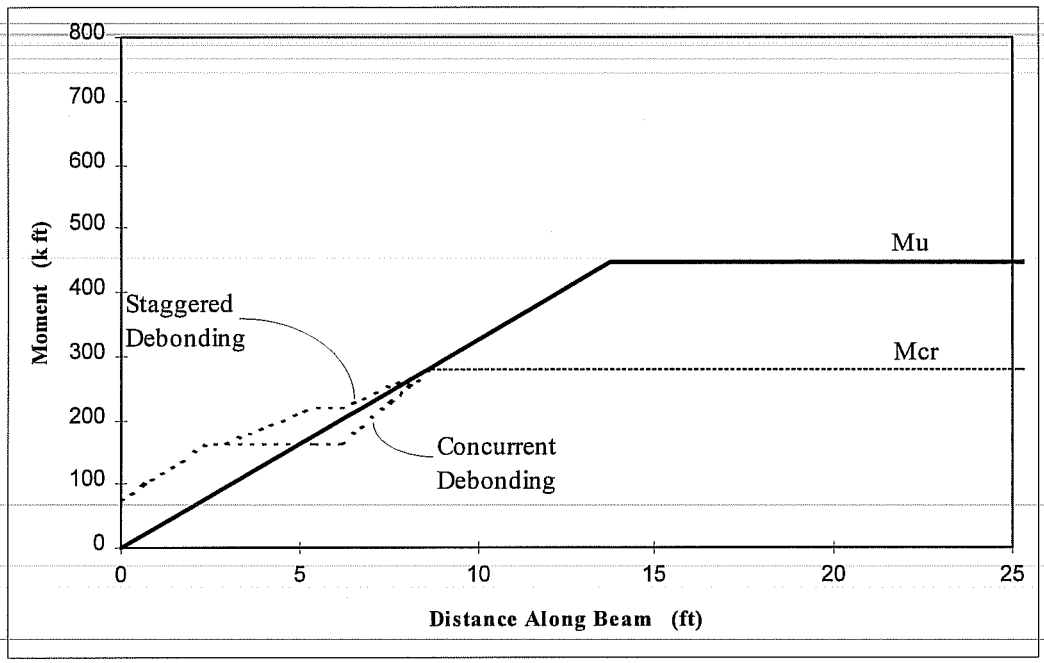

Figure 3.11 Staggered vs. Concurrent Debonding
Russell and Burns (1993)

Results from fatigue loadings indicated that in most cases, slip due to overloads increased under repeated loadings but they were very small and stabilized under a finite number of loadings. There was an instance where the slips became larger, which is cause for concern with any loading situations which involve an increasing stress range.

From these results, the report made the following recommendations for design of pretensioned beams with debonded strands:

- Implement a conservative value of the transfer length as opposed to the current code equation which approximates an average value;

$$L_t = \frac{f_{se}}{2} d_b$$

- An expression was developed that would avoid cracking in the transfer zone of debonded strands. This is based on the parabolic shape of a moment envelope for a design vehicle loading;

$$(Lb + Lt) = \frac{SPAN}{2}\left[1 - \sqrt{1 - \frac{Mcr}{Mu}}\right]$$

- If $V_{cw} < V_u$, then horizontal and vertical shear reinforcement should be provided to prevent propagation of shear cracks into the transfer zone of prestressed strands.
- Include top strands in the design of pretensioned beams to significantly reduce the number of debonded strands required to control end stresses. In this manner an acceptable level of cracking moment and shear resistance in the end region of the beam is maintained.

Other papers include a PCI report by Horn and Preston[20] which gives an overview of research on transfer and development length for debonded strands. It provides design procedures and an example to follow for prestressed girders containing debonded strands. Another by Ghosh and Fintel[21] gives an overview of research that helped to establish ACI code provisions for development length of debonded strands. It includes comments by individuals from the precast/prestressed concrete industry on the fabrication of prestressed concrete beams with debonded strands.

CHAPTER 4

TEST PROGRAM

4.1 Test Beam Section and Analysis

The test beams for this study were Type I AASHTO precast prestressed concrete standard sections (see Figure 4.1) with mild reinforcement as provided in the Texas Department of Transportation (TxDOT) standard. Beams were fabricated in Victoria, Texas at Texas Concrete Company, and a 6.5 inch thick by 60 inch wide slab was placed on the beam in Austin, Texas at Ferguson Structural Engineering Laboratory (FSEL). Details of mild reinforcement are located in Appendix C. Figure 4.1 is a detail of the completed cross section. There were three beam designs for the three ranges of concrete strength used. Table 4.1 gives the jacking stress of the prestressing strand and a list of which strands were debonded. Information on test beam labeling and concrete strength data is given in Tables 4.2 and 4.3.

TABLE 4.1
TEST BEAM STRAND DETAILS

Concrete Strength Group	Bottom Strands*		Top Strands*		Debonded Strands	
	Number	f_{jack} ksi	Number	f_{jack} ksi	A2 & A5 in	A3 & A4 in
Low	8	202.5	2	202.5	36	72
Medium	8	202.5	2	46.0	36	72
High	8	202.5	0	-	36	72

*Strand locations are given in Figure 4.1

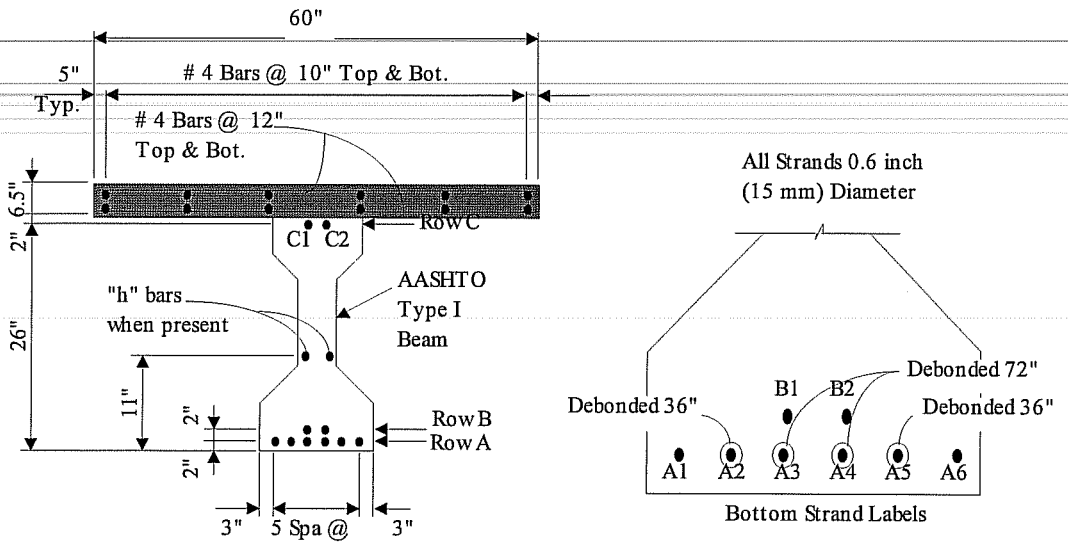

A) Beam Cross Section

B) Detail of Bottom Strands

Figure 4.1 Test Beam Section

Test beams were cast in pairs, two for each of the three concrete strength groups given in Table 4.2, making a total of 6 test beams. In one end of a pair of beams, or one out of four tests, "h" bars were placed in addition to the standard reinforcement. These bars are shown in Figure 4.1 and extended from the end of the beam for 12.5 feet (150 inches). This is about 78 inches beyond the beginning of bond for the 72 inch debonded strands. Further details are shown in Appendix C. This reinforcement was included to determine if these bars would limit crack widths in the transfer region of the prestressing strand in order to control end slip while the beam was under an applied load.

Table 4.2 defines the symbols used in labeling each test and beam for the various embedment length tests. For example, test M4b0n is made of medium strength concrete with four strands debonded, bright strand condition, no "h" bars are included in this beam, and the north end of beam M4b0 was tested.

TABLE 4.2
TEST BEAM LABELING

Example	Description	Symbol Definition
M	Concrete Strength	L - Low, M - Medium, H - High
4	No. of Debonded Strands	4 - 4 strands Debonded
B	Surface Condition	B - Bright
0	"h" Bar	0 - none, 1 - "h" Bar at north end
N	Beam End Tested	N - North, S - South

Three design mixes provided by Texas Concrete Company were used to obtain the various concrete strengths. Mix designs for the test beams are located in Appendix A. The proposed strength and average strength attained for each group is listed in Table 4.3. Concrete strengths for beams at the time of testing are listed in Chapter 5, and Appendix A has plots of time versus strength gain for the test beams. The high strength concrete did not reach the full expected strength and was roughly one ksi higher than the average medium strength in this particular series of tests as listed in Table 4.3. Data for the high strength class will remain separate from the medium strength class of concrete to determine the effects the different mix design had on the test results for each group of beams.

TABLE 4.3
CONCRETE STRENGTH DATA

Concrete Strength Group	Proposed Strength		Avg. Act. Strength	
	Beam ksi	Slab ksi	Beam ksi	Slab ksi
Low	5.0 to 7.0	6.0	6.20	6.12
Medium	9.5 to 11.5	6.0	10.40	6.01
High	13.0 to 15.0	6.0	11.43	5.90

Behavior of the test beams was based on strain compatibility analysis of the section. Stress-strain properties for concrete, prestressing steel and mild reinforcement were modeled by using known curves for these materials. Deflection predictions for test beams under load were based on a moment-curvature analysis[28].

The stress-strain relationship used for concrete is shown in Figure 4.2. It is based on a curve established by Hognestad[26, 27] as modified by Burns[28]. The compressive force acting on the concrete in the top part of the section is determined by integrating this equation over the beginning and end strains where the beam and slab are in compression as shown in Figure 4.3. The centroid for forces C1 and C2 was obtained by integrating this equation between two known strains to determine a factor γ. This factor γ is multiplied by the distance between the locations of the two known strains to determine the centroid as shown in Figure 4.3. This assumes that the slab and flange of the beam in compression are of a constant width. All equations derived are found in Appendix C. This method of determining the compressive force and centroid has been documented

by Park and Paulay[29] as an accurate analysis for predicting moment-curvature response for a composite prestressed concrete cross section.

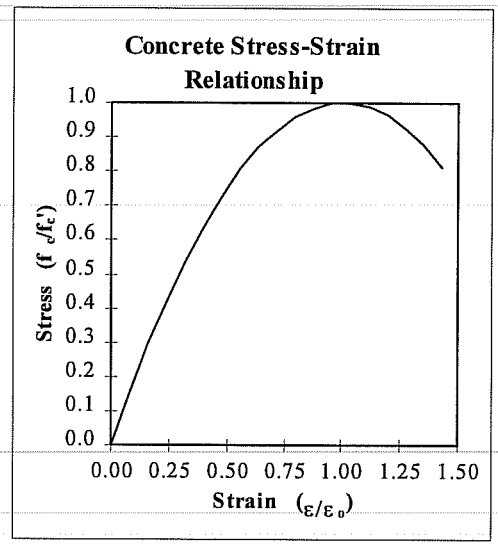

Figure 4.2 Concrete Stress-Strain Relationship

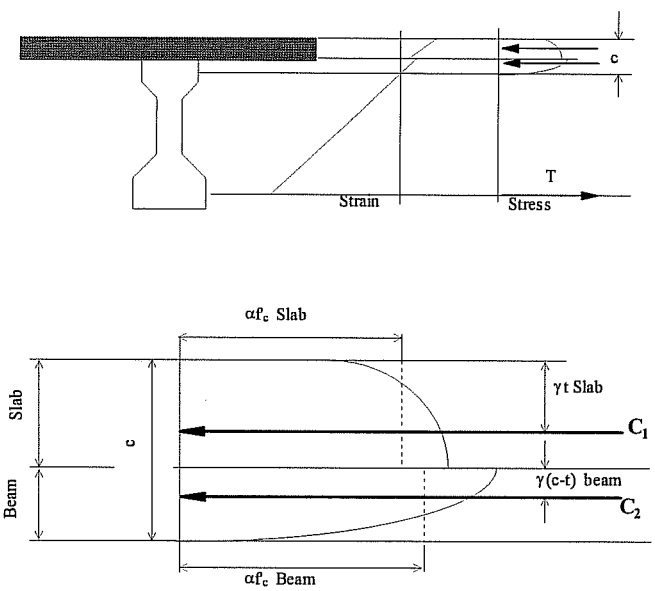

Figure 4.3 Stress Block Used in Analysis of Test Beams

The stress-strain curve used for 0.6 inch (15 mm) diameter prestressing seven wire strands is modified from that presented in the PCI Design Handbook[4] to model strand with an ultimate strength of 275 ksi based on ultimate strength tests results, and is presented in Appendix A. A bilinear stress-strain curve for mild steel reinforcement (unstressed) with an ultimate strength of 60 ksi is used.

Effective prestress was determined by subtracting prestress losses due to shrinkage, creep, elastic shortening and strand relaxation from the initial jacking force applied to the prestressing strand. Prestress losses were measured two ways. The first method was based on readings from internal strain gauges. These gauges were placed on a piece of reinforcing bar which was tied to the beam reinforcement at the centroid of prestressing steel, for both the top and bottom strands. Strain measurements were taken before and after the transfer of prestress, and again at times before testing. This was done so that an effective initial prestress (f_{si}) and the effective prestress (f_{se}) at the time of testing could be determined.

The second method was to use the concrete surface strain from the DEMEC readings used to determine the transfer length in the end regions of the beams. The increased strain in the concrete corresponded with a decrease in strain in the bonded prestressing strands, and the effects of strand relaxation were included based on curves provided in the PCI Design Handbook[4]. The results from calculations using both of these methods are included in Appendix A.

Equations were placed in an spreadsheet and the moment capacity was determined by iteration to obtain equilibrium of section forces due to prestressing

steel, mild reinforcement in the slab (and "h" bars when present), and concrete compressive forces (C_1 and C_2 from Figure 4.3). The iteration was accomplished by writing a macro in Excel which would solve by trial and error the curvature for various levels of strain based on the sum of section forces until the error was less than .0001 kips for each strain increment. The ultimate strain gradient at equilibrium included the effects of load on the beam alone before the composite slab was added. The composite section strains shown in Figure 4.3 were used after the beam cracked. Slab shrinkage strains were combined with the strains from moment carried by the cross section to obtain the rotation required to reach ultimate flexural capacity. From this analysis a moment-curvature relationship was established for the section for a particular top fiber strain. These points were combined to define the moment-curvature relationship of the section. Using this relationship the deflection was calculated by use of the moment-area method.

4.2 Measurement of Transfer Length

Transfer lengths were determined for the 0.6 inch (15 mm) prestressing strand based on measurement of concrete strains for the beam at the centroid of the bottom prestressing strand. Strain was measured mechanically using DEMEC points bonded to the surface of the beam immediately before transfer of the prestress. These points were set approximately 200 mm on center with overlapping 50 mm spacings, and strains were measured with an accuracy of about 5×10^{-6} with the DEMEC gauge. Once the prestress force was released and transferred to the concrete, the increments between points were measured again. The difference between the before and after-release measurements provided the strain in the concrete due to transfer of prestress.

The data obtained using a gauge length of 200 mm provided more output for the DEMEC strains and reduced the error in measurements. The method for reducing the data took into account the overlapping of the 200 mm lengths for gauge points located 50 mm on center. Transfer length was measured immediately after transfer and again before the development length test was performed after the composite slab had been placed on the beam. This was to determine the effect time had on transfer lengths. Figure 4.4 is a photograph of the concrete strain being measured with a DEMEC gauge.

The strains, as measured above, were averaged with adjacent points to smooth the curve when plotted along the length of the beam. Once plotted the transfer length was determined by one of two methods; the 95 percent plateau method and the slope intercept method. The results of both methods are compared and discussed further in Chapter 5.

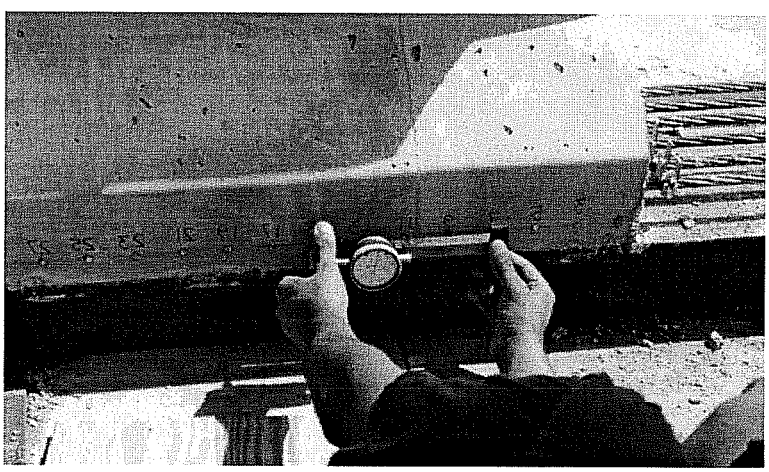

Figure 4.4 Measurement of Transfer Length Using a DEMEC Gauge

In order to indicate the characteristics of bond of the prestressing strand used, pull-out tests and end slip measurements at transfer were performed. In the pull-out test, strand was placed in a concrete block and was placed under tension to measure its resistance at failure. This test is based on the Moustafa method as reported in a paper by Donald R. Logan[12]. Measurement of end slip at transfer (pull-in) is another method in which to determine transfer length and is reported to be a good indicator of bond behavior of prestressing strand. This is based on a theory by Mast reported in the same paper in which pull-out testing was studied by Logan[12].

A complete report on all details of the transfer length measurements is given in Reference 30, which reports on another series of beams in the present study. While that study had no debonded strands, the techniques for measurement of transfer and development length were identical.

4.3 Measurement of Development Length

Measurement of development length cannot be made directly but is determined by testing various embedment lengths. Embedment length is the distance from the beginning of bond of a strand to the first load point, or critical section, as discussed in Chapter 3 and shown in Figure 4.5.

Debonded length is L_{db} and the embedment length is L_e for these strands, as shown in Figure 4.5. In this study the debond length was staggered; two strands had 36 inches and two had 72 inches debonded. An embedment length in which no strand slip occurs and the full capacity of the beam is reached, demonstrates a bonded length of strand in excess of the required development

length (L_d). When the embedment length is short enough that slip occurs and the capacity of the beam is not reached, then L_e is less than the required L_d.

Tests were performed on both ends of a beam making a total of 12 tests which are reported in this study. They are labeled as indicated in Table 4.3 with "n" or "s" indicating whether the north or south end of the beam was tested relative to placement of the beam in the Laboratory.

The total beam length (L_{beam}) was 54 feet, and a span length (L_{test}) of 30 feet was used when testing the embedment length. This test span provided a symmetrical test loading when the longest embedment length of 96 inches was used. This provided a loading geometry in which the test end of the beam would be subjected to larger shears and moments for the remaining tests which had smaller embedment lengths. This arrangement of L_{test} and L_{beam} also prevented excessive damage to the beam's interior which might affect the performance of the other end of the beam. Figure 4.5 shows the test setup.

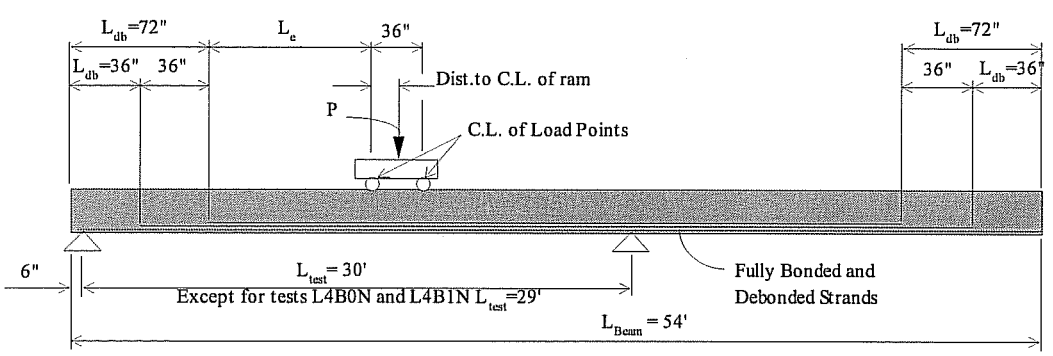

Figure 4.5 Development Length Test Setup

An electronic data collection system was used to monitor strand slip during loading. End slip for each individual strand was measured by placing linear potentiometers on the strand to measure its movement relative to the beam end. This instrumentation is shown in Figure 4.6. For this study, when a slip of 0.01 inch occurred (this is discussed further in Chapter 5), it was considered initiation of bond failure. Ultimate slip was defined as the total end slip at the end of testing, regardless of weather the test was terminated due to bond or flexural failure, or a combination of both.

Strains on top of the slab were measured at eight locations between the load points as shown in Figure 4.7. Electronic resistance strain gauges (ERSG) were placed on the slab prior to testing with a fast curing epoxy, and were wired into the data collection system which monitored strains at each load increment. A photograph of the strain gauges in place on the slab is shown in Figure 4.8.

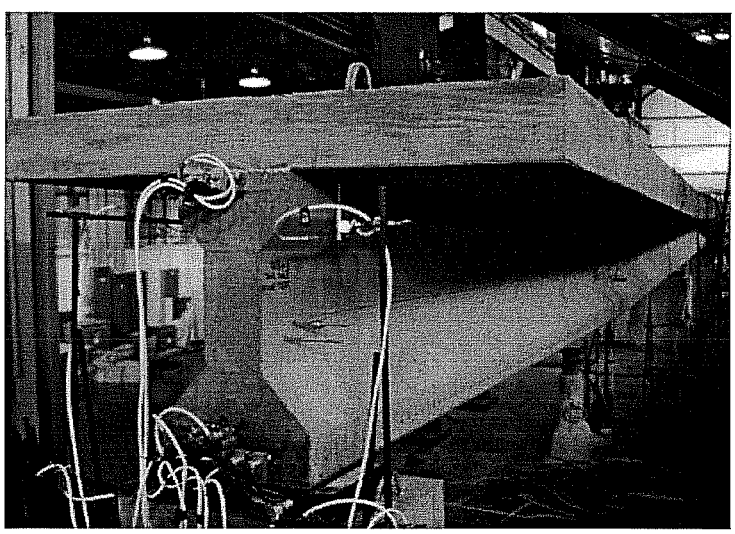

Figure 4.6 Linear Potentiometers at End of Beam to Measure Strand Slip

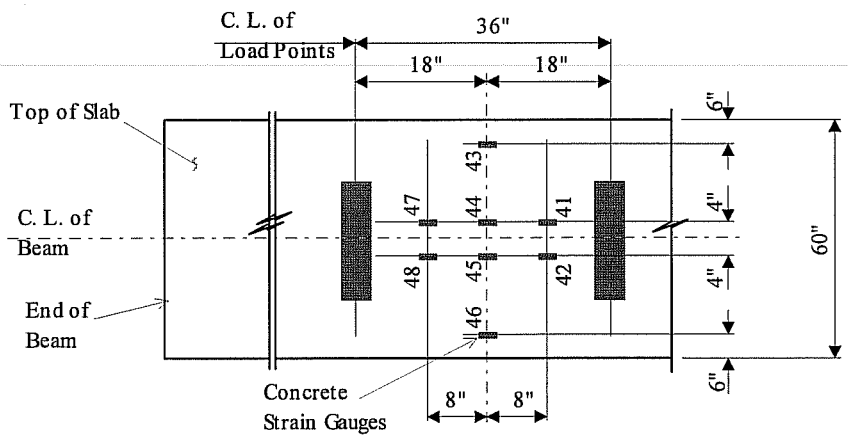

Figure 4.7 Concrete Strain Gauge Placement

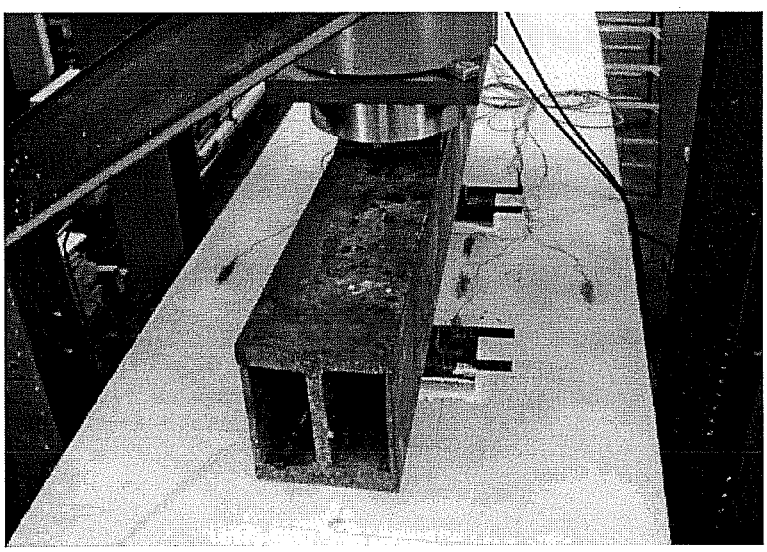

Figure 4.8 Photograph of Strain Gauges on Top of the Slab

In order to plot a load-deflection response, deflections were monitored midway between the two load points and at each load point located as shown in

Figure 4.5. Deflections were measured with the same type of linear potentiometers used to measure strand end slip. Deflection at the center of the load points is the location where both the calculated and measured load-deflection response was compared. Figure 4.9 shows the linear potentiometers in the test setup which were connected to the data acquisition system to record beam deflections at each load increment during the test.

A complete description of this same test setup for development length evaluation is given in Reference 30. All details are the same except the beams of that study had no debonded strands with different test span lengths.

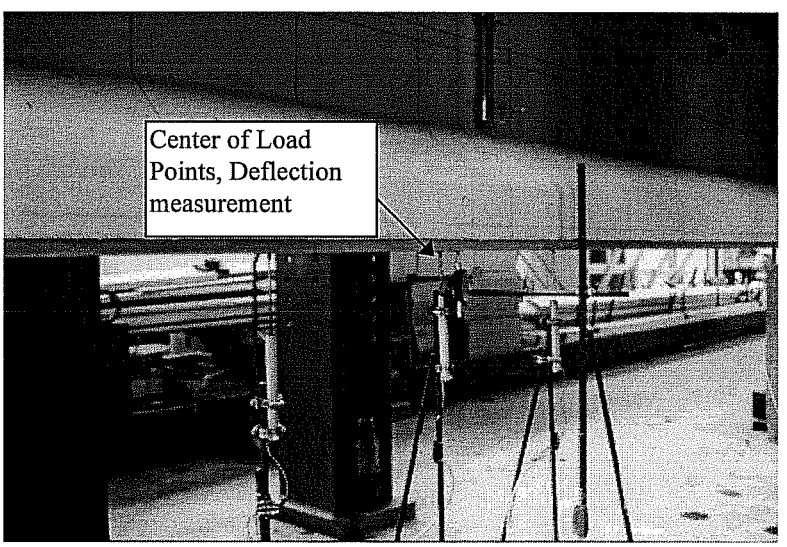

Figure 4.9 Linear Potentiometers to Measure Deflection

CHAPTER 5
TEST RESULTS

5.1 Introduction

Results from transfer and development length tests are presented in this chapter. A complete set of plots from which transfer lengths were determined is found in Appendix B. Plots of data from the development length tests are in Appendix D, and material information is presented in Appendix A.

5.2 Transfer Length

Strain data measured as described in Chapter 4 with the Demec gauge were input into a spreadsheet for interpretation. Each reading was averaged with the two adjacent points, a process referred to as three-point smoothing. In this way a more smooth plot was generated that is easier to interpret. The technique is commonly used with data of this nature[11]. Once the curve was constructed, the plateaus corresponding to the various levels of debonding were identified as shown in Figure 5.1. Based on the regions where the apparent plateaus existed, an average was calculated, and the lines were plotted on the graph as 95 or 100 percent plateau levels. Also identifiable were the slopes where the transfer of stress from the prestressing strand to concrete occurred. In these regions an average slope was constructed. Figure 5.1 is an example where the points have been smoothed and the above mentioned lines constructed.

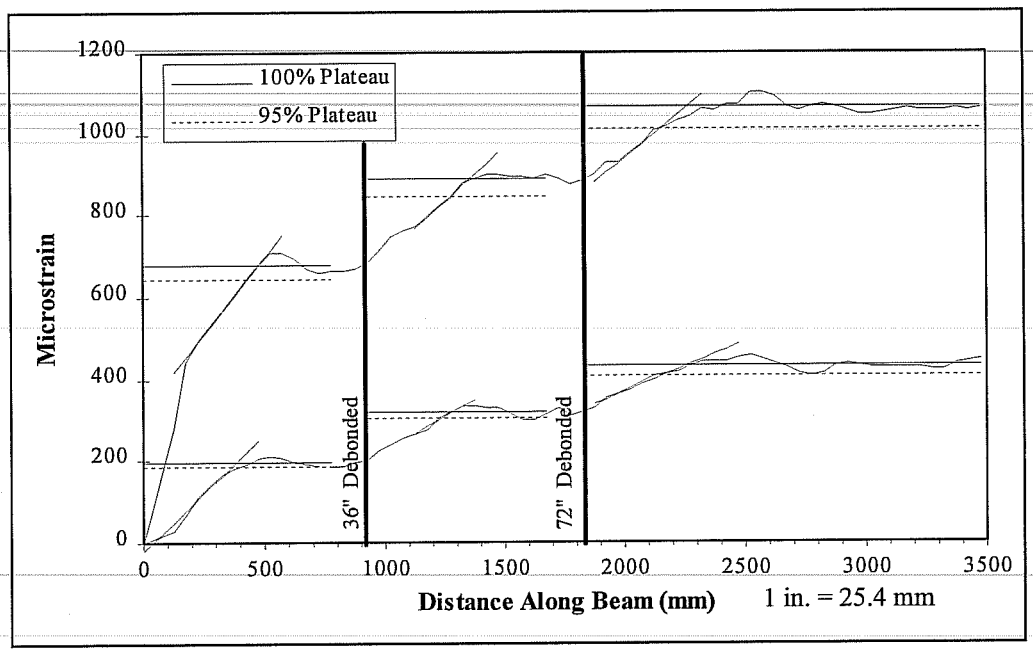

Figure 5.1 Plot of Smoothed Transfer Data

In Figure 5.1, 100 and 95 percent of the average strain plateau is constructed at each level of bonding. Two methods of determining the transfer length are used. The first method, the one recommended by C. D. Buckner in his report for the Federal Highway Administration (FHWA),[11] is the intersection of the 95% plateau with the curve created by the data points. The second method, which will be referred to as the Slope-Intercept Method, defines the end of transfer as the intersection of the average plateau with a line which represents an average slope of the transition region. This second method has been used by

TABLE 5.1
MEASURED TRANSFER LENGTHS (in)
95% PLATEAU METHOD

Beam End	Immediately After Transfer			After Deck Placement		
	Debond Length			Debond Length		
	0"	36"	72"	0"	36"	72"
L4B0S	21.7	24.7	14.7	24.7	23.8	13.8
L4B0N	15.3	15.4	11.9	19.5	15.5	12.1
L4B1S	21.2	12.1	13.3	-	-	-
L4B1N	15.7	12.4	13.1	17.0	14.5	12.5
M4B0S	14.5	11.6	14.4	14.6	13.2	10.4
M4B0N	12.4	13.2	9.5	15.1	12.8	10.4
M4B1S	14.3	14.9	13.8	16.5	15.6	13.1
M4B1N	14.2	13.8	10.6	13.9	10.6	12.1
H4B0S	11.5	13.8	16.0	13.4	11.8	14.6
H4B0N	13.6	12.0	14.9	16.1	14.0	13.9
H4B1S	14.5	13.3	15.2	15.5	14.1	16.4
H4B1N	12.6	14.0	12.3	13.7	14.7	6.2

TABLE 5.2
MEASURED TRANSFER LENGTHS (in)
SLOPE-INTERCEPT METHOD

Beam End	Immediately After Transfer			After Deck Placement		
	Debond Length			Debond Length		
	0"	36"	72"	0"	36"	72"
L4B0S	22.4	25.3	19.4	26.3	27.4	18.5
L4B0N	15.3	15.4	14.8	20.8	18.1	16.4
L4B1S	21.8	13.6	16.0	-	-	-
L4B1N	15.0	14.5	16.8	18.9	17.5	17.0
M4B0S	14.4	14.9	17.9	14.7	16.1	14.6
M4B0N	13.1	15.8	13.1	13.6	16.3	14.1
M4B1S	14.5	17.1	16.6	14.3	18.1	17.1
M4B1N	14.0	16.3	14.2	13.5	13.3	16.0
H4B0S	11.8	17.6	19.6	13.3	15.3	17.8
H4B0N	12.8	15.3	17.6	13.0	16.6	17.1
H4B1S	12.8	14.7	20.0	12.7	15.8	21.0
H4B1N	12.7	14.3	15.4	13.0	14.7	15.4

other researchers[15]. Using both of these methods, transfer length was measured immediately after transfer and after the composite deck was placed on the beam. Results of the 95% Plateau Method and Slope-Intercept Method are listed in Tables 5.1 and 5.2, respectively.

5.3 Development Length

5.3.1 Failure Mode

Bond and flexural failure are two modes of failure which define the capacity of a test specimen in the study. Shear failure was not encountered, as the reinforcement was more than adequate to prevent its occurrence. A test was determined to be a flexural failure if the actual test load applied to the beam met or exceeded the calculated flexural resistance based on strain compatibility as detailed in Chapter 4. Usually in a flexural failure either crushing of the slab or rupture of the prestressing strands takes place. In some cases, the test was terminated for safety reasons before total flexural failure occurred; failure was imminent as indicated by the concrete strains monitored during the test. Plots of concrete strain versus applied load are shown in Appendix D. A bond failure is defined as an event where the calculated ultimate moment resistance is not reached and the beam continues to deform, but with no increase in load as further slip occurres.

The final failure mode that occurred was a combination of both bond and flexure, which will be classified as a hybrid failure. This is defined as a test in

which there was considerable strand slip but the specimen's test capacity reached or exceeded the calculated ultimate moment resistance.

5.3.2 Test Span and Loading Configuration

The maximum embedment length tested was equal to the development length calculated by the ACI Code and AASHTO Standard Specification, which was 96 inches. This length was used to determine the span necessary to load the test span symmetrically. All tests were set up with a 30 foot span, except tests, L4B0N and L4B1N, which had test spans of 29 feet with an embedment length of 48 inches. The center of the load ram was placed to produce a constant moment region over the 3 foot length between load points from the spreader beam as shown in Chapter 4, Figure 4.5. Table 5.3 shows test setups for all tests performed. Moments calculated based on this loading geometry included the test load and beam weight, which included the cantilevering portion of the beam.

TABLE 5.3
DEVELOPMENT LENGTH
TEST SETUP

Test	L_e	$L_{d\ ACI}$	$Span_{test}$	*C.L. Ram
	in	%	ft	in
L4B0N	48	50	29	14.00
L4B1N	48	50	29	14.00
L4B1S	60	63	30	14.81
L4B0S	96	100	30	19.25
M4B0S	48	50	30	13.31
M4B1S	56	58	30	14.38
M4B1N	56	58	30	14.38
M4B0N	60	63	30	14.81
H4B0S	50	52	30	13.63
H4B0N	56	58	30	14.38
H4B1S	62	65	30	14.63
H4B1N	62	65	30	14.63

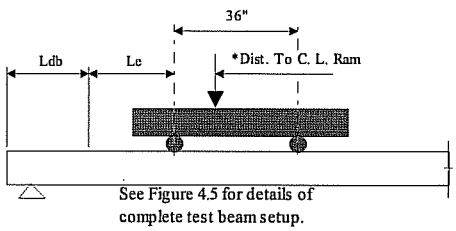

5.3.3 Analysis of Test Beams

Test beams were analyzed, as outlined in Chapter 4, based on the match-cured cylinder strength. This is defined as a cylinder that was cured at the same temperature as the beam before release of the prestressing force. There was usually about a 24 hour curing period before the minimum initial release strength was reached, at which time transfer occurred. The results of these concrete strength tests are located in Appendix A.

Effective prestress was determined as described in Chapter 4 by the use of internal strain gauges, and DEMEC readings. These calculations are shown in Appendix A, with the final values shown in Table 5.4. Initial prestress is denoted as f_{si}, and prestress at the time of testing is identified as f_{se}. Initial prestress for the all test beams was approximately equal. Final prestress for the low strength beams was somewhat lower than that measured for the medium and high strength beams as shown in Table 5.4.

The effect of time-dependent deflection is included in the analysis of the test beams. This is primarily a result of shrinkage of the slab relative to that of the beam. This phenomenon, discussed in depth in the study performed by Russell and Burns[13], decreases compressive stress in the bottom of the section. While the ultimate moment capacity of a section is largely unaffected, it has a significant impact on the cracking moment, reducing it by as much as 15 percent for this series of test beams. Figure 5.2 shows the residual stresses to which a section is subjected. Calculated moment resistance at cracking, M_{cr}, for test beams is shown in Table 5.5 with and without slab shrinkage considered. Table 5.4 also shows

the calculated ultimate moment capacity for each test beam based on the concrete strength and effective prestress at the time of testing. The calculation for the ultimate moment capacity is discussed in Chapter 4.

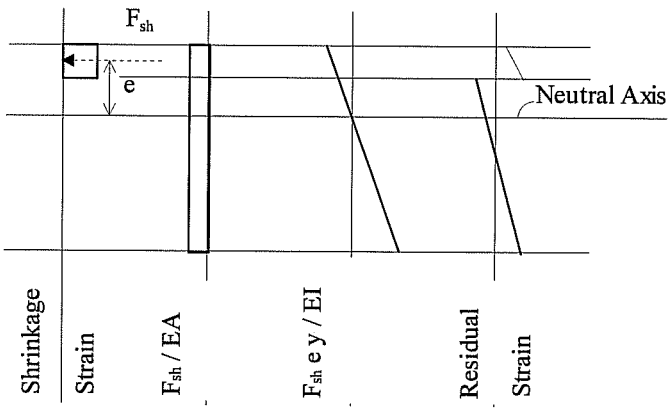

Figure 5.2 Residual Stresses Due To Slab Shrinkage

TABLE 5.4
RESULTS OF ANALYSIS
BASED ON MATERIAL PROPERTIES AT TIME OF TESTING

Test	Slab Age days	f'c Beam psi	f'c Slab psi	$M_{cracking}$ (k ft) With Shrinkage	$M_{cracking}$ (k ft) Without Shrinkage	$M_{ult.\ calc.}$ k ft
L4B0N	64	6040	6550	779	903	1348
L4B0S	13	6280	5740	814	898	1337
L4B1N	63	6110	6580	777	909	1391
L4B1S	13	6350	5620	809	897	1335
M4B0N	13	10620	5500	849	975	1326
M4B0S	16	10620	5700	853	977	1331
M4B1N	26	10180	6550	825	988	1388
M4B1S	21	10180	6270	816	981	1342
H4B0N	14	11260	5400	892	996	1275
H4B0S	17	11260	5560	895	996	1275
H4B1N	27	11590	6390	911	1012	1327
H4B1S	20	11590	6260	906	1007	1282

f_{su}= 275 ksi
f_{si}= 188 ksi
f_{se}= 171 ksi (L4BX)
f_{se}= 178 ksi (M4BX & H4BX)

5.3.4 Test Results

The cracking of a pretensioned girder in the transfer zone of a prestressing strand may precipitate bond failure as has been well documented in preceding research[6, 8, 13]. The introduction of tensile stress into the bottom fiber of a beam due to time-dependent deflection (differential slab shrinkage) results in cracking in the transfer region at a load less than that predicted by ACI and AASHTO equations for these test beams. Table 5.5 lists the cracking moments that occurred under test loading compared to those calculated by strain compatibility with and without shrinkage considered. Shrinkage strain was based on values suggested by the PCI Design Handbook[4] for the age of the composite slab at the time of testing. When shrinkage was not considered, the actual cracking moments were a significantly lower than the calculated values based on material properties at the time of testing. This can have a significant impact on initial bond failure as cracking in the transfer zone may occur at a lesser load than predicted.

Table 5.6 summarizes the test results with respect to final load and the mode of failure for each beam. In some cases a test was labeled a hybrid or flexural failure before crushing of the slab or rupture of the strands occurred, but the capacity exceeded the calculated strength when the test was stopped. All embedment lengths, except test L4B0S, were well below the minimum development length as predicted by ACI and AASHTO equations. Still, capacities exceeded or were within four percent of the calculated capacities.

TABLE 5.5
CRACKING MOMENTS

Test	Date	$M_{cr\ test}$	$M_{cr\ test} / M_{cr\ calc.}$	
		k ft	With Shrinkage	Without Shrinkage
L4B0N	01/30/97	771	0.99	0.85
L4B0S	12/10/96	811	1.00	0.90
L4B1N	02/06/97	777	1.00	0.85
L4B1S	12/18/96	822	1.02	0.92
M4B0N	03/10/97	848	1.00	0.87
M4B0S	03/13/97	818	0.96	0.84
M4B1N	03/26/97	819	0.99	0.83
M4B1S	03/21/97	826	1.01	0.84
H4B0N	04/22/97	908	1.02	0.91
H4B0S	04/25/97	901	1.01	0.90
H4B1N	05/08/97	911	1.00	0.90
H4B1S	05/01/97	906	1.00	0.90

TABLE 5.6
DEVELOPMENT LENGTH
TEST RESULTS

Test	L_e	Final Load			Failure Mode	Slab Crushing (Gauge)	Final Slab Strain in/in
	in	P meas. kips	M meas. k ft	$\frac{M_{mea}}{M_{calc}}$			
L4B0N	48	215	1287	0.96	Bond	NO (41)	0.00268
L4B1N	48	225	1349	0.97	Bond	NO (42)	0.00293
L4B1S	60	214	1373	1.03	Hybrid	YES (43)	0.00312
L4B0S	96	198	1319	0.99	Flexure	NO (45)	0.00266
M4B0S	48	207	1277	0.96	Bond	YES (41)	0.00317
M4B1S	56	207	1313	0.98	Bond	YES (41)	0.00338
M4B1N	56	219	1389	1.00	Bond	NO (41)	0.00318
M4B0N	60	217	1390	1.05	Hybrid	YES (41)	0.00448
H4B0S	50	202	1256	0.99	Bond	NO (41)	0.00256
H4B0N	56	206	1307	1.02	Hybrid	YES (41)	0.00275
H4B1S	62	206	1327	1.04	Hybrid	NO (41)	0.00294
H4B1N	62	217	1398	1.05	Hybrid	NO (44)	0.00346

Table 5.7 lists the end slips that occurred in the three and six foot debonded strands during testing. Based on the strain compatibility model used in analysis of the test beams, the stress in the strand at the critical section is calculated for different events during testing. Included in Table 5.8 is the average stress in the strand at a slip of 0.01 inches. When cracks propagated across the transfer zone, this was the order of magnitude that strands slipped. Also for comparison to strand stress at ultimate is the stress at a slip of 0.10 inches. Plots of strand stress versus end slip for individual tests are located in Appendix D.

TABLE 5.7
END SLIP
TEST RESULTS

Test	L_e	End Slip (in)				End Slip in 6' Debonded Strands		
		L_{db}= 3'	L_{db}= 6'	L_{db}= 6'	L_{db}= 3'	0.01	0.1	Final
						f_s	f_s	f_{su}
	in	A2	A3	A4	A5	ksi	ksi	ksi
L4B0N	48	0.082	1.013	1.034	0.080	201.6	247.1	270.7
L4B1N	48	0.062	1.204	1.182	0.059	180.0	247.1	273.9
L4B1S	60	0.026	0.494	0.427	0.020	257.9	273.0	273.7
L4B0S	96	0.001	-0.001	-0.001	0.004	-	-	273.7
M4B0S	48	0.016	1.347	1.392	0.024	213.9	245.3	271.3
M4B1S	56	0.019	0.981	1.013	0.019	201.6	250.6	272.0
M4B1N	56	0.041	0.814	0.703	0.035	215.3	252.2	273.6
M4B0N	60	0.003	0.316	0.531	0.002	250.4	271.6	273.7
H4B0S	50	0.008	0.882	0.646	0.009	237.2	266.1	272.3
H4B0N	56	0.006	1.125	1.094	0.004	187.4	267.2	273.8
H4B1S	62	0.013	0.756	0.711	0.010	239.0	262.1	274.0
H4B1N	62	0.011	0.686	0.563	0.008	246.6	261.5	274.0

The following is a discussion of the three types of failure modes encountered during testing: flexural, bond and hybrid. Load-deflection plots for all tests performed are located in Appendix D.

Flexure:

Test L4b0s was the only purely flexural failure with no measurable end slip occurring. Cracking of the section occurred at a load 8 percent lower than that calculated without considering the effects of slab shrinkage (Table 5.5). Shear cracking occurred at 176 kips but did not propagate or attain any significant width. This was expected since shear reinforcement was more than adequate to resist applied shear during loading, even considering the reduction of prestress at the end of the beam due to debonding. Cracking across the transfer zone of fully or debonded strands did not occur nor did a general bond failure. Figure 5.3 shows the actual and calculated load-deflection relationship. A higher load could have been attained but due to difficulties with the hydraulic pump used during testing, no additional load was applied. The beam had reached 99 percent of the calculated capacity without measurable slip, and concrete strains were close to crushing at about 0.0027.

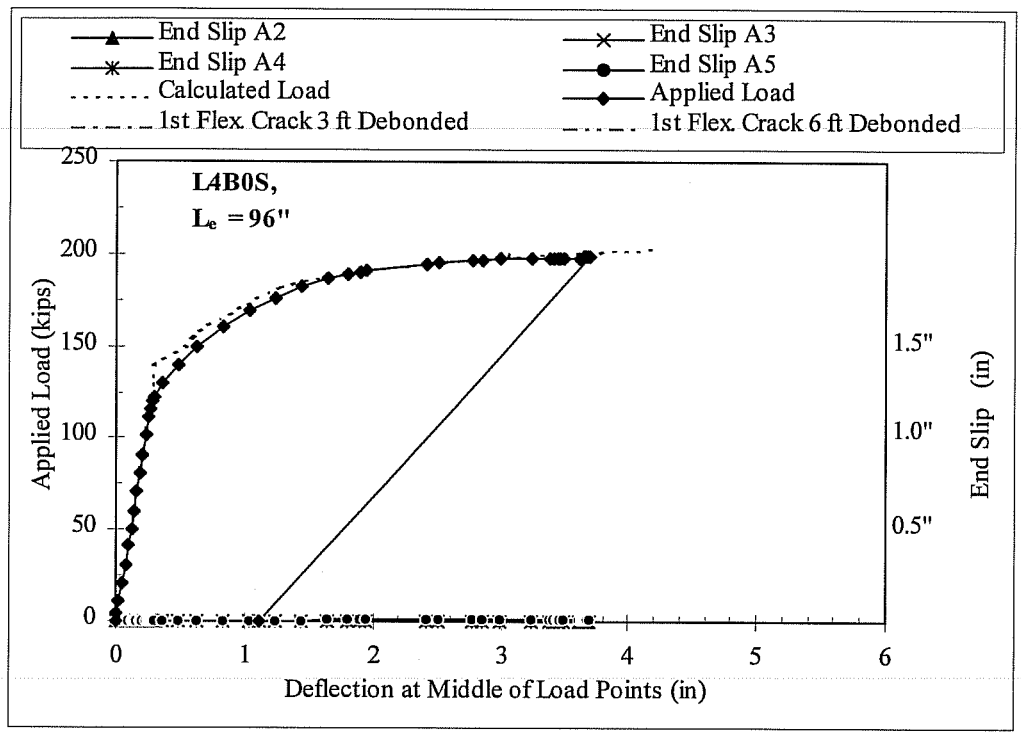

Figure 5.3 Load-Deflection Relationship for Test Beam L4B0S Flexural Failure

Bond Failure

Six of the tests failed in bond at loads that did not reach the predicted ultimate resistance. The embedment lengths were very short compared to the 96 inch development length determined by the ACI expression. They varied from 50 to 58 percent of the calculated development length.

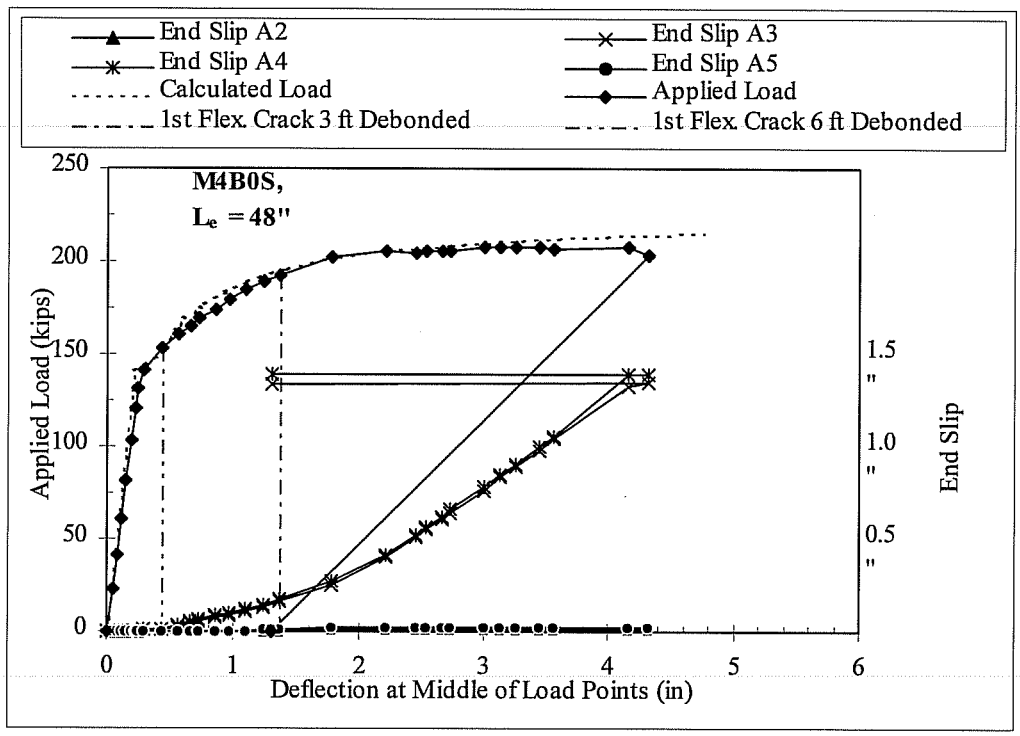

Figure 5.4 Load-Deflection Relationship for Test Beam M4B0S Bond Failure

Test M4b0s had an embedment length of 48 inches which is $.50L_{d,\ ACI}$. The load-deflection curve in Figure 5.4 is typical for the bond failures in this series of beams. Included in Figure 5.4 is the strand slip for all four debonded strands, and the point at which flexural cracking occurred in the transfer zones of the debonded strands.

Flexural cracking first occurred for test M4b0s within the maximum moment region of the span. As flexural cracking occurred through the transfer zone of the 72 inch debonded strands at a load of 154 kips, these strands experienced small end slip on the order of 0.01 inch. Figure 5.4 shows that as the crack formed, end slip began and continued through failure of the beam. For test

beam M4b0s the final end slip for the 72 inch debonded strands was 1.392 inches (from Table 5.7). This initial cracking through the transfer zone resulted in the initiation of bond failure. For test beam M4b0s the final crack width was 0.028 inches (Table 5.8) for the 72 inch debonded strands. Final crack widths through the transfer zone of the 72 inch debonded strands in tests for which a bond failure occurred, ranged from 0.02 to 0.12 inch at the final load at which a general bond failure occurred.

TABLE 5.8
CRACK WIDTHS

Test No.	L_e in	Final Crack Width $L_{db} = 36"$ in	Final Crack Width $L_{db} = 72"$ in	Failure Mode
L4B0N	48	0.013	0.031	Bond
L4B1N	48	0.016	0.039	Bond
L4B1S	60	-	-	Hybrid
L4B0S	96	none	none	Flexure
M4B0S	48	0.006	0.028	Bond
M4B1S	56	0.004	0.016	Bond
M4B1N	56	0.006	0.035	Bond
M4B0N	60	none	0.028	Hybrid
H4B0S	50	0.006	0.118	Bond
H4B0N	56	none	0.039	Hybrid
H4B1S	62	0.012	0.020	Hybrid
H4B1N	62	0.0098	0.0354	Hybrid

If a crack formed in the transfer zone of the 36 inch debonded strands, initial bond slip also occurred, but the crack width did not increase, or increased very little, with additional load. The rate at which these strands slipped was minimal, and final end slip did not exceed 0.08 inches in any of the twelve tests

performed. For test beam M4b0s, the slip was only 0.024 inch (Table 5.7) with L_{db}=36 inches. Even though slip in these strands did occur, a complete bond failure did not since the ultimate capacity of the strand was developed with very small final slips measured. Final crack widths in the transfer zone of all debonded strands are listed in Table 5.8. Crack widths in the transfer zone of 36 inch debonded strands are consistently less than for those in the transfer zone of the strands debonded 72 inches.

In addition to the flexural cracking across strands, longitudinal cracks formed on the bottom of the beam. These cracks formed near the center of the bottom flange in the region of strands A3 and A4, which are the strands debonded 72 inches, shortly after slip had begun. Bond resistance along the flexural bond length is primarily due to mechanical interlocking. Longitudinal cracking was due to radial stresses from the strand acting on the surrounding concrete. This could indicate that the bond mechanism is similar to that of a deformed reinforcing bar. This is a crushing-type resistance against the bar deformations, and in the case of prestressing strand, the surface irregularities formed by the helical twist of individual wires. Figure 5.5 is a photograph of the cracking pattern on the side and bottom of the beam for test M4B0S.

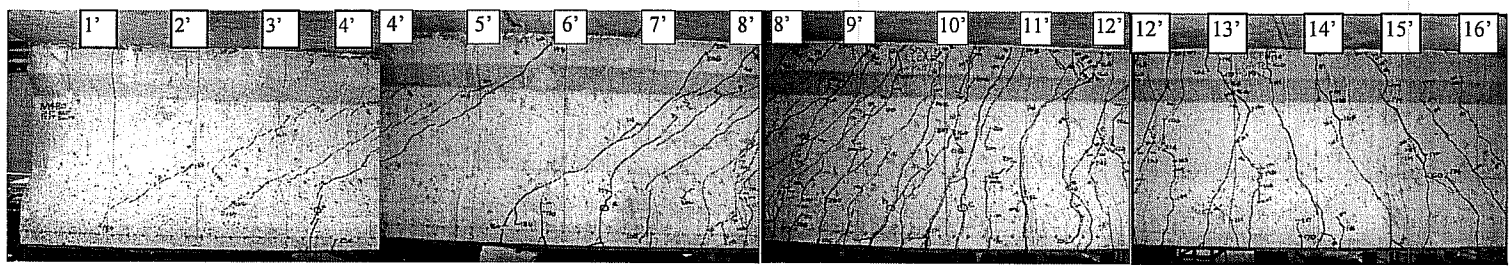

East Face

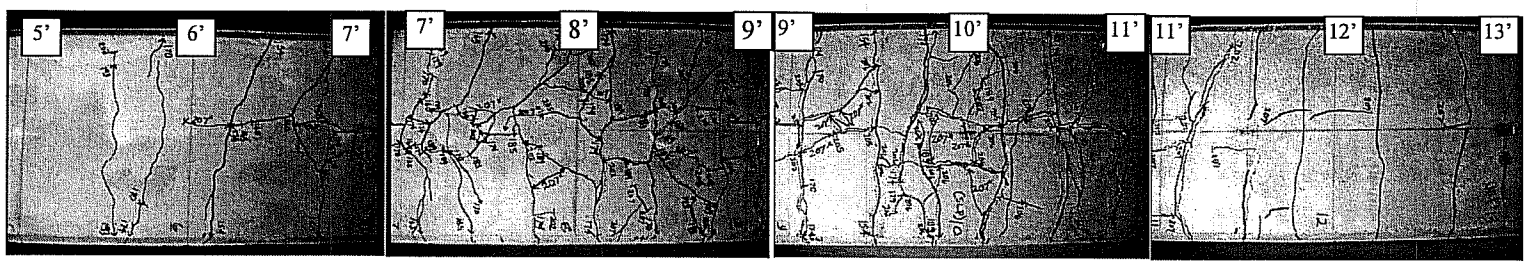

Bottom of Beam

Figure 5.5 Cracking Pattern for Test Number M4B0S.

Hybrid Failure

A hybrid failure occurred in a very similar manner to a bond failure, the primary difference being that the debonded strands which had slipped maintained enough resistance to develop the full calculated flexural capacity of the beam. Table 5.9 shows the test load as a fraction of the calculated ultimate capacity at initial slip (0.01 inch), at a slip of 0.1 inch and at final slip. Here it can be seen that typically, over 80 percent of expected moment had been reached when bond failure initiated. In hybrid failures at a slip of 0.1 inch, which is small, about 91 to 97 percent of capacity had been reached (see Table 5.9) prior to failing in flexure by crushing of the slab or rupture of the strands.

TABLE 5.9
FLEXURAL CAPACITY AT
VARIOUS SLIP INCREMENTS

Test	L_e	0.01	0.1	Final	Failure
		M/M_{ult}	M/M_{ult}	M/M_{ult}	Mode
L4b0n	48	0.71	0.84	0.96	Bond
L4b1n	48	0.63	0.82	0.97	Bond
L4b1s	60	0.75	0.91	1.03	Hybrid
L4b0s	96	-	-	0.99	Flexure
M4b0s	48	0.71	0.86	0.96	Bond
M4b1s	56	0.71	0.85	0.98	Bond
M4b1n	56	0.70	0.85	1.00	Bond
M4b0n	60	0.82	0.97	1.05	Hybrid
H4b0s	50	0.83	0.95	0.99	Bond
H4b0n	56	0.82	0.95	1.02	Hybrid
H4b1s	62	0.83	0.92	1.04	Hybrid
H4b1n	62	0.85	0.92	1.05	Hybrid

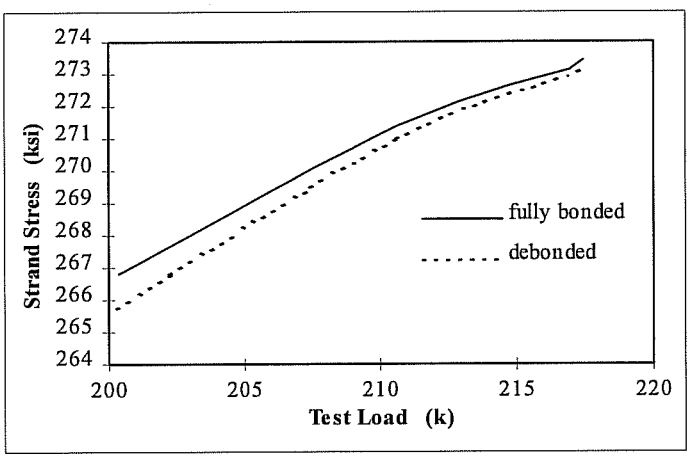

Figure 5.6 Stress in 72 Inch Debonded Strands of Test M4B0N

An interesting failure occurred in test H4b0n in which the flexural failure was reached by rupture of six of the eight prestressing strands. The two strands that did not rupture were A3 and A4, the 72 inch debonded strands, with an ultimate slip of 1.125 and 1.094 inches, respectively. As FOR the previously discussed test, the stress in the debonded strands was very close to the strands that had not slipped, but the strain was significantly different due to the large amount of slip. The remaining six strands exceeded the strain which precipitated rupture (slightly more than 3.5 percent guaranteed ultimate strain) while the debonded strands that had slipped had a strain 0.75 percent less ($[L_{slip}/(L_e + 18)]/2 = .0075$). Figure 5.7 is a photograph of the ruptured strands and strands A3 and A4 which were cut with a torch during destruction of the test beam. Figure 5.8 is a plot of the load-deflection response for the loading test. The large drop in load from 207.5 to 15.5 kips and the increase in deflection by 0.39 inch is the point where strand rupture occurred. Figure 5.9 is a photograph showing the cracking pattern of test H4b0n after the final load had been removed.

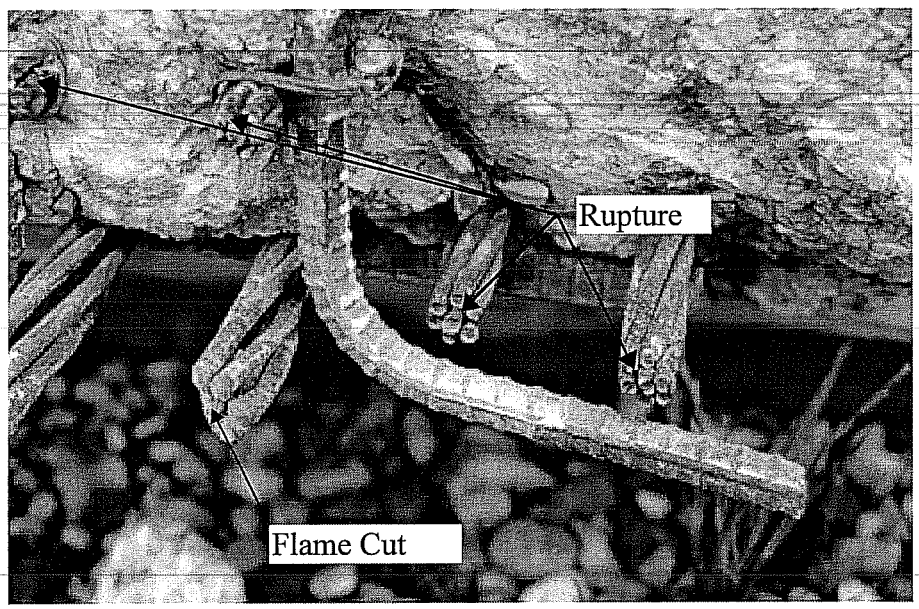

Figure 5.7 Debonded Strands Were Flame Cut While The Remaining Strands Ruptured During Testing of H4b0n.

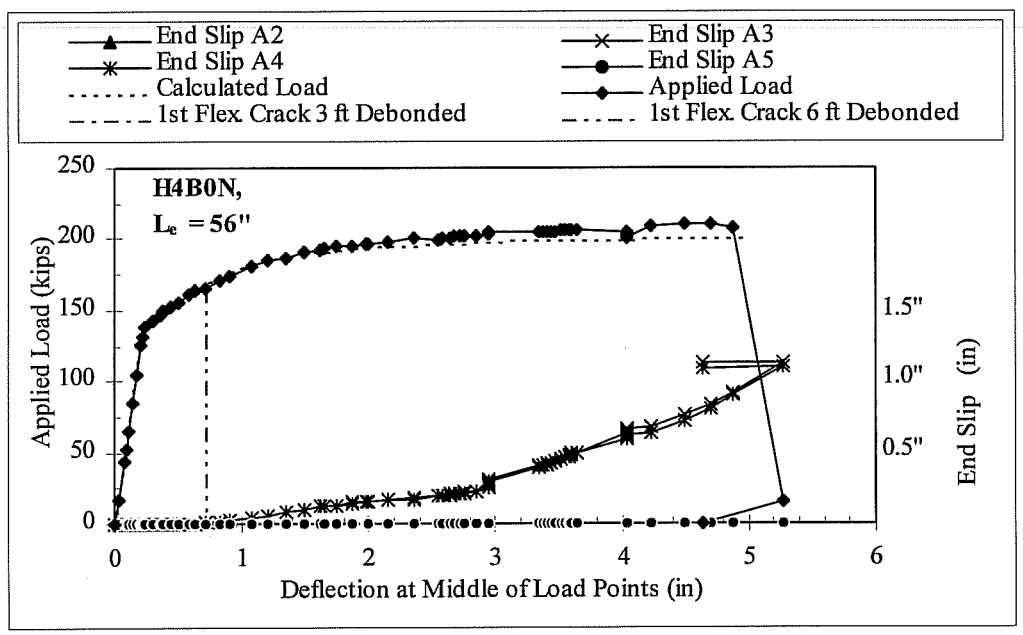

Figure 5.8 Load Deflection Relationship of Test H4B0N, by Rupture of Strands

In hybrid failures, while the actual stress in the strands was very close to those that experienced slip, there was a significant difference in the strain. This could cause an early failure if the strand that slipped did not develop enough stress to resist external loads, leaving the remaining strands to provide load-carrying capacity for the member. This was the case in the tests that were classified as a bond failure, but still the debonded strands developed enough stress to come within 4 percent of calculated capacity of the beam as shown in Table 5.8.

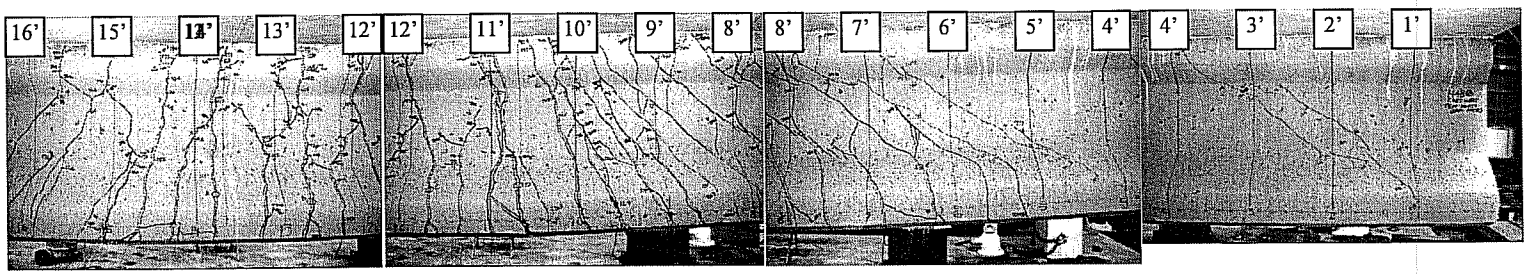

East Face

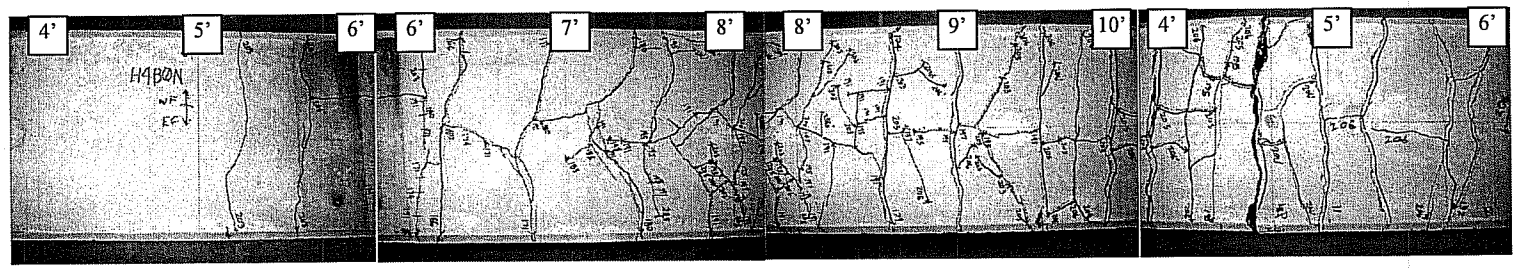

Bottom of Beam

Figure 5.9 Cracking Pattern for Test Number H4B0N.

CHAPTER 6
DISCUSSION OF TEST RESULTS

6.1 Introduction

The following is a discussion of the results presented in Chapter 5. The effects of bond characteristics, concrete strength, time and debonding are the focus of discussion. Details of all data and plots are located in Appendices B, D and E.

6.2 Transfer Length

6.2.1 Quality of Bond

A major factor in determining the transfer and development length of prestressing strand is the bond characteristics of prestressing strand. Many of the factors that affect this quality were discussed in Chapter 2. The strand in this study had a bright surface condition, which would generally produce longer transfer and development lengths.

In a recent study[12], pull-out tests were investigated as a method to indicate the bonding characteristics of prestressing strand and more accurately predict transfer and development lengths. In the research summarized by Logan[12], tests were performed on 1/2 inch diameter strand placed in a standard pull-out block based on the Moustafa method[22]. Strand that resisted a force equal to 235 ksi (36

kips) of stress before pulling out of the concrete, performed well in transfer and development length tests. When surface conditions were such that a resistance of 78 ksi (12 kips) or less was reached in the strand, performance was considerably less desirable. Bond slip failure was observed in test beams using this same strand in transfer length measurements and development length tests.

The focus of this project is on 0.6 inch diameter strand, but when compared to the acceptable stresses produced in the Logan[12] paper, a qualitative comparison can be made. Pull-out tests were performed for each pair of beams tested, with the full results listed in Appendix E and summarized in Table 6.1. The results from these tests for the low and medium strength concrete designs were well above the 235 ksi or $0.87f_{pu}$ and the transfer lengths reflect good bond behavior.

TABLE 6.1
SUMMARY OF
PULL-OUT TEST RESULTS

Concrete Strength	Average Stress @ Failure (ksi)	Percent f_{pu}	L_t after trans. in
Low	244	90%	17.5
Medium	285	106%	15.2
High	180	67%	15.4
235 ksi /f_{pu} =		87%	
78 ksi /f_{pu} =		29%	

The high strength concrete pull-out tests did not resist above $0.87f_{pu}$ but still produced transfer lengths in beams made with this concrete approximately equal to transfer lengths for the medium strength concrete beams as shown in

Table 6.1. Behavior of strand with a pull-out resistance between $0.87f_{pu}$ $0.29f_{pu}$ was not defined, but here strand with a resistance of $0.67f_{pu}$ performed well. This pull-out test resistance is still well above the $0.29f_{pu}$ value that indicated poor performance in the tests by Logan[12]. It should be noted that in the pull-out block for the high strength concrete, considerable temperature and shrinkage cracking had occurred around the embedded strand which might have contributed to the inferior pull-out test results. The average transfer lengths for all series of beams (15.2 to 17.5 inches) were very short compared to other studies and the ACI/AASHTO equation which is approximately 32 inches. This would indicate that even though the strand condition is considered bright, it has very good bond characteristics.

6.2.2 Effect of Concrete Strength

Several studies have looked at the influence concrete strength has on transfer and development length[9, 23, 25], all of which indicate that shorter transfer lengths are produced in beams with higher concrete strength. For both methods used to determine the transfer length (95 % Plateau and Slope Intercept Methods), the medium and high strength concrete designs (which were very close in actual strength) produced shorter transfer lengths than the low strength concrete specimens. As is common with transfer data, there is a large degree of scatter. To present the results in a more meaningful manner, it is beneficial to show the results statistically. Tables 6.2 and 6.3 show average transfer lengths and the standard deviation which indicates the degree of scatter. Data is separated into the different concrete strength ranges, low, medium and high.

Figures 6.1 and 6.2 are plots of the cumulative distributions of the data in Tables 6.2 and 6.3 immediately after transfer of prestress. The cumulative distribution for a measurement gives the percentage of values that would be lower than that measurement. As an example one of the low strength concrete measured transfer lengths was 22.4 inches using the slope intercept method and the cumulative distribution is 0.90. This means that this value is greater than 90 percent of transfer lengths measured in this data set, based on the average and standard deviation for this set of data.

TABLE 6.2
AVERAGE TRANSFER LENGTHS (IN.)
95 % PLATEAU METHOD

Average Concrete Strength		Imm. After Transfer		After Deck Placement	
Design	ksi	Lt in.	Std Deviation	Lt in.	Std Deviation
Low	6.2	16.0	4.26	17.0	4.67
Medium	10.4	13.1	1.70	13.2	2.06
High	11.4	13.6	1.38	13.7	2.68

TABLE 6.3
AVERAGE TRANSFER LENGTHS (IN.)
SLOPE-INTERCEPT METHOD

Concrete Strength		Imm. After Transfer		After Deck Placement	
Design	ksi	Lt in.	Std Deviation	Lt in.	Std Deviation
Low	6.2	17.5	3.77	20.1	4.04
Medium	10.4	15.2	1.55	15.1	1.54
High	11.4	15.4	2.77	15.5	2.43

The low strength concrete design had a higher degree of scatter which is also reflected in Figures 6.1 and 6.2 by the flatter curve (i.e. a higher standard deviation). Results for the medium and high strength concrete were very similar as were their actual strengths.

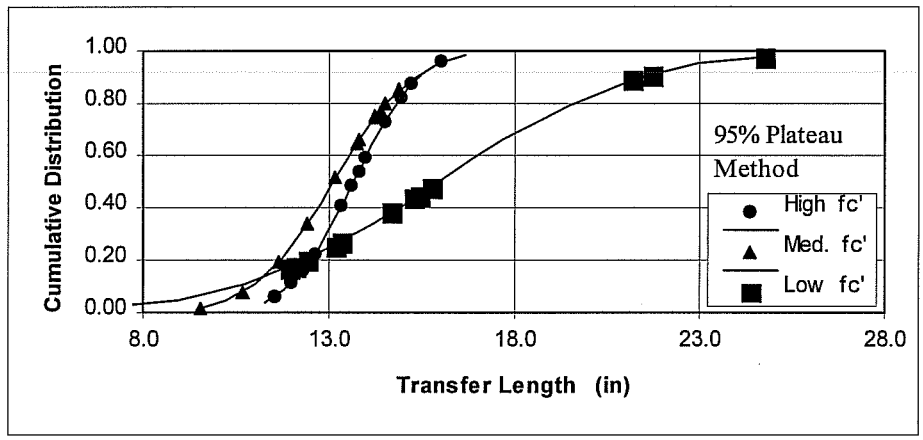

Figure 6.1 Cumulative Distribution of Transfer Data Using the 95% Plateau Method

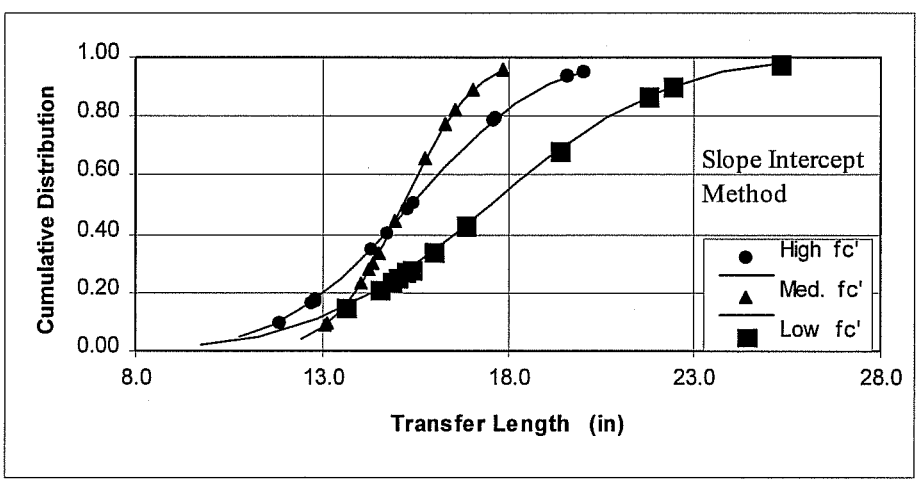

Figure 6.2 Cumulative Distribution of Transfer Data Using the Slope-Intercept Method

Table 6.4 shows transfer lengths as calculated by various researchers whose equations included the effects of concrete strength, compared with those produced in this study. Most transfer lengths calculated in Table 6.4 are greater

than lengths measured as indicated by the cumulative distribution shown. Those proposed by Zia et. al.[25] give results closest to the average of those measured in this study. As previously noted, the Zia expression from Reference 25 is probably a better representation of values for strand with excellent bonding characteristics and not the average of all strand produced with the wide range of surface conditions found.

TABLE 6.4
COMPARISON OF TRANSFER LENGTH (in)
EQUATIONS WITH
CONCRETE STRENGTH AS A VARIABLE

Concrete Strength	Measured *L_t	Zia, et al[25]	Cumulative Distribution	Cousins, et al[5]	Cumulative Distribution	Mitchell et al[23]	Cumulative Distribution
Low	17.5	30.5	1.00	43.1	1.00	29.7	1.00
Medium	15.2	14.9	0.43	33.9	1.00	22.1	1.00
High	15.4	13.3	0.22	32.5	1.00	21.2	0.98

* Results from all data using the slope intercept method.
Lt = 32 in. (ACI).

Transfer lengths measured in this study are shorter than those predicted by ACI/AASHTO indicating that the bond characteristics were very good. End slips measured at transfer of prestress and before testing of development length also indicated this. End slip measurements are located in Appendix D. By the above figures it was demonstrated that the prestressing strand in the medium and high strength concrete beams had shorter transfer lengths than the low strength beams. Concrete strength had a definite impact on the transfer length which was reduced with an increase in concrete strength.

6.2.3 Effect of Time

Tables 6.2 and 6.3 also indicate that for medium and high strength concrete, there was little change in the transfer length over the short period of time between measurements (60 to 115 days). The low strength concrete did show some increase which was more significant when the Slope-Intercept Method was used. Figure 6.3 is a cumulative distribution plot of transfer lengths for the medium strength beams before and after deck placement for both methods of measurement. The slope-intercept method had less scatter when measurements were compared with respect to time but for both methods the after-deck-placement measurements generally followed the before-deck measurements Plots of this data for the other concrete beams are located in Appendix B.

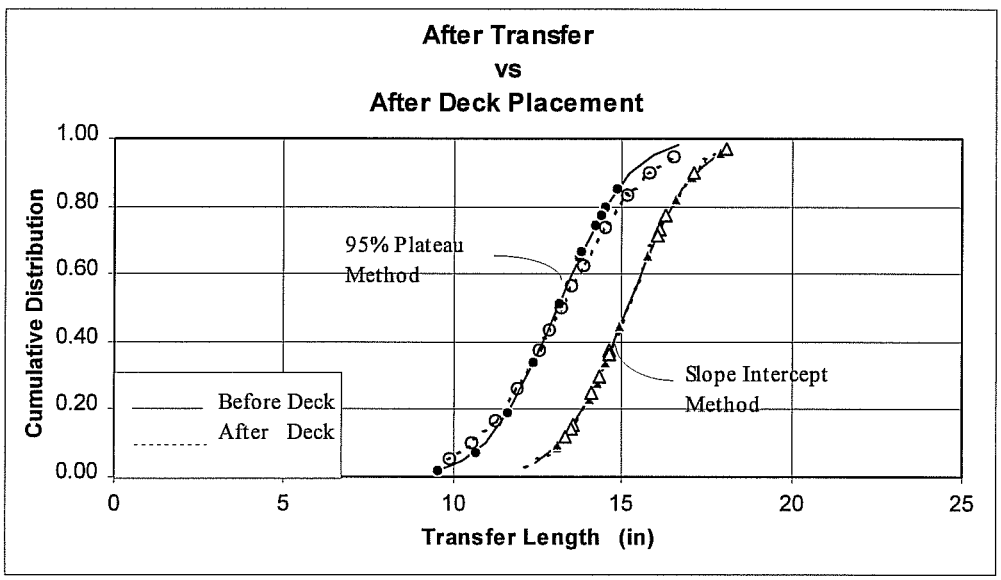

Figure 6.3 Effect of Time on Transfer Length

6.2.4 Effect of Debonding

Another consideration was the differences between fully-bonded and debonded strands. In Tables 6.5 and 6.6 the data shown are for measurements taken immediately after transfer for both methods used to determine the transfer length. Here the fully-bonded strands for both methods are practically identical given the degree of scatter. The biggest difference is exhibited in the fully bonded versus debonded strands. The Slope-Intercept method generally produces transfer lengths for debonded strands that are longer than those produced by using the 95% Plateau Method.

TABLE 6.5
AVERAGE TRANSFER LENGTHS
95 % PLATEAU METHOD

Average Concrete Strength		Fully Bonded		Debonded	
		Lt	Std	Lt	Std
Class	ksi	in.	Deviation	in.	Deviation
Low	6.2	18.5	3.45	14.7	4.24
Medium	10.4	13.9	0.97	12.7	1.91
High	11.4	13.1	1.27	13.9	1.41

TABLE 6.6
AVERAGE TRANSFER LENGTHS
SLOPE-INTERCEPT METHOD

Average Concrete Strength		Fully Bonded		Debonded	
		Lt	Std	Lt	Std
Class	ksi	in.	Deviation	in.	Deviation
Low	6.2	18.6	4.03	17.0	3.79
Medium	10.4	14.0	0.64	15.7	1.56
High	11.4	12.5	0.48	16.8	2.22

In C. D. Buckner's[11] discussion of transfer length measurement, the benefits of using the 95% Plateau Method were that it indirectly compensated for gauge length, three point smoothing and shear lag. These three items are reported to be responsible for the curvature found in the plot of strain readings when the data points transition from the transfer region to the strain plateau. In Dr. Buckner's discussion the 95% plateau intersected the plot in the curved portion thereby indirectly including these three effects. When looking at the debonded data this was not often the case as can be seen in the example shown in the previous chapter in Figure 5.1 and Appendix B. This is demonstrated graphically in Figure 6.4.

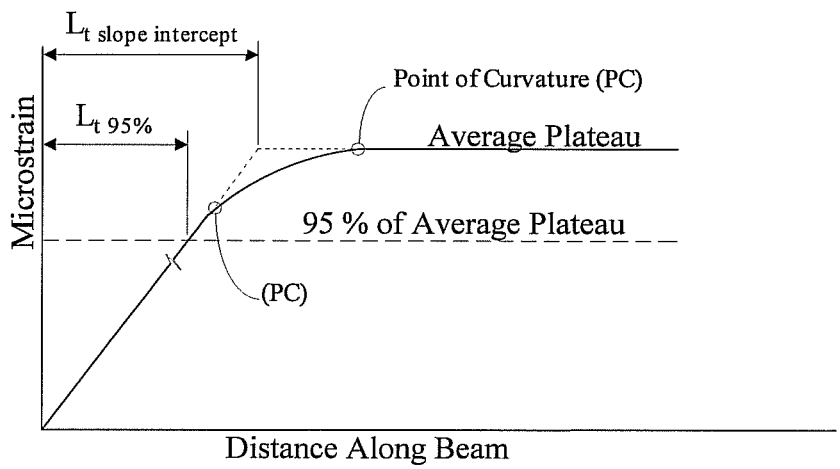

Figure 6.4 Typical Intersection of 95 % Plateau for Debonded Strands

The 95 % plateau intersection (see Figure 6.4) would produce a transfer length that is not conservative as implied by Buckner. The Slope Intercept Method provided lengths that were about 16 to 24 percent longer and had a lower standard deviation in most cases. From the results of this study, the slope-intercept method seemed to provide more consistent and conservative transfer lengths for debonded

strands. This would imply that transfer lengths in debonded strands for this series of test beams were slightly longer than those for fully bonded strands.

In determining transfer lengths from concrete strains in debonded strands, these results would be affected by the method of determining the 95 percent plateau. If 95 percent of the strain difference between plateaus were taken instead of the total strain for a given prestress in a region of the beam, the 95 percent plateau as shown in Figure 6.4 would be higher than the one shown. The intersection of the curve would be higher and therefore the transfer length would be longer. These results could be more similar to the results produced by the slope-intercept method. As pointed out by C. D. Buckner[11], this is part of the reason for the variability of data from different studies. Different interpretations of transfer length by different researchers adds to scatter in transfer lengths when all data is compared collectively.

Figure 6.5 is a plot of cumulative distribution vs. transfer length for fully-bonded and debonded strands for medium strength concrete beams as an example. The transfer length values for the slope-intercept method for debonded strands are greater than the values found using the 95 % plateau method. This is shown numerically in Tables 6.5 and 6.6. Plots for the remaining beams are located in Appendix B. Again, the transfer lengths are shorter than the ACI code in all cases.

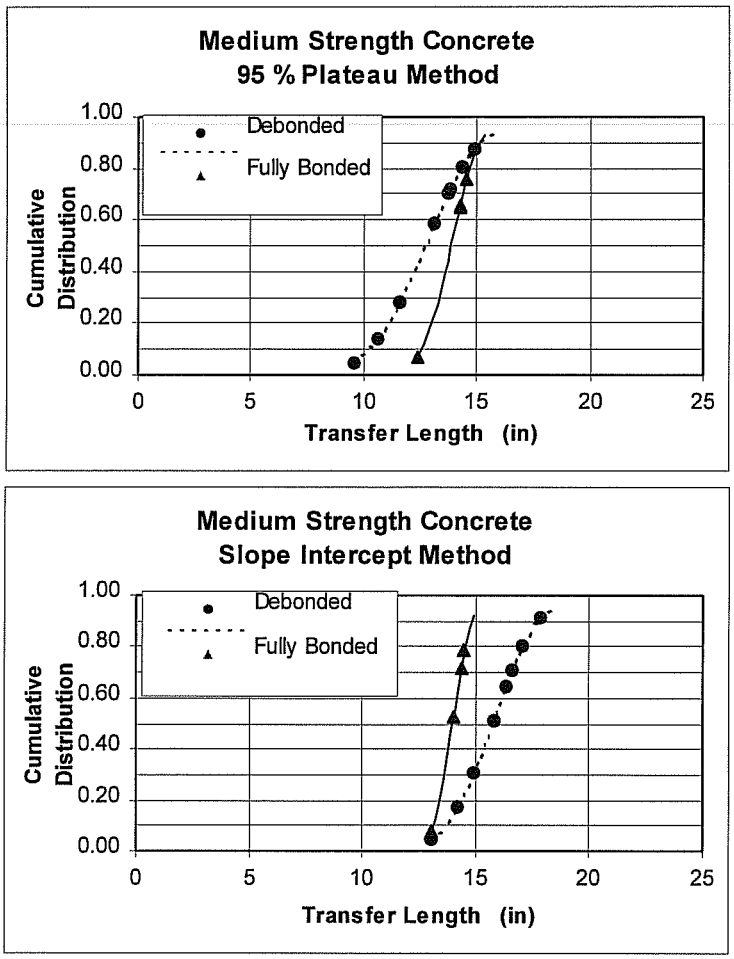

Figure 6.5 Fully Bonded vs. Debonded Transfer Lengths

6.3 Development Length

6.3.1 Quality of Bond

As mentioned in the discussion above of transfer length, pullout tests indicated that the bonding characteristics of the strand used in this project were very good. This is reaffirmed in development length tests performed on various embedment lengths. Three tests were performed with embedment lengths that were 50 percent of the 96 inch value calculated by the ACI and AASHTO

At a slip of only 0.1 inch, the stress in the debonded strands at the critical section was practically identical to the stress in the fully-bonded strands. This is because the level of strain in the strand was in the plateau region of the stress-strain curve for prestressing steel. Figure 5.6 shows the difference in stress between fully-bonded and debonded strands versus the applied load after a slip of 0.1 inches had been reached in test M4b0n. Even though debonded strands continue to slip they also developed additional stress as the beam continued to pick up load until crushing occurred in the slab. Ultimate slip at failure was 0.53 inches in strand A4 for test M4B0N.

A conservative approximation was used in calculating the steel strain resulting from slip shown in Figure 5.6, since we do not know at what point along the beam the strand stops slipping. As can be seen in Table 5.9, 97 percent of calculated capacity in test M4b0n had been developed when a slip of 0.1 inches had been reached in this test. Ultimately the failure load exceeded the calculated capacity by 5 percent. The debonded strands had developed a level of strain that provided a resistance very close to ultimate capacity for test M4b0n.

development length equation. While they ultimately failed in bond, over 96 percent of the beam capacity was developed. Bond between concrete and strand surface for debonded strands was adequate to develop the tensile capacity of the strands even though large slips occurred. Figure 6.6 is a summary of the capacities test beams reached before failure as a ratio of the calculated capacity.

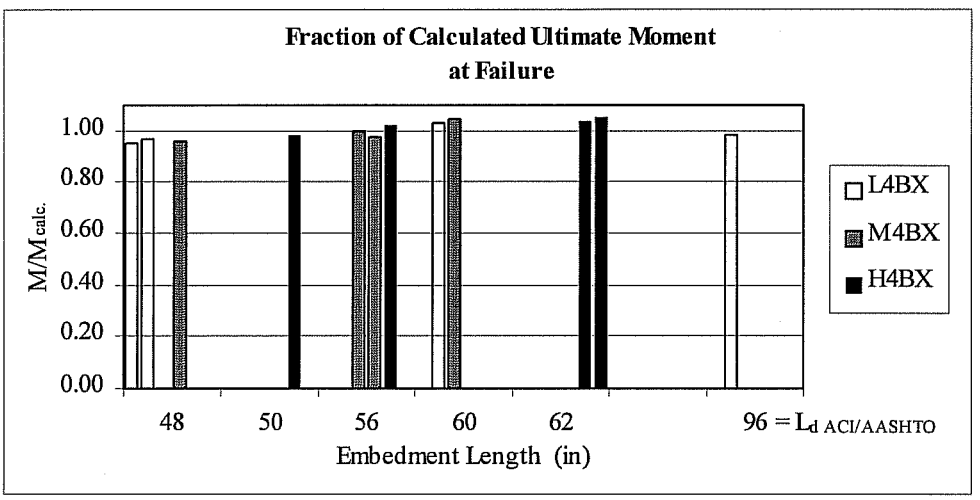

Figure 6.6 Embedment Length Test Results
Percent Moment Attained

According to a theory by Robert Mast[12], the flexural bond length of a beam is proportional to the factors that affect end slip at transfer (L_t). He provided the relationship listed in Table 6.7 between end slip at transfer and the calculated development length by ACI/AASHTO. Strand end slips measured at transfer in this study are, in most cases, less than 0.09 inches, which indicates that development lengths will be less than that calculated by the code equation, which is consistent with Mast's theory. Embedment lengths tested which reached a flexural failure in this study were significantly shorter than the code equation. This theory predicted that the bond characteristics for transfer and development

lengths would be good for this strand, as did the data from pull-out tests. End slip measurements at the time of transfer are summarized in Appendix E and are compared to measured transfer length as determined by the slope-intercept method.

TABLE 6.5 MAST'S THEORY	
Magnitude of Slip	$\frac{L_{d\ Actual}}{L_{d\ ACI}}$
< .09	< 1
= .09	= 1
> .09	> 1

Tests that were classified as a hybrid failure reached or exceeded the calculated flexural capacity while undergoing large slips in the 72 inch debonded strands. These slips created a significant difference in strain between the debonded and fully bonded strand at the point of failure for the beams. Due to the fact that the magnitude of these strains were in the plateau region of the stress-strain curve for prestressing strand, the stress variation was not significant. Thus, the prestressing force was maintained and therefore almost full flexural capacity was preserved. Test H4b0n failed in flexure by rupturing six of the eight strands. The six foot debonded strands did not rupture because the strain was much less due to the magnitude of slip which had occurred in these strands. Still the capacity was not compromised.

Compared to other research performed, these results are indicative of strand with very good bond characteristics. It is clear that due to the wide range of results from other research, that the surface conditions of strand from different fabricators vary widely which significantly adds to the scatter in the existing data

base. Another important factor that did not occur in this study is contamination of the strand during fabrication of the beam which can harm bond capacity, as noted by Russell and Burns[13].

6.3.2 Flexural Bond Length

Development length is not measured directly, as is transfer length, and is not as easily defined. To better understand behavior of anchorage in a pretensioned beam, it is beneficial to consider the flexural bond length (L_{fb}). From the final capacities reached, as shown in Figure 6.6, all tests performed very well and it is difficult to draw definite conclusions. Figure 6.7, reproduced from a report by the Federal Highway Administration (FHWA)[11], summarizes results of flexural bond length from the study by Hanson and Kaar[8]. This information from Reference 11 was used by ACI Committee 323 in establishing the current development length equation.

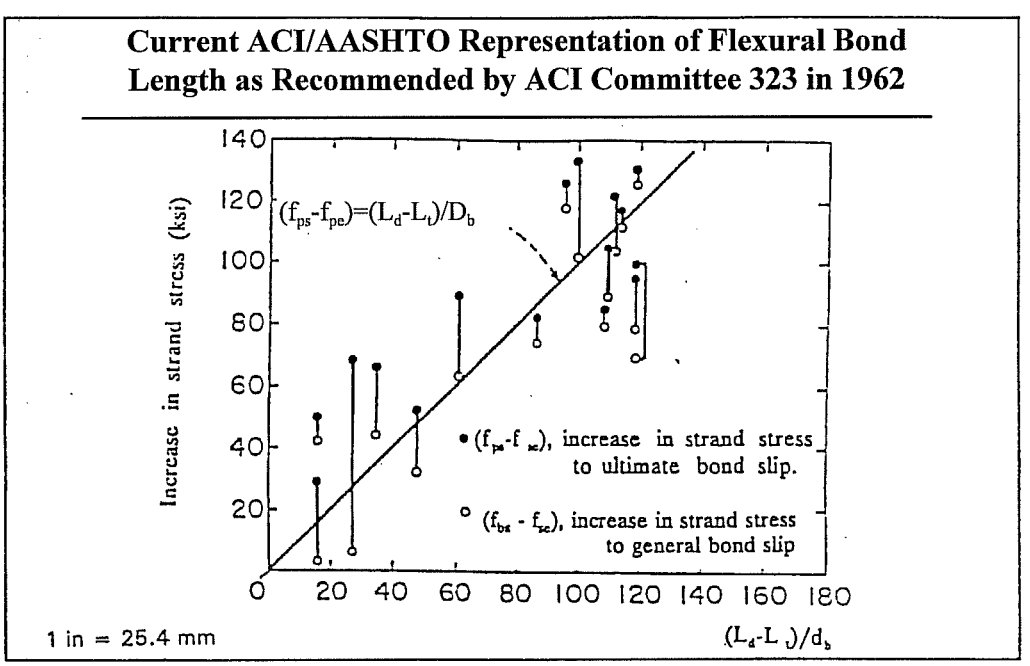

Figure 6.7 Results from Hanson and Kaar

For the data presented in Chapter 5, a plot similar to that of Figure 6.7 may be made of the flexural bond length divided by the strand diameter for data taken in the present study. Strand stress was estimated by using the previously described strain compatibility model to analyze the section at an applied load, and was not measured directly. While this is not exact, it does give a good representation of the behavior, as the model followed the test load versus deflection response very closely. Figure 6.8 includes data from the 36 inch debonded strands and the 72 inch debonded strands. The 36 inch debonded strands have an embedment length 36 inches longer than the 72 inch debonded strands located in the same test as shown in Figure 4.5. Figure 6.8 also includes the line representing the code equation for L_{fb} currently used in design. Also shown are lines which represent the equations developed by C. D. Buckner[11], which doubles the required flexural bond length, and by Zia and Mostafa[26], which increased this length by 25 percent. The intermediate point of 0.1 inch slip is shown to indicate the magnitude of slip which would occur for a stress increase as predicted by equations plotted on the graph for the given flexural bond lengths.

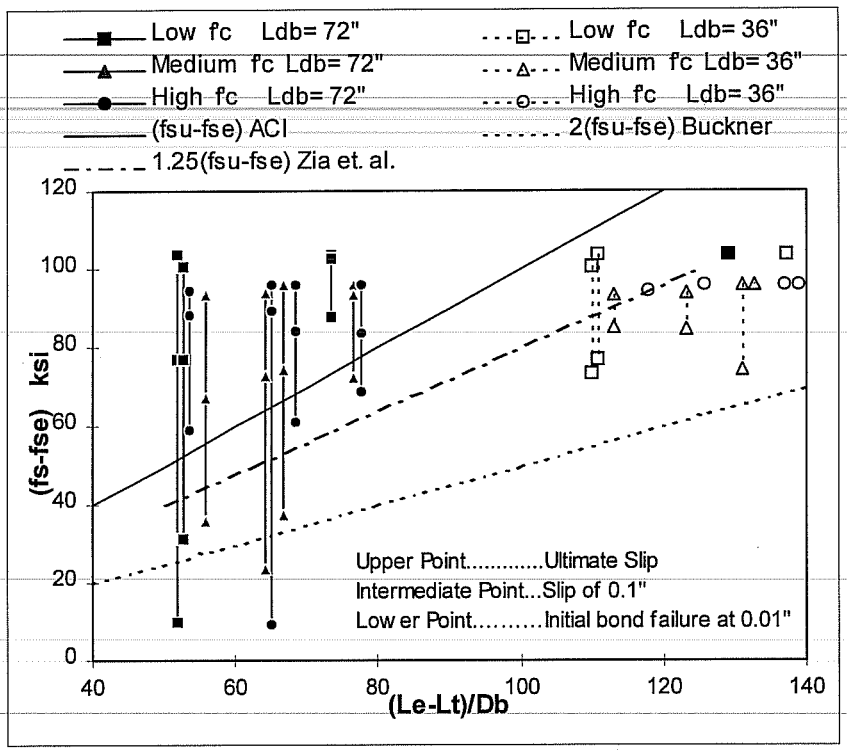

Figure 6.8 Flexural Bond Length from Test Results

For the strand tested in this project, Figure 6.8 demonstrates that the ACI equation would estimate a development length in which minimal slip would occur. Slip is less than 0.1 inches at the calculated stress increase over the effective prestress (f_{se}). In other words the line representing the ACI equation passes through the plot of the data at a point where the strand had slipped less than 0.1 inches for the strands that had been debonded 72 inches.

In C. D. Buckner's discussion of the ACI equation, he notes that in the Hanson Kaar data at (L_e-L_t) greater than $80D_b$ the equation was not conservative. In Figure 6.7 there is no indication of the slips that were reached in Hanson and Kaar's data with flexural bond lengths above $80d_b$. Slips shown in data from the

present study with a flexural bond length greater than $80d_b$ (i.e. strands debonded 36 inches) were between 0.0 and 0.1 inches when slip occurred after the ultimate tensile capacity of the strand had been reached. Figure 6.9 shows the low concrete strength test data with the ultimate slip noted for each test, and plots for the remaining concrete strength groups are located in Appendix D. For the 36 inch debonded strands the capacity of the strand was exceeded in the beam test so the fact that the ultimate slip is below the ACI line is not significant. Note that since only very small or no slip occurred, the stress level in the strand was essentially unaffected.

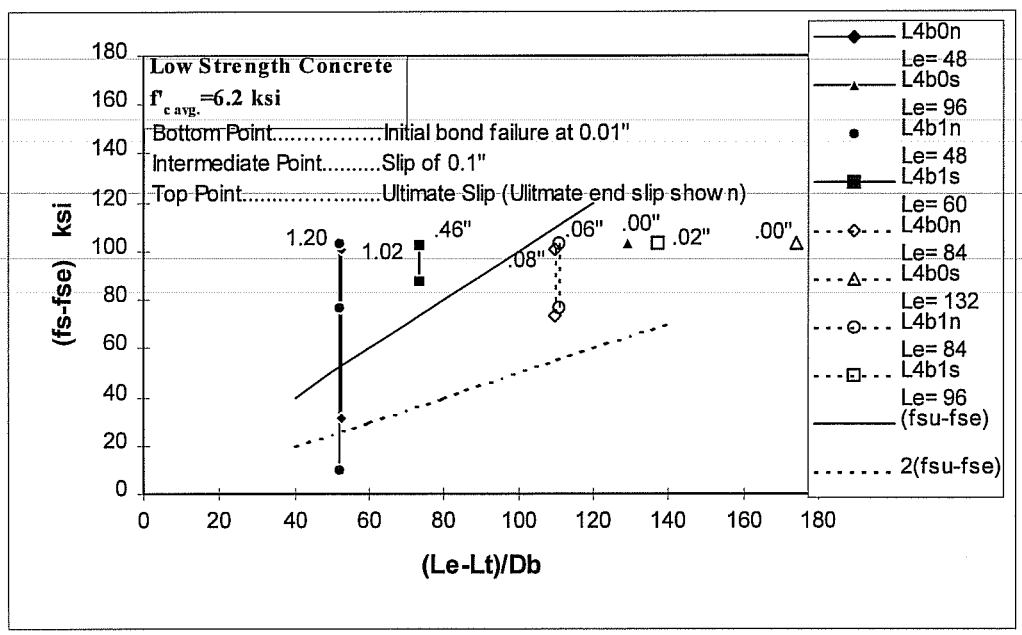

Figure 6.9 Flexural Bond Length from Low Strength Concrete Test Results

Strand slip does not increase linearly with an increase in strand stress. Figure 6.10 is a plot of strand stress versus slip for test L4b0n with the ultimate stress back-calculated from the ACI/AASHTO equation for flexural bond length ($f_{su}=\{L_e-L_t\}/d_b+f_{se}$). Here this calculated ultimate stress is for comparison only. It

shows that, for a flexural bond length of 48 inches with very good bonding characteristics as has been demonstrated for this strand, an ultimate stress of about 223 ksi would be allowed. The slip at this stress level is approximately 0.02 for test L4b0n which would be acceptable if the beam were designed to fail with the strand having a design ultimate strength of 223 ksi. Plots of stress versus slip for the remaining tests are located in Appendix D. In the Hanson and Kaar data (Figure 6.7) this information is not presented but it is possible the capacity of the strand had been exceeded with minimal slips occurring, which is the case in this study.

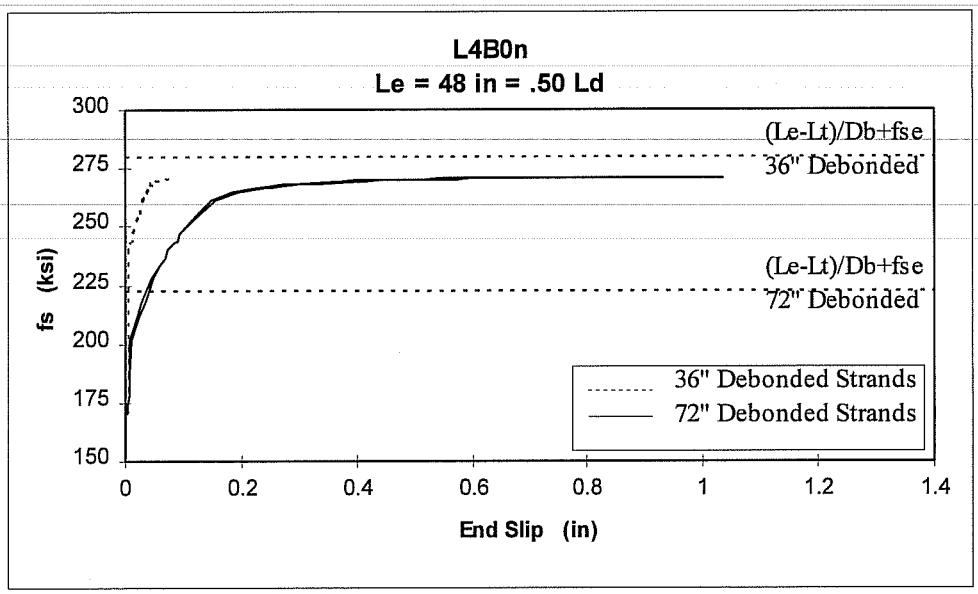

Figure 6.10 Strand Stress vs. Slip for Test L4b0n

6.3.3 Effect of Concrete Strength

The impact that concrete strength has on development length is not as apparent as in the measurement of transfer length. Figure 6.8 shows that the flexural bond length is affected to some degree by concrete strength. In general

the initial bond failure occurred at a lower strand stress for the low strength concrete than for the medium and high strength designs. Table 6.8 shows the results of three different equations developed by various researchers[5, 23, 25] that have concrete strength as a variable.

TABLE 6.8
COMPARISON OF L_d (IN)
EQUATIONS WITH CONCRETE
STRENGTH AS A VARIABLE

Average Concrete Strength		Zia,	Cousins,	Mitchell
Class	ksi	et al[25]	et al[5]	et al[23]
Low	6.2	109	158	83
Medium	10.4	88	117	60
High	11.4	86	112	58

*Results from all data using transfer lengths from the slope intercept method.
The following variables were used in the Zia et. al. equation

Ut'= 6.7 $L_{d\ ACI}$= 96"
Ud'= 1.32
B= 300 psi/in

Included in Figure 6.8 is a plot of the equation for flexural bond by Zia and Mostafa, which is not a function of concrete strength but increased the ACI length by 25 percent. It is fairly conservative for flexural bond length, but when combined with the transfer length, which is dependent on concrete strength, it produces a development length that appears conservative but not excessive. For the low strength concrete the result is greater than 96 inches as calculated by the ACI equation. For this data, a purely flexural failure was attained at an embedment length of 96 inches, so that the 109 inch length by Zia et. al. would be conservative.

Tests H4B1S and H4B1N, which had an embedment length of 62 inches, experienced a hybrid failure so that while failing in flexure, some slip did occur. The results of the Zia recommendation seems to be adequate for design since the beams reached a capacity 4 to 5 percent greater than that predicted. At 92 percent of calculated moment capacity of the test beam, the 72 inch debonded strands (62 inch embedment) had slipped only 0.1 inches.

The equation by Mitchell, Cook, Khan, and Tham did a good job of producing lengths that were equal to embedment lengths where hybrid failures took place. While these embedment lengths were adequate to reach a flexural failure, it would be more appropriate to use a conservative value for design. Strand in this study demonstrated that it has very good bonding characteristics, but strand provided by different manufacturers, due to variations in processes performed during production, has proven to vary widely in quality of surface conditions. So while the equation proposed by Mitchell et. al. predicted a flexural failure, considerable slip did occur at ultimate load, and other strand might not perform as well.

6.3.3 Effect of Debonding

The anchorage zone of debonded strands is subjected to different loads compared to that of fully-bonded strands located at the end of a beam. At the center line of bearing at the end of a beam, the moment is zero and increases to some value at the end of the anchorage zone. In the anchorage zone of a debonded strand the moment is not zero but is a function of the applied load. Also, there is no bearing pressure on a debonded strand, which has been shown to

improve anchorage due to the resulting pressure. Strand that is debonded is subjected to greater sectional forces which affect the anchorage. Russell and Burns stated that transfer and development lengths are a function of load geometry. Most researchers address development length by estimating safe transfer and flexural bond stresses. As shown in their research and verified in this test program, a crack across the transfer zone initiates bond failure. Russell and Burns approach the matter of development length by controlling the cracking moment in the transfer region of a strand.

In several of the beams tested a crack formed in the transfer region of the 36 inch debonded strands. While this caused an initial slip, the flexural bond stresses were able to provide enough resistance so that the strand did not move much beyond the initial slip and the total slip remained well below 0.1 inches. Strands that were debonded 72 inches had cracking occur in their transfer zone in all beams except the purely flexural failure. The strands in tests that underwent a hybrid failure still developed the ultimate capacity of the strand even though some slip occurred. While a crack may have passed through the transfer zone of a strand, if enough flexural bond length existed, the slip was resisted at an adequate level where the beam could develop its full calculated capacity.

See Appendix D for plots of load-deflection responses for all tests performed. In these figures the initial crack in the 72 inch debonded strands is plotted and it can be seen that the initial strand slip occurred at this point, and continued at varying rates, depending on the embedment length and concrete strength.

Two studies[3, 18] reviewed in Chapter 3 applied a test load in order to simulate the parabolic curve of the moment envelope of a highway loading. The remaining studies used a loading geometry such that the moment diagram was linear as was the case for the load in this test program. The parabolic shape increases the capacity demands in the portion of the beam where anchorage of the strand is being developed, having a greater impact than a linear moment diagram. An envelope of moments can be made as a plot of all loads that will produce the maximum moment at any section along a girder. A girder would not be subjected to all of these moments at one time from a single load. While an envelope is probably an overly conservative approach, providing a parabolic moment diagram, it is a good method to test the effect that loading geometry has on development length. In the Load and Resistance Factor Design (LRFD) the HL93 loading includes a lane load with the design vehicle, an HS20 or tandem truck. The effect of the lane load would make the moment diagram more parabolic, and the effect would be amplified in longer spans.

Figure 6.11 shows the moment envelope, and the controlling HL93 loading at a distance of .15L away from the center of the span. This 125 foot span is relatively long for a pretensioned concrete girder, giving the lane and dead loads a larger impact on the moment diagram and making it more parabolic in shape than would occur in a short span. It can be seen that for an extreme case of the critical section being .15L distance away from the center of the beam, a parabolic shape results and can be compared to the tangent section shown in Figure 6.11. As a critical section moves closer to the end of the beam, this curve flattens out and more closely resembles a linear moment diagram in the anchorage region of the beam. The two studies mentioned by Kaar and Magura[3] and Rabbat

et. al.[18] were on the conservative side, and slips were small when the bond failure occurred due to flexure.

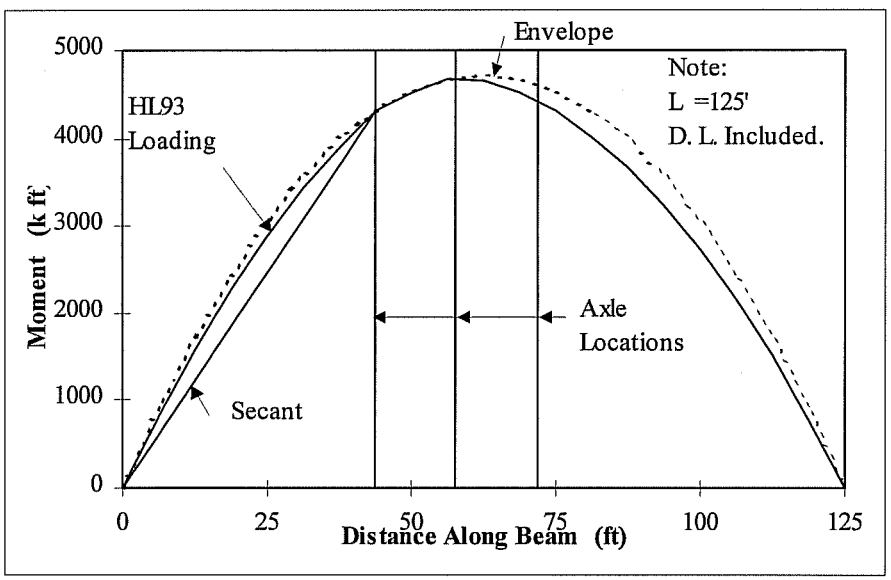

Figure 6.11 HL-93 Moment Envelope (LRFD)

Tests performed by Russell and Burns showed that during fatigue loading, slips that occurred due to overloads, stabilized and did not slip further under repeated loads. Tests that experienced a hybrid failure were able to reach loads over 92 percent of capacity before slip increased above 0.1 inch. As shown in Figure 6.12, 72 inch debonded strand performed very well, even in tests where the embedment length was 50 percent of calculated development length by ACI/AASHTO. The average cracking moments for the low, medium and high strength concrete beams are, 59, 62 and 70 percent of the calculated ultimate strength respectively. These first cracking moments are considerably lower than the 92 percent of calculated ultimate resistance before 0.1 inch of slip occurred.

The beams that had a hybrid failure would therefore perform well for overloads less than 92 percent of the ultimate capacity.

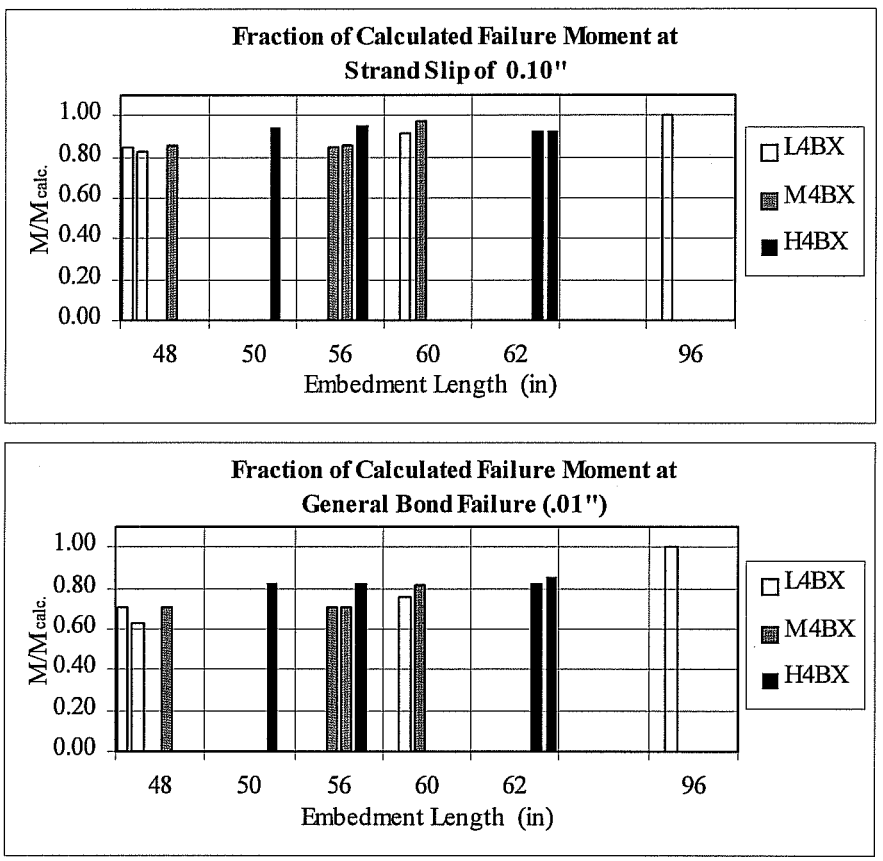

Figure 6.12 Applied Moment at 0.01 and 0.10 Inches of Slip

Hybrid failures for the medium and high strength concrete beams did not exhibit a general bond failure until 82 to 85 percent of the ultimate load was reached. Strand in the low strength concrete beams initially slipped at about 75 percent of ultimate. In service the beam would have to exceed the cracking moment by 12 to 20 percent of the ultimate capacity in order to produce an initial bond failure at 0.01 inch of slip and 22 to 30 percent to produce 0.1 inches of slip.

While ultimately the hybrid failures had significant slip, it did not occur until a major portion of the capacity had been developed. This data is summarized in Table 6.9.

TABLE 6.9
FLEXURAL CAPACITY AT
VARIOUS SLIP INCREMENTS

Test	L_e	0.01	0.1	Final	Failure
		M/M_{ult}	M/M_{ult}	M/M_{ult}	Mode
L4b0n	48	0.71	0.84	0.96	Bond
L4b1n	48	0.63	0.82	0.97	Bond
L4b1s	60	0.75	0.91	1.03	Hybrid
L4b0s	96	-	-	0.99	Flexure
M4b0s	48	0.71	0.86	0.96	Bond
M4b1s	56	0.71	0.85	0.98	Bond
M4b1n	56	0.70	0.85	1.00	Bond
M4b0n	60	0.82	0.97	1.05	Hybrid
H4b0s	50	0.83	0.95	0.99	Bond
H4b0n	56	0.82	0.95	1.02	Hybrid
H4b1s	62	0.83	0.92	1.04	Hybrid
H4b1n	62	0.85	0.92	1.05	Hybrid

One other consideration in comparing the calculated versus embedment length is the ultimate strand strength used to determine the development length. All studies reviewed, including this one, use f_{ps} equal to the equation in ACI which results in values of approximately 268 ksi for grade 270 strand and 243 ksi for grade 250 strand, which is less than the guaranteed ultimate tensile strength (GUTS). The actual ultimate tensile strength for this study was about 275 ksi in

tensile tests, and in the pullout tests up to 280 ksi of resistance was exhibited. This can make a significant difference in the calculated development length. Figure 6.13 is a plot of actual ultimate tensile strength versus percent increase in calculated development length for grades 250 and 270 prestressing strand.

Table 6.10 shows the increase in development length calculated if the actual ultimate strength of the prestressing strand is used for the studies pertaining to debonded strand reviewed in Chapter 3. The effect for the grade 250 is more significant due to the larger difference, but even for grade 270 Table 6.10 shows that use of the actual strand ultimate strength can have a significant impact on the results of development length calculations.

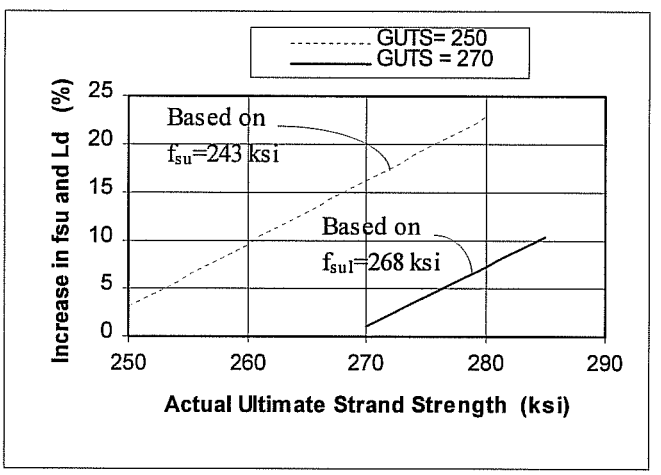

Figure 6.13 Development Length Increase vs. Actual Strength

TABLE 6.10
COMPARISON OF CALCULATED DEVELOPMENT LENGTH
BASED ON FSU AND ACTUAL ULTIMATE TENSILE STRENGTH

Study	Strand Dia. (in)	f_{su} ksi	$f_{su\ Actual}$ ksi	f_{se} ksi	L_d		
					Reported	$W/f_{su\ Act.}$	% Incr.
Kaar & Magura	0.375	240	277	140	55	69	25
Dane and Bruce	0.375	240	268	160	50	61	21
	0.438	240	268	155	60	72	20
Rabbat et. al.	0.438	244	264	140	66	75	13
Russell and Burns	0.500	268	283	162	80	88	9
	0.600	268	283	162	96	105	9
Current Study	0.600	269	275	162	96	100	4

CHAPTER 7
SUMMARY AND CONCLUSIONS

7.1 Summary

Anchorage of 0.6 inch diameter prestressing strand in a debonded application was the focus of this research. Strand of 0.6 inch diameter was placed in standard full sized Type I AASHTO girders at a 2 inch grid spacing which is common to the precast/prestressed concrete industry. All strand had a bright surface condition and was kept in a protected area to prevent the surface from rusting significantly prior to casting the beams. The effect of three different concrete strengths on transfer and development length of 0.6 inch strand was studied with two beams (four tests) for each concrete strength. The concrete strength ranged from 6.2 to 11.4 ksi. The addition of horizontal "h" bars in the anchorage region to control crack widths was investigated with one of the four tests in each of the three concrete strength groups.

Test beams were fabricated in Victoria, Texas at the Texas Concrete Company in the same manner as a typical highway girder. Release of the prestressing force at the plant was by torch cutting both ends at the same time for the beams of this study. Once the beams were received at Ferguson Structural Engineering Laboratory (FSEL), a concrete deck slab was placed on the beam to provide composite action during loading. Three pairs of beams were fabricated using the three different concrete design mixes. Both ends of each beam was tested making a total of 12 tests.

Transfer length was determined by mechanically measuring external concrete strains at the centroid of the prestressing strand at each end of the precast/prestressed concrete beams. This was done by placing DEMEC points on the concrete surface at two inch spacing before release of the prestress force. An 8 inch gauge length was used to measure concrete strains in the end regions of the beams where transfer occurred. This was done immediately before and after transfer of the prestress force. These same DEMEC points were used to get another set of strains 60 to 120 days after transfer, when the composite deck had been placed and before the load test was performed on the completed composite beam. From these readings strain profiles were constructed. The transfer lengths were determined from the strain profiles constructed using the DEMEC data taken after release of the prestress force.

Development lengths were determined indirectly by loading 12 beam ends at different embedment lengths. If a beam failed in pure flexure, the embedment length was considered to be greater than the development length. If failure occurred before the calculated capacity was reached for the test beam due to bond failure with slipping of the strand, then it was considered to be less than the development length. Embedment lengths ranged from 50 to 100 percent of the development length as calculated by the ACI/AASHTO equation. Throughout the loading process end slip was measured in each of the prestressing strands for the end being tested. The concrete strains on the top of the slab were measured also to determine when crushing strain was being approached. Crack patterns were marked and crack widths recorded after each load increment during a beam test. Deflections of the beam were monitored and recorded at each load increment so

that a load-deflection response could be constructed and compared to predicted behavior.

Pull-out tests were performed on pieces of the 0.6 inch seven wire strand to give an indication of the quality of bond characteristics of the strand. Results of the pull-out tests were evaluated to determine how well they predict bond behavior in the transfer and development of prestressing strand.

7.2 Conclusions

Based on the test results of this study, the following conclusions can be made.

7.2.1 Transfer Lengths

1) On the average, transfer lengths for 0.6 inch diameter strand with bright surface condition decreased with an increase in concrete strength. Measurements in the low strength concrete beams ($f'_{c\ avg.}$ = 6.2 ksi) averaged about 17.5 inches and the medium ($f'_{c\ avg.}$ = 10.4 ksi) and high ($f'_{c\ avg.}$ = 11.4 ksi) strength concrete beams averaged 15.2 and 15.4 inches respectively.
2) With an increase in concrete strength, the measured transfer lengths had a decreasing amount of variation, and less scatter from one beam end to another.
3) Over a period of time between 60 to 120 days between measurement of initial transfer lengths (immediately after transfer) and after placement of the slab, only a small increase in the transfer length occurred. This could be attributed to scatter inherent in the methods of measurement used.

4) Transfer lengths in the debonded strands when determined using the 95 percent plateau method, were generally less than the transfer length for the fully-bonded stands. When the slope-intercept method was used, the debonded strands produced transfer lengths slightly longer than the fully-bonded strands. The slope-intercept method in general had less scatter, producing slightly more consistent results (See Table 6.3 and 6.4 for a summary of the results).

5) Pull-out tests for the low and medium strength concrete indicated that the bonding characteristics were very good and this was confirmed by the short transfer lengths measured. The high strength pull-out test was in the region that was not defined in the article by Logan[12] but produced transfer lengths which were about equal to the values obtained for medium strength concrete.

6) The ACI/AASHTO equation for transfer length of strand with this high quality of bond, as indicated by the pull-out resistance, is conservative. Equations by Mostafa et. al. gave predicted transfer lengths which were slightly under the average measured values for the higher strength concrete beams, and not excessively conservative for the low strength concrete beams. Results from equations proposed by Mitchell et. al. were conservative but not excessive for all concrete strengths.

7.2.2 Development Lengths

1) As indicated by the short transfer length measurements and pull-out test results, the performance of bond in these 0.6 inch seven wire strands proved to be very good in the development length tests. Strands debonded 72 inches with an embedment length as little as 63 percent of the ACI/AASHTO code

equation were able to develop full flexural capacity. Even though there was a significant amount of slip, they were able to develop enough resistance to exceed calculated flexural capacity. The anchorage of debonded strands which are not anchored at the end of a beam, performed very well despite being subjected to flexural moment at sections all along the member.

2) In Figure 6.8 increase in strand stress is plotted versus test embedment lengths from the point when initial bond failure (a slip of 0.01 inches) began until ultimate slip occurred. In general, slips of 0.1 inches showed correlation with stress increases at ultimate which are higher than required by the ACI/AASHTO equation for flexural bond length.

3) Cracking moment through the transfer region of a strand was found to cause initiation of bond failure but not general bond failure of strand. In several of the tests, cracking occurred in the transfer zone of the 36 inch debonded strands. The flexural bond length was long enough to develop adequate bond resistance to resist further load and no more significant slip occurred in these strands.

4) In the failures that were considered hybrid, initial bond failure (0.01 inch slip) did not occur until test load levels of over 82 percent of the calculated capacity had been reached. When 0.1 inches of slip had developed for debonded strands, the applied load had reached 92 percent of the ultimate flexural capacity.

5) The results of this series of tests show that the ACI/AASHTO equation for development length of 0.6 inch seven wire strand with good bond characteristics is conservative. With embedment of 60 inches, which is 63 percent of the ACI/AASHTO code required length, the full calculated flexural strength was developed for beams tested in this study.

7.2.3 Quality of Bond

Anchorage of strand in this study performed very well compared to results reported in previous studies which varied widely, indicating that there is a wide range of surface conditions in the production of prestressing strand. Different producers provide strand with widely varying surface conditions which adds to the scatter of data collected by various studies. It appears that a method of testing the bond characteristics of prestressing strand before it is used in a pretensioned application is necessary in order to achieve more consistent results. Logan[12] presents one method in which this might be accomplished by the use of pull-out testing. Also presented in this paper is the use of end slip measurement at the time of release of prestress (pull-in), which gives a good estimate of the transfer length and an indication of strand behavior during development of strand ultimate capacity.

APPENDIX A

MATERIAL PROPERTIES

- **Concrete Strength vs. Time**
- **Summary of Concrete Strength at Testing**
- **Strand Stress-Strain Curve**
- **Strand Relaxation**
- **Strand Shrinkage**
- **f_{si} & f_{se}**
- **Concrete Design Mixes**

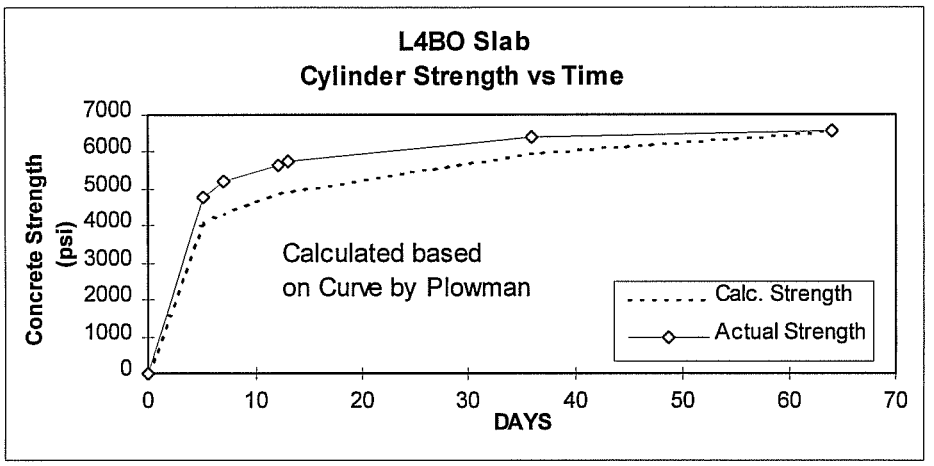

Figure A.1 Compressive Strength of Slab on Beam L4BO

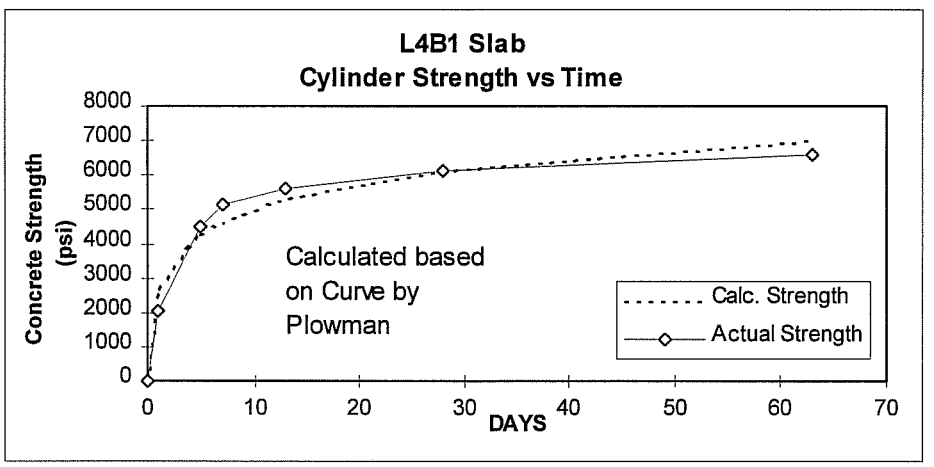

Figure A.2 Compressive Strength of Slab on Beam L4B1

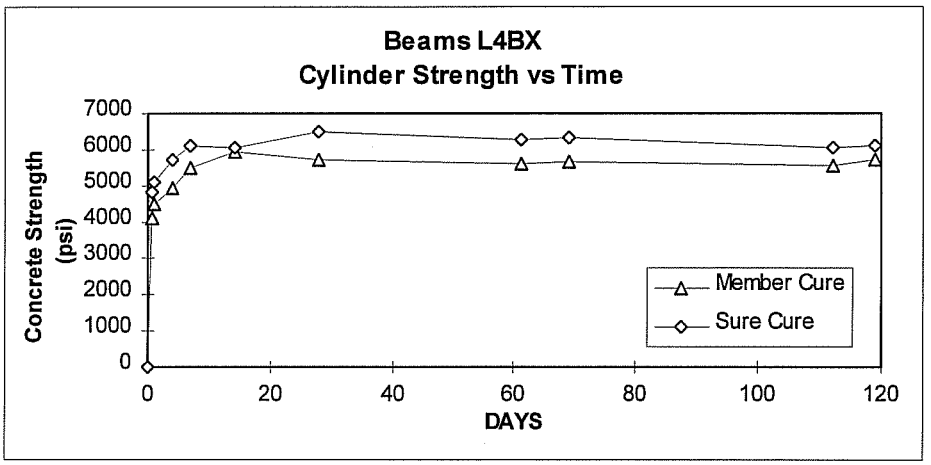

Figure A.3 Compressive Strength of Beams L4BO & L4B1

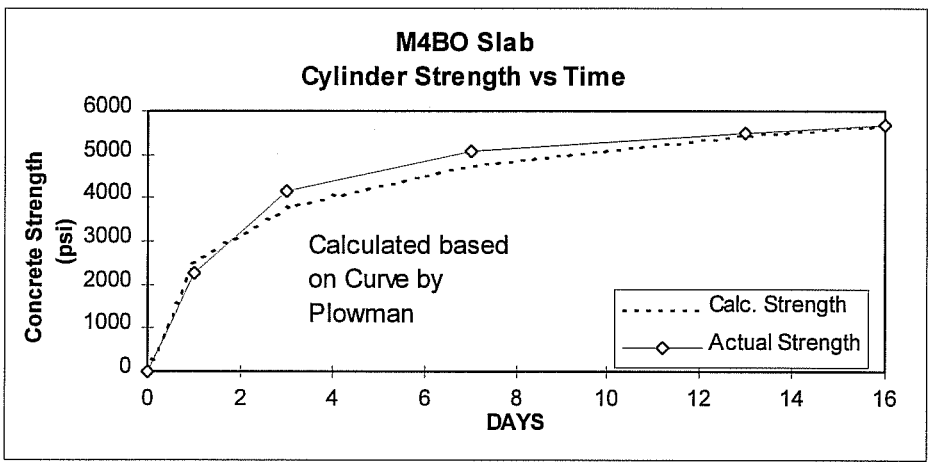

Figure A.4 Compressive Strength of Slab on M4BO

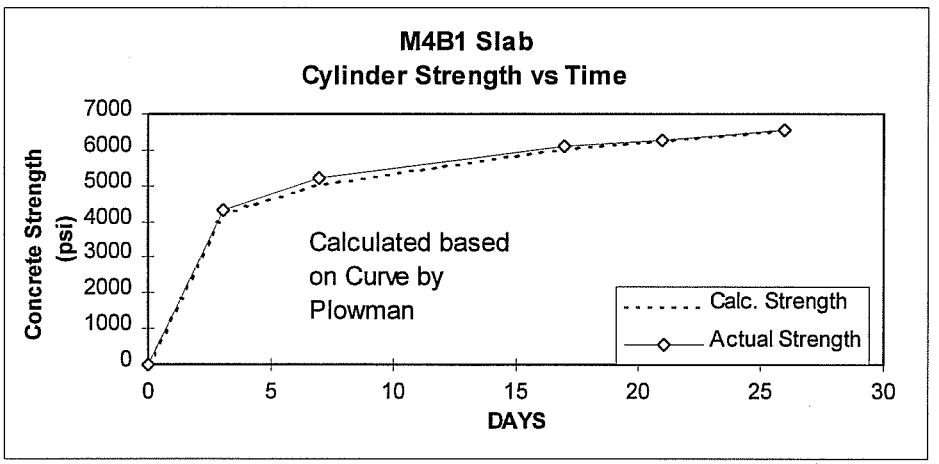

Figure A.5 Compressive Strength of Slab on M4B1

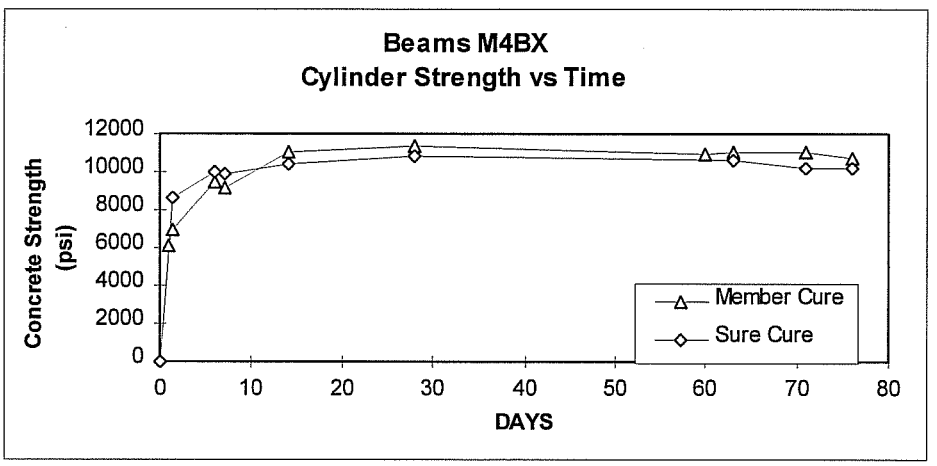

Figure A.6 Compressive Strength of Beams L4BO & L4B1

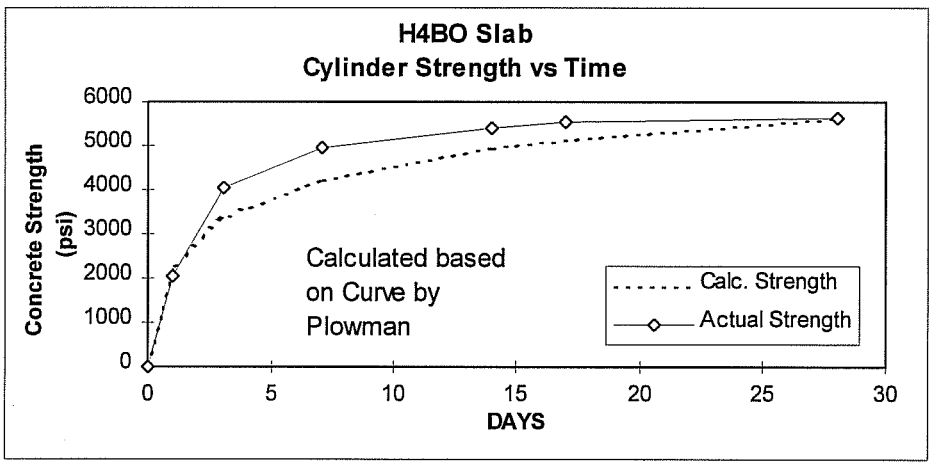

Figure A.7 Compressive Strength of Slab on H4B0

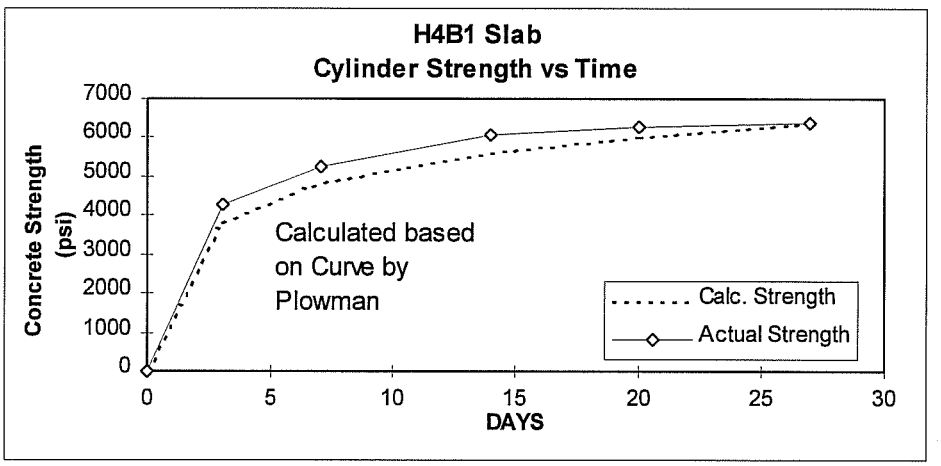

Figure A.8 Compressive Strength of Slab on H4B1

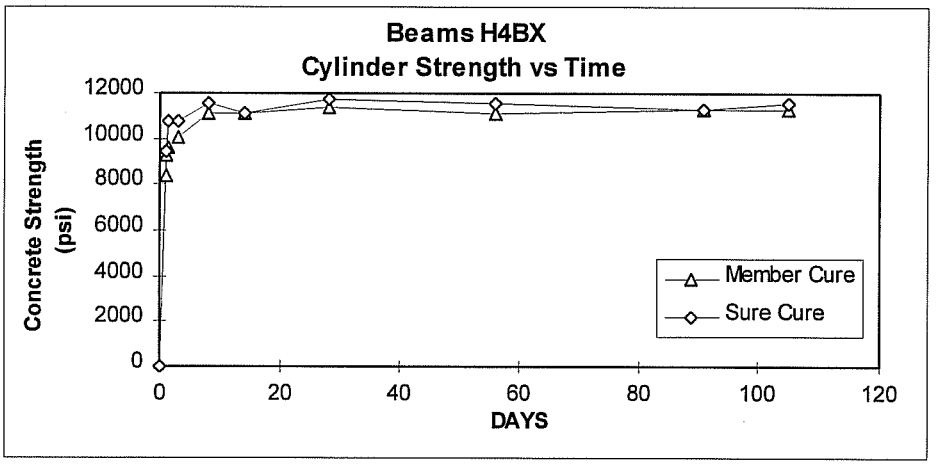

Figure A.9 Compressive Strength of Beams H4BO & H4B1

TABLE A.1
SUMMARY OF CONCRETE STRENGTHS
AND MATURITY DURING TESTING

Test No	Date Tested	Conc. Strength psi		Date Cast		Age at Test	
		Slab	Beam	Beam	Slab	Beam	Slab
L4B0N	01/30/97	6550	6040	10/10/96	11/27/96	112	64
L4B0S	12/10/96	5740	6280	10/10/96	11/27/96	61	13
L4B1N	02/06/97	6580	6110	10/10/96	12/05/96	119	63
L4B1S	12/18/96	5620	6350	10/10/96	12/05/96	69	13
M4B0N	03/10/97	5500	10620	01/09/97	02/25/97	60	13
M4B0S	03/13/97	5700	10620	01/09/97	02/25/97	63	16
M4B1N	03/26/97	6550	10180	01/09/97	02/28/97	76	26
M4B1S	03/21/97	6270	10180	01/09/97	02/28/97	71	21
H4B0N	04/22/97	5400	11260	01/21/97	04/08/97	91	14
H4B0S	04/25/97	5560	11260	01/21/97	04/08/97	94	17
H4B1N	05/08/97	6390	11590	01/21/97	04/11/97	107	27
H4B1S	05/01/97	6260	11590	01/21/97	04/11/97	100	20

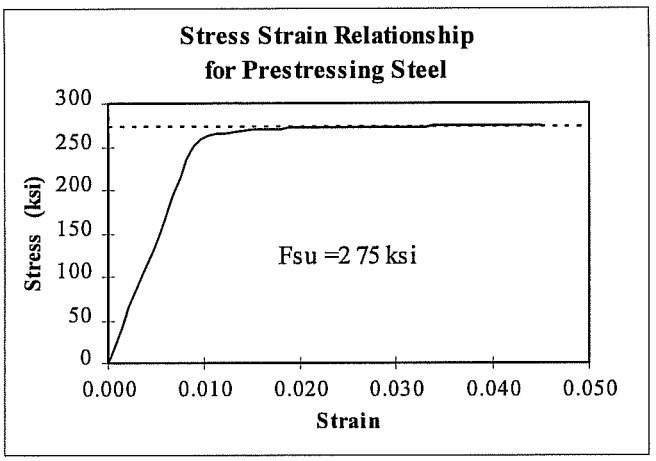

Figure A.10 Stress-Strain Relationship for Prestressing Steel

$$f_{ps} = 28{,}500\varepsilon_{ps} \qquad \text{for:} \quad \varepsilon_{ps} \le 0.00867$$

$$f_{ps} = 270.1 - \left(\frac{.0468}{\varepsilon_{ps} - .007}\right) \qquad \text{for:} \quad \varepsilon_{ps} > 0.00867 \text{ Effective Prestress}$$

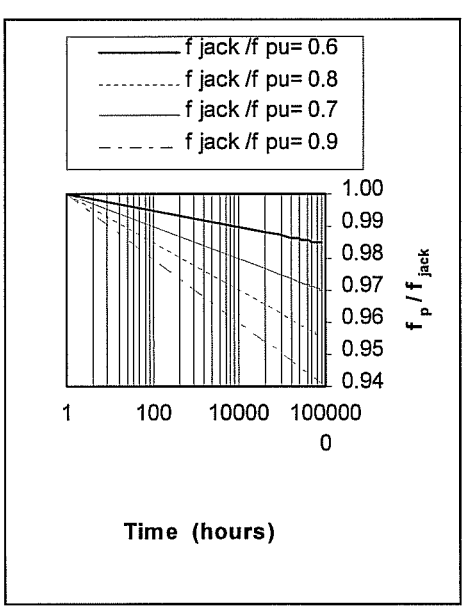

Figure A.11 Relaxation of Prestressing Steel

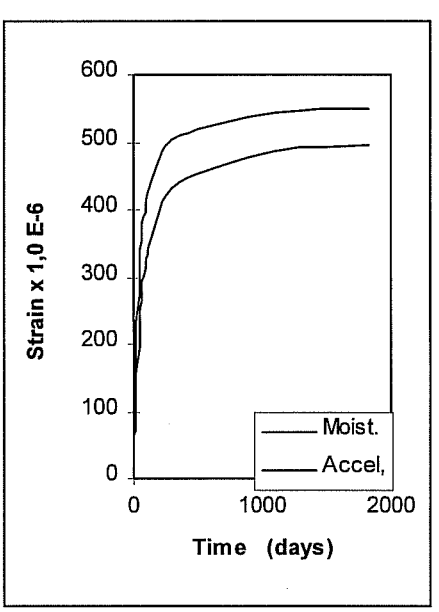

Figure A.12 Shrinkage of Concrete

TABLE A.2
EFFECTIVE PRESTRESS FOR INTERNAL
ERSG's AND DEMEC READINGS

Test	Le	BOTTOM STRANDS				TOP STRANDS	
		DEMEC Gauge		Internal ERSG		Internal ERSG	
		fsi	fse	fsi	fse	fsi	fse
Number	in	ksi	ksi	ksi	ksi	ksi	ksi
L4B0N	48	187.3	170.2	188.3	175.1	106.0	96.9
L4B0S	96						
L4B1N	48	187.1	169.7	186.1	170.3	105.7	97.1
L4B1S	60						
M4B0N	60	189.0	180.5	187.7	180.8	39.8	37.0
M4B0S	48						
M4B1N	56	188.8	180.0	187.9	179.9	42.0	34.5
M4B1S	56						
H4B0N	56	188.3	179.3	187.5	177.8		
H4B0S	50						
H4B1N	62	188.0	180.3	185.0	178.5		
H4B1S	62						

CONCRETE MIX DESIGNS:

TABLE A.3 LOW STRENGTH BEAM CONCRETE MIX DESIGN	
Material	Quantity Qty / yd^3
Type III Cement	528 lb
Fly Ash	205 lb
Water	242 lb
Coarse Aggregate	1799 lb
Fine Aggregate	1120 lb
Air	5 %
Admixtures: High Range Water Reducer Air Entraining Agent	

TABLE A.4 MEDIUM STRENGTH BEAM CONCRETE MIX DESIGN	
Material	Quantity Qty / yd^3
Type III Cement	564 lb
Fly Ash	162 lb
Water	202 lb
Coarse Aggregate	1999 lb
Fine Aggregate	1153 lb
Air	2 %
Admixtures: High Range Water Reducer Air Entraining Agent	

TABLE A.5 HIGH STRENGTH BEAM CONCRETE MIX DESIGN	
Material	Quantity Qty / yd^3
Type III Cement	671 lb
Fly Ash	319 lb
Water	246 lb
Coarse Aggregate	1882 lb
Fine Aggregate	1052 lb
Air	2 %
Admixtures: High Range Water Reducer Air Entraining Agent	

APPENDIX B

TRANSFER MEASUREMENTS
DATA AND RESULTS

- **Affect of Time on Lt: 95 % Plateau Method**
- **Affect of Time on Lt: Slope-intercept Method**
- **Affect of Debonding on Lt: 95 % Plateau Method**
- **Affect of Debonding on Lt: Slope-intercept Method**
- **Concrete Strain vs. Distance Along Beam**

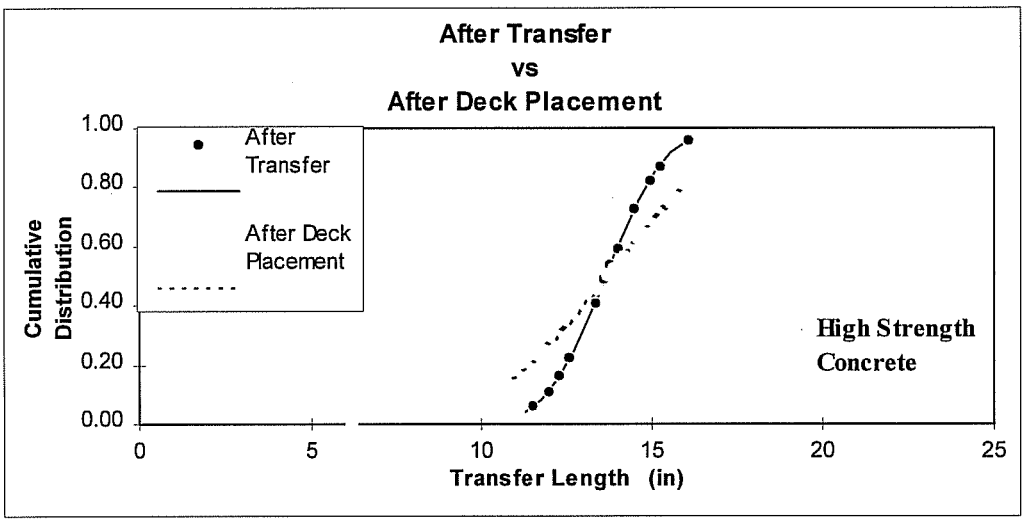

Figure B.3 Cumulative Transfer Data vs. Time: High Strength Concrete (11.4 ksi)

TABLE B.1				
95 % Plateau Method				
Concrete Strength	Imm. After Transfer		After Deck Placement	
	Lt in	Std Deviation	Lt in	Std Deviation
Low	16.0	4.26	17.0	4.67
Medium	13.1	1.70	13.2	2.06
High	13.6	1.38	13.7	2.68

% PLATEAU METHOD

Effect of Time on Lt

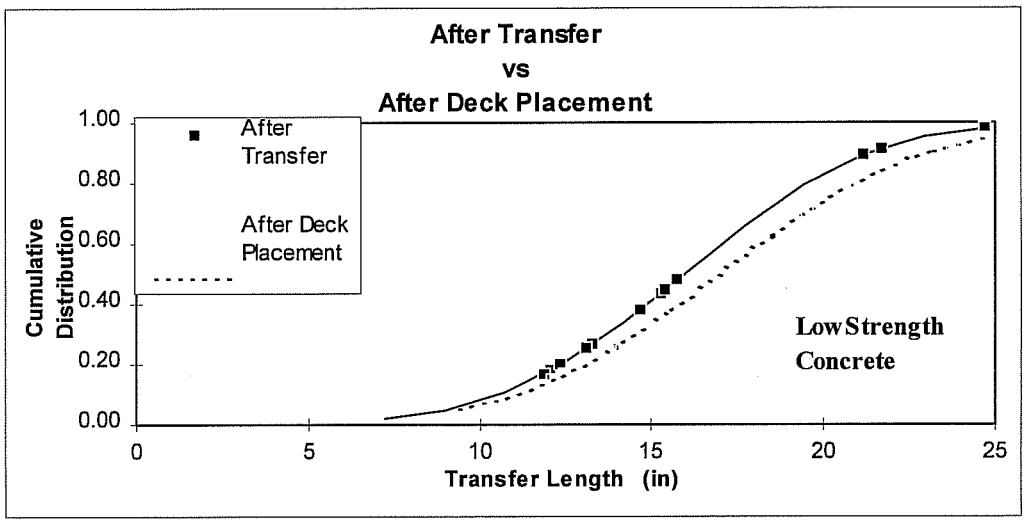

Figure B.1 Cumulative Transfer Data vs. Time: Low Strength Concrete (6.2 ksi)

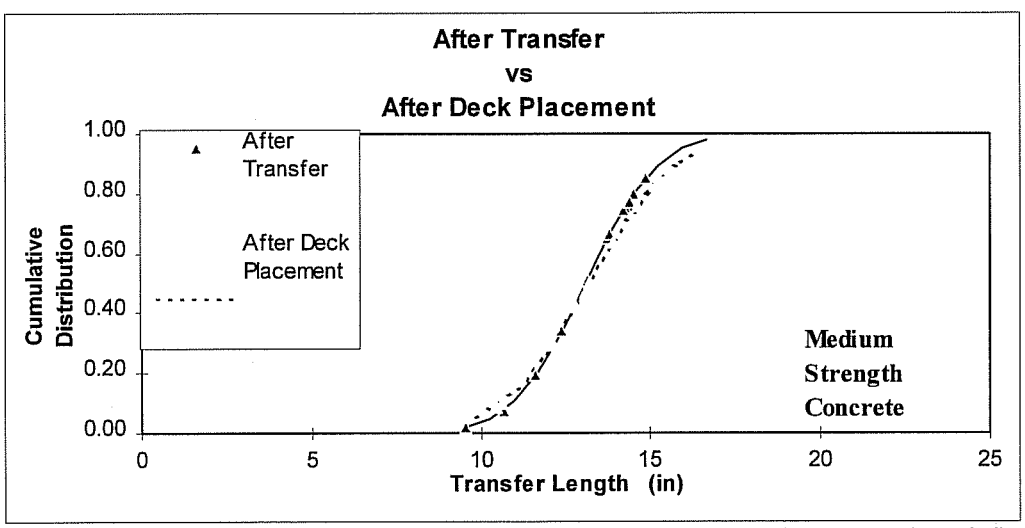

Figure B.2 Cumulative Transfer Data vs. Time: Medium Strength Concrete (10.4 ksi)

SLOPE-INTERCEPT METHOD

Transfer vs. Time

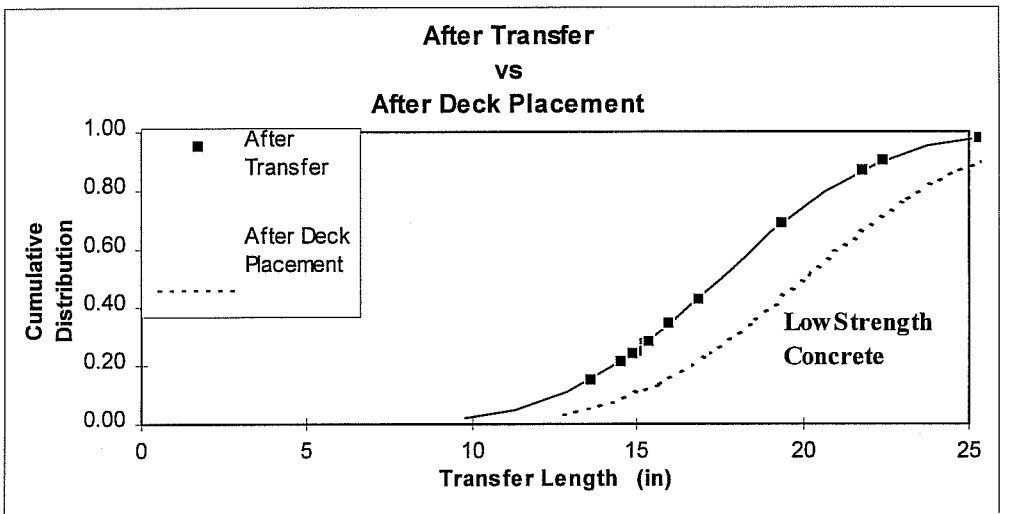

Figure B.4 Cumulative Transfer Data vs. Time: Low Strength Concrete (6.2 ksi)

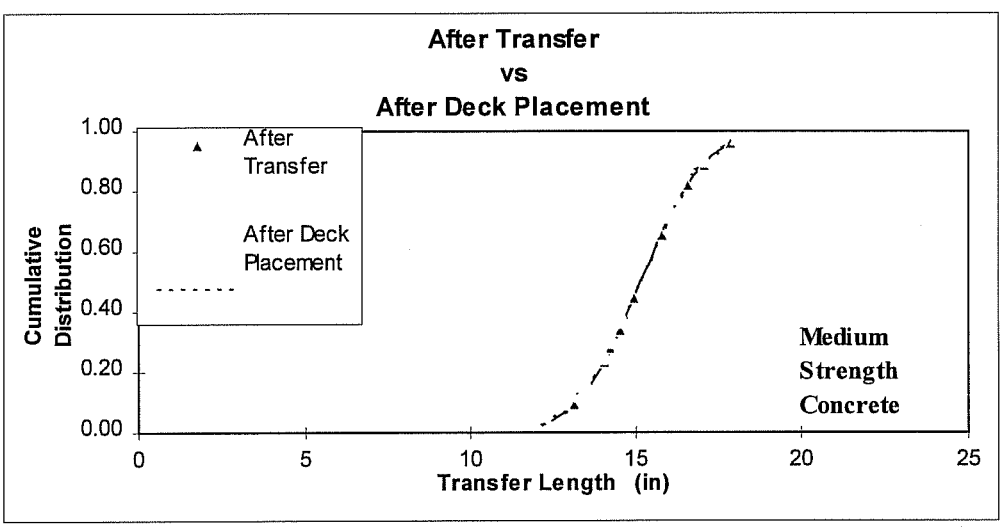

Figure B.5 Cumulative Transfer Data vs. Time: Medium Strength Concrete (10.4 ksi)

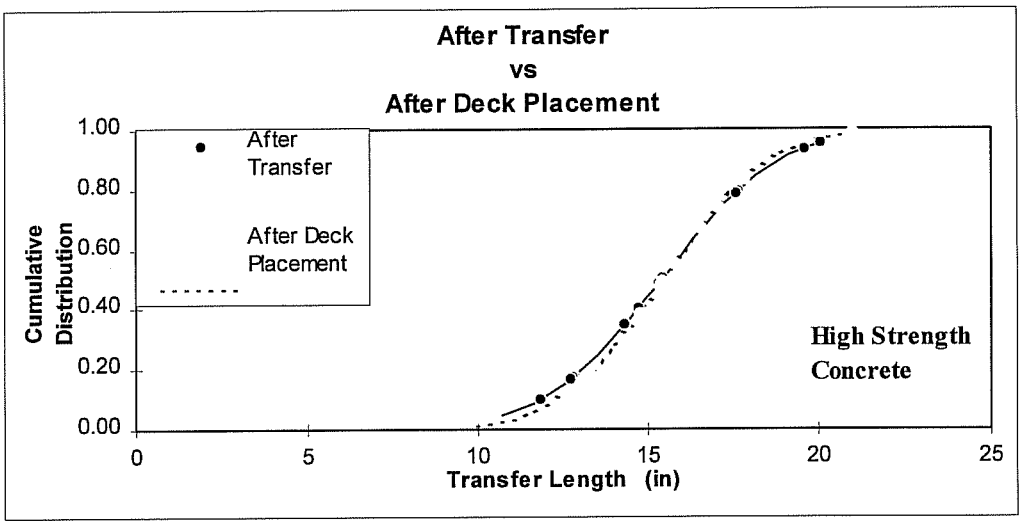

Figure B.6 Cumulative Transfer Data vs. Time: High Strength Concrete (11.4 ksi)

TABLE B.2				
Slope-Intercept Method				
Concrete Strength	Imm. After Transfer		After Deck Placement	
	Lt in	Std Deviation	Lt in	Std Deviation
Low	17.5	3.77	20.1	4.04
Medium	15.2	1.55	15.1	1.54
High	15.4	2.77	15.5	2.43

95 % PLATEAU METHOD
Fully-bonded vs. Debonded

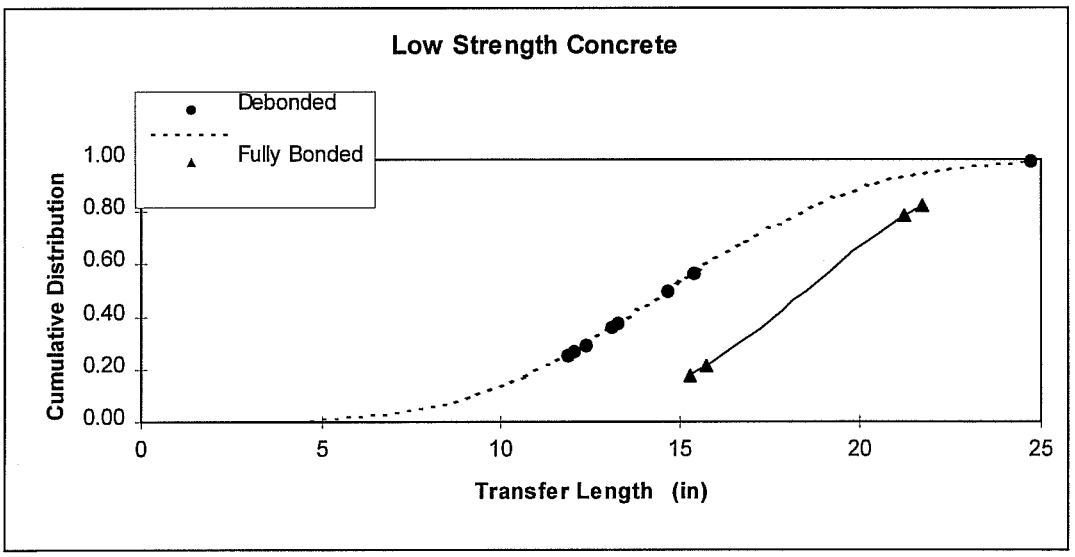

Figure B.7 Cumulative Transfer Data vs. Time: Low Strength Concrete (6.2 ksi)

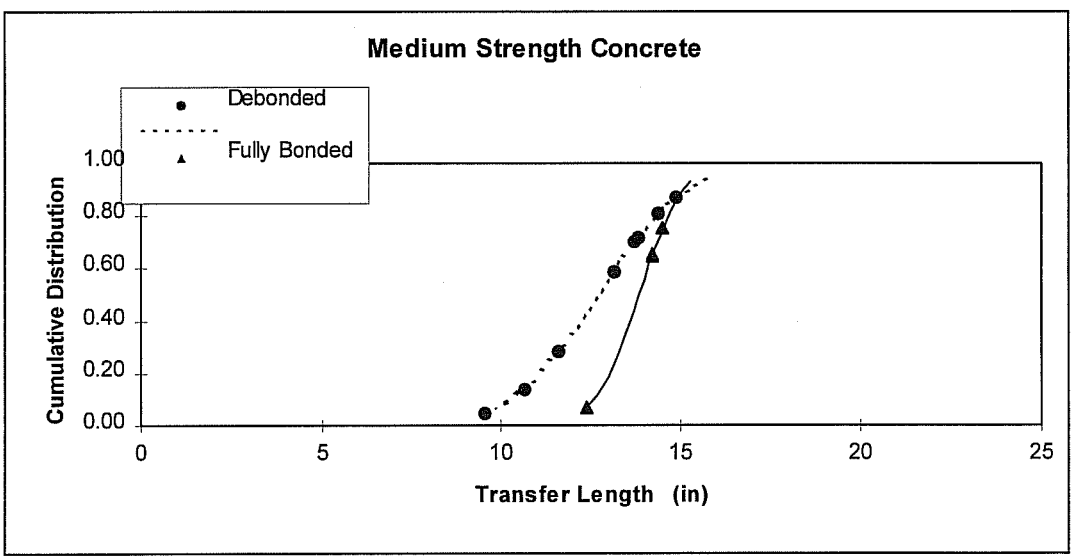

Figure B.8 Cumulative Transfer Data vs. Time: Medium Strength Concrete (10.4 ksi)

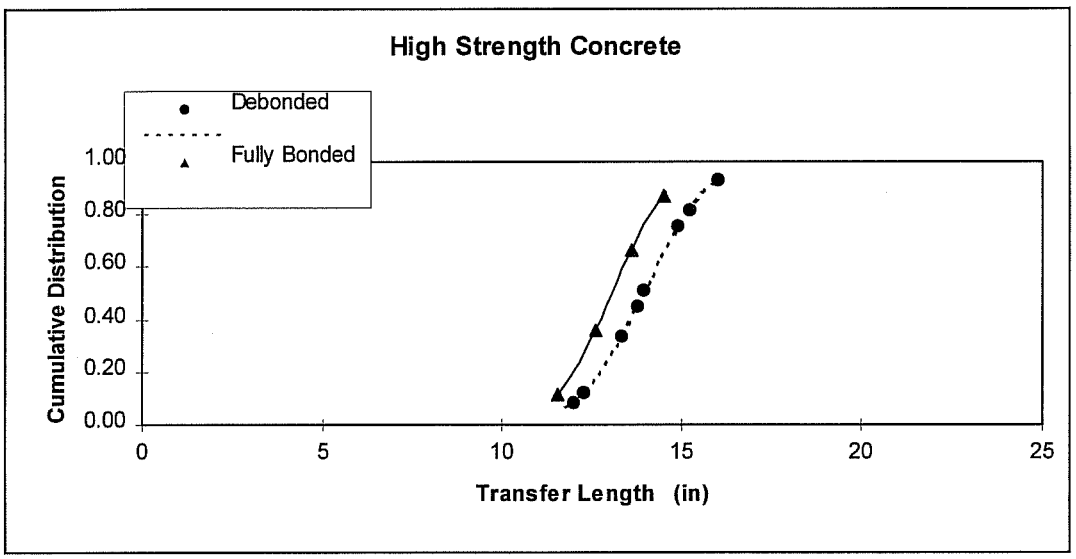

Figure B.9 Cumulative Transfer Data vs. Time: High Strength Concrete (11.4 ksi)

TABLE B.3				
95 % Plateau Method				
Concrete Strength	Fully-bonded		Debonded	
	Lt in	Std Deviation	Lt in	Std Deviation
Low	18.5	3.45	14.7	4.24
Medium	13.9	0.97	12.7	1.91
High	13.1	1.27	13.9	1.41

SLOPE-INTERCEPT METHOD
Fully-bonded vs. Debonded

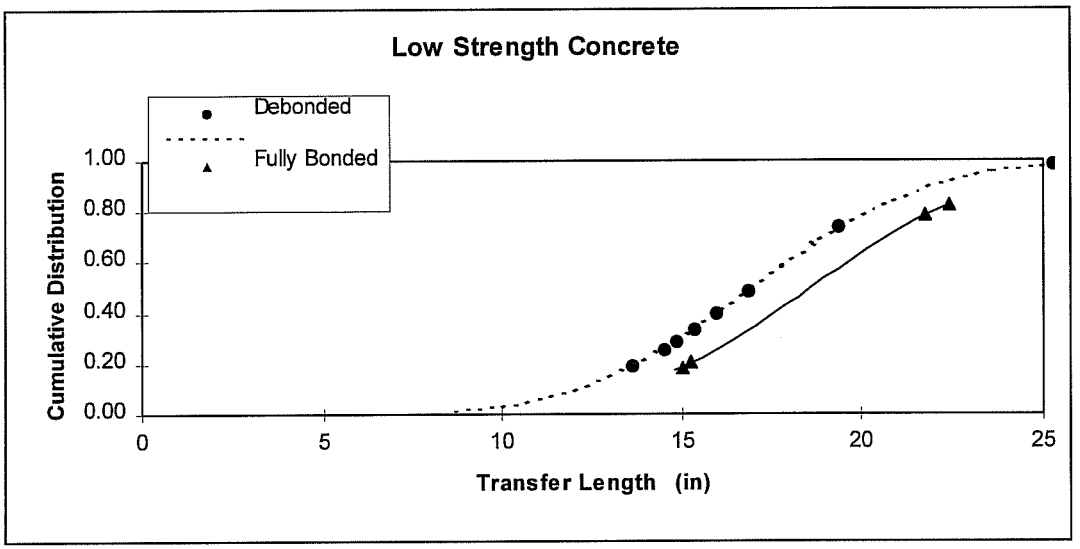

Figure B.10 Cumulative Transfer Data vs. Time: Low Strength Concrete (6.2 ksi)

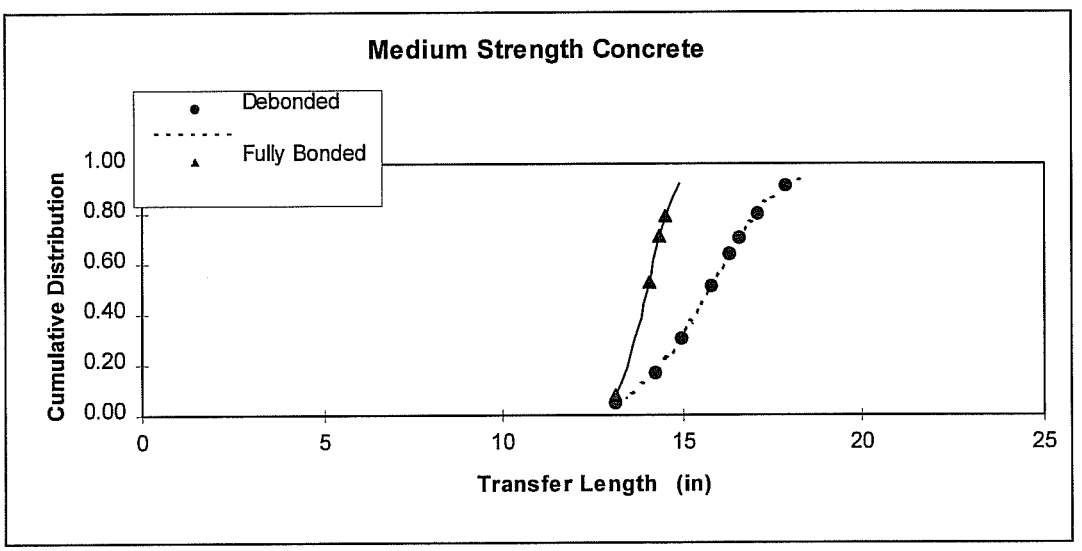

Figure B.11 Cumulative Transfer Data vs. Time: Medium Strength Concrete (10.4 ksi)

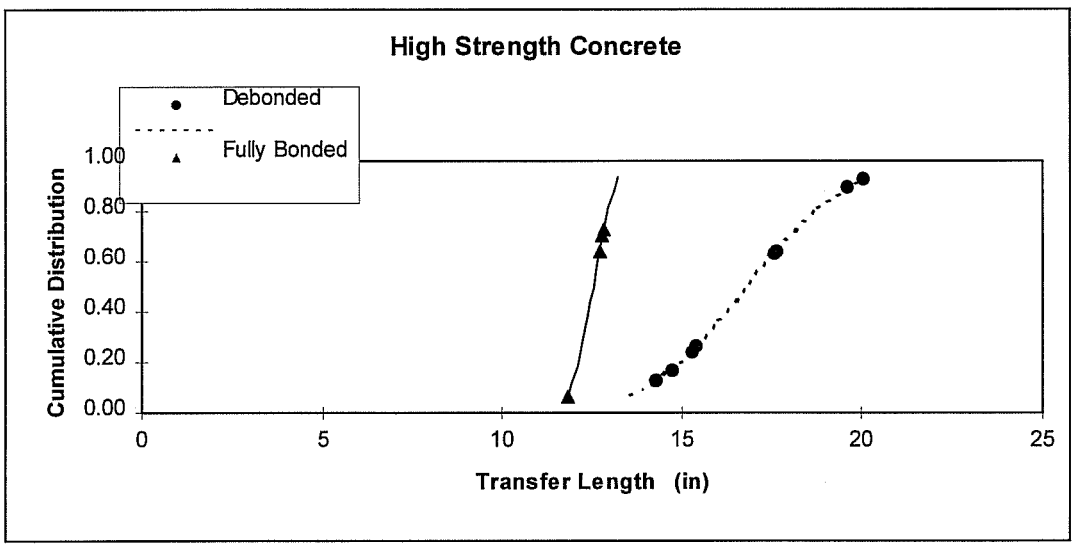

Figure B.12 Cumulative Transfer Data vs. Time: High Strength Concrete (11.4 ksi)

TABLE B.4				
Slope-intercept Method				
Concrete Strength	Fully-bonded		Debonded	
	Lt in	Std Deviation	Lt in	Std Deviation
Low	18.6	4.03	17.0	3.79
Medium	14.0	0.64	15.7	1.56
High	12.5	0.48	16.8	2.22

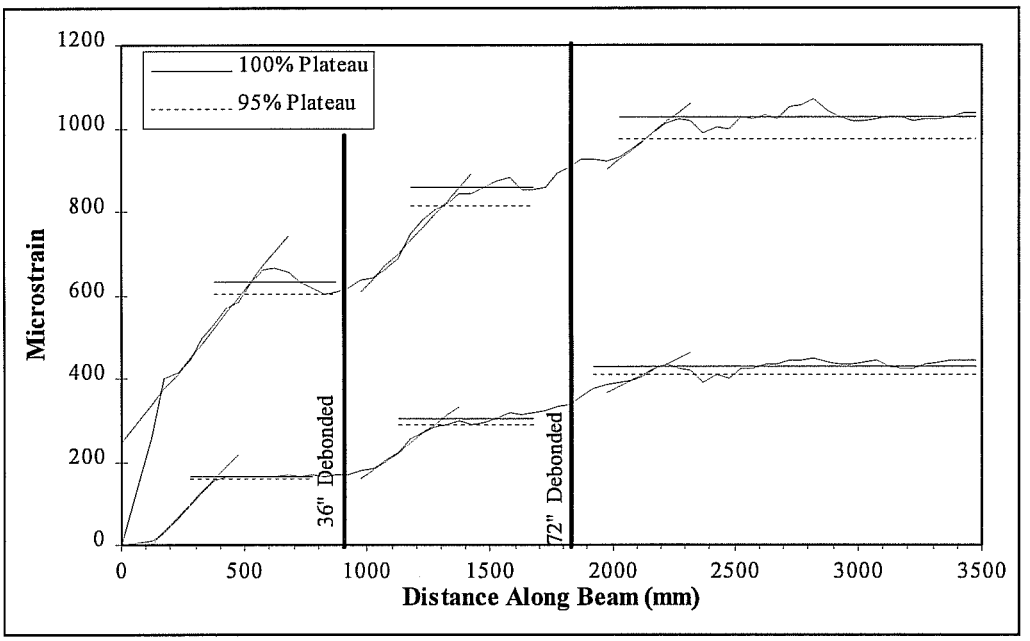

Figure B.13 Transfer Length Data: L4B0 West

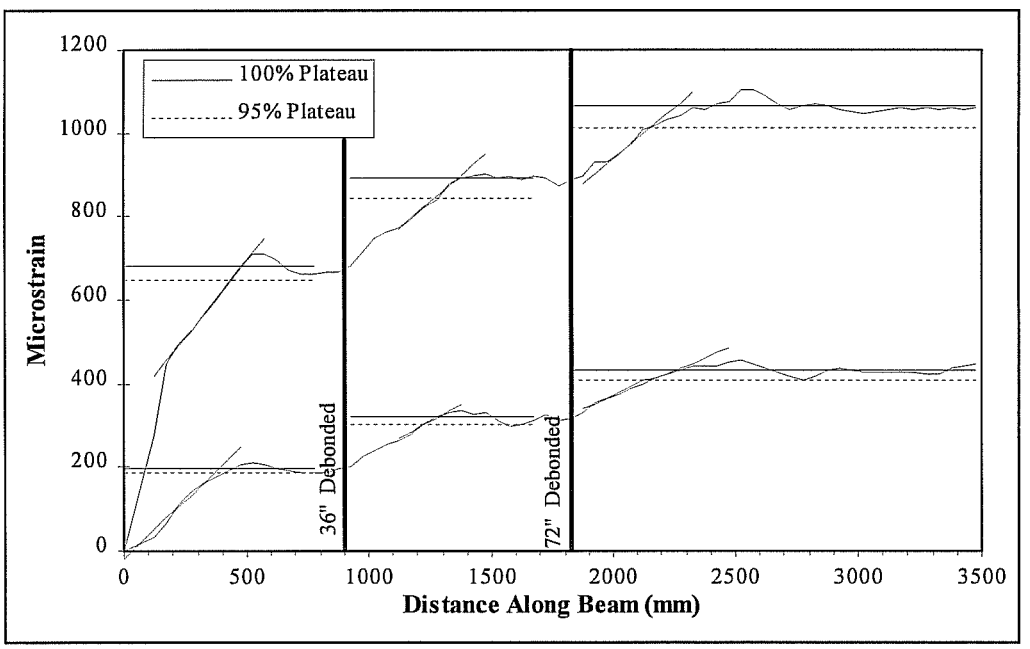

Figure B.14 Transfer Length Data: L4B1 West

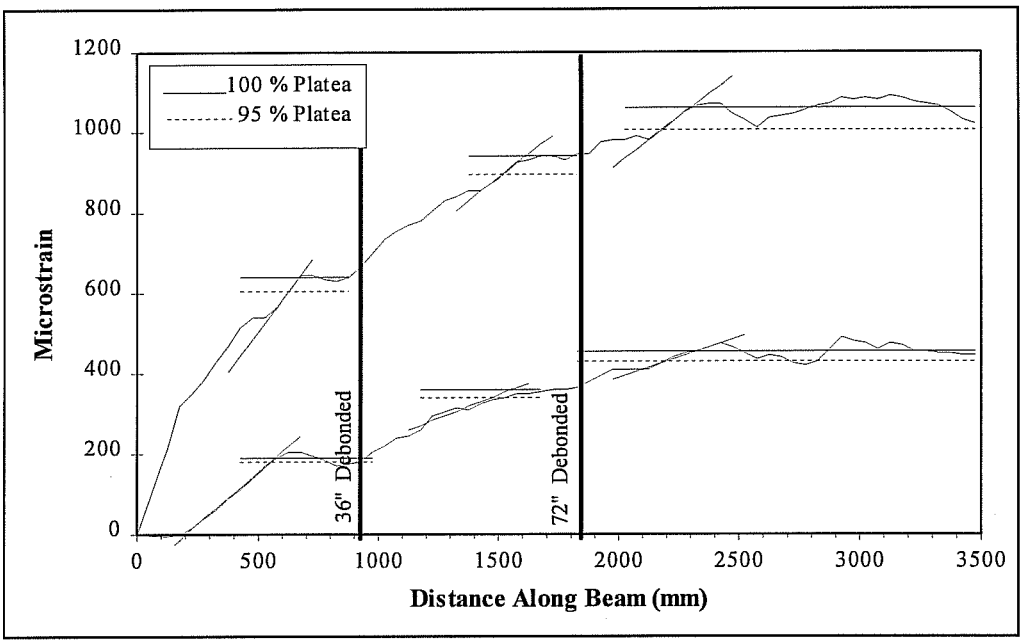

Figure B.15 Transfer Length Data: L4B0 East

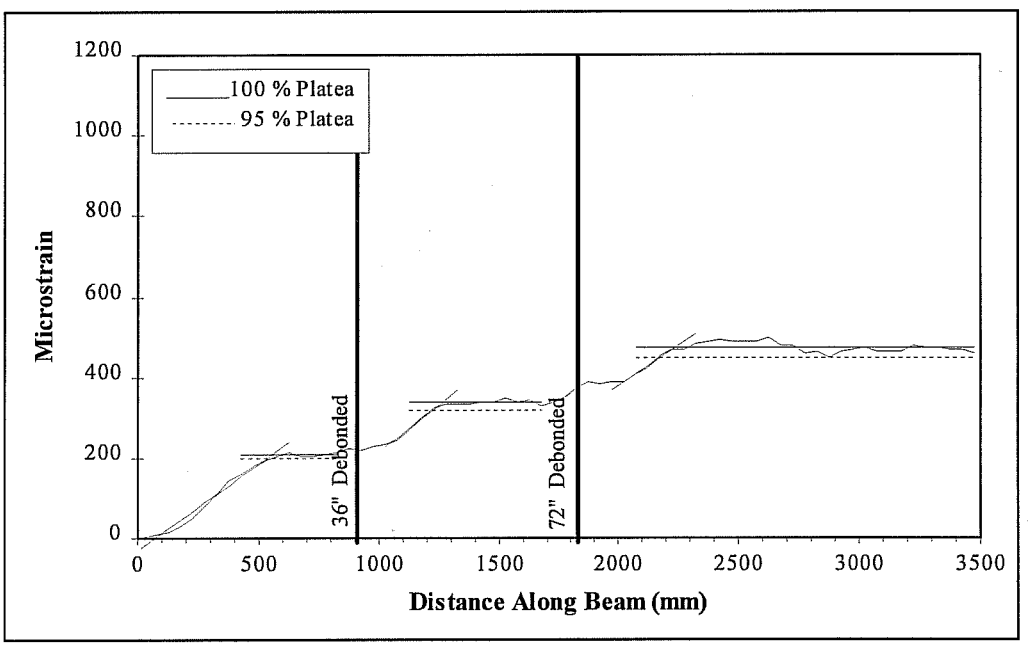

Figure B.16 Transfer Length Data: L4B1 East

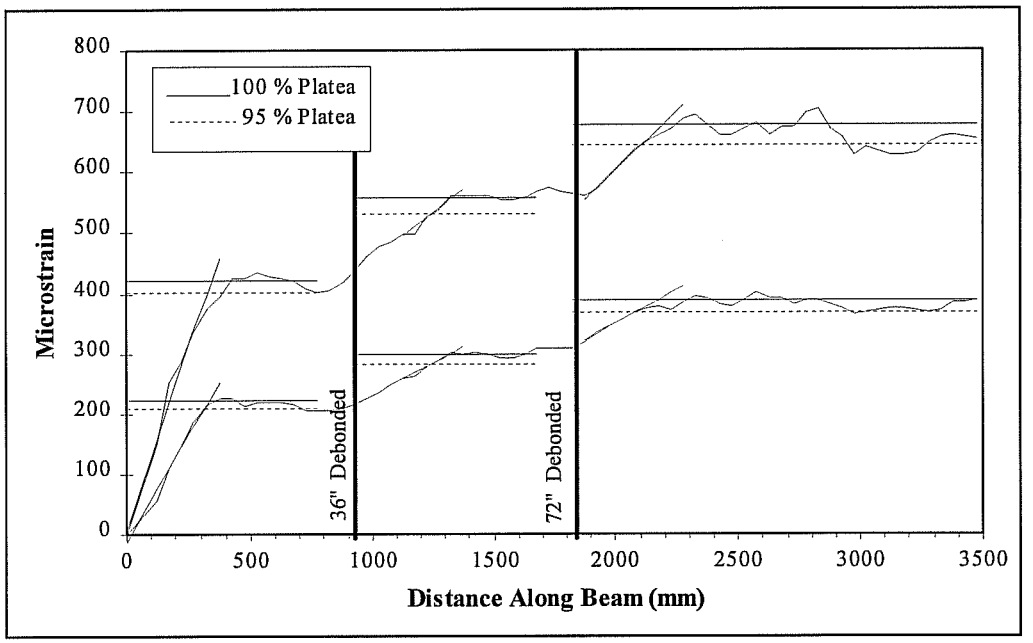

Figure B.17 Transfer Length Data: M4B0 West

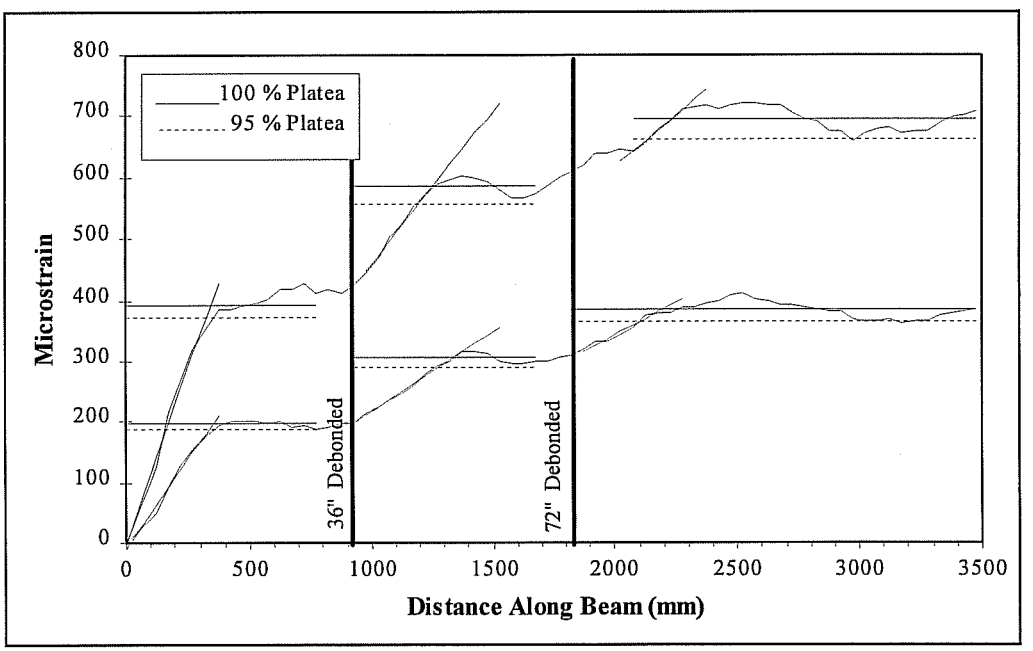

Figure B.18 Transfer Length Data: M4B1 West

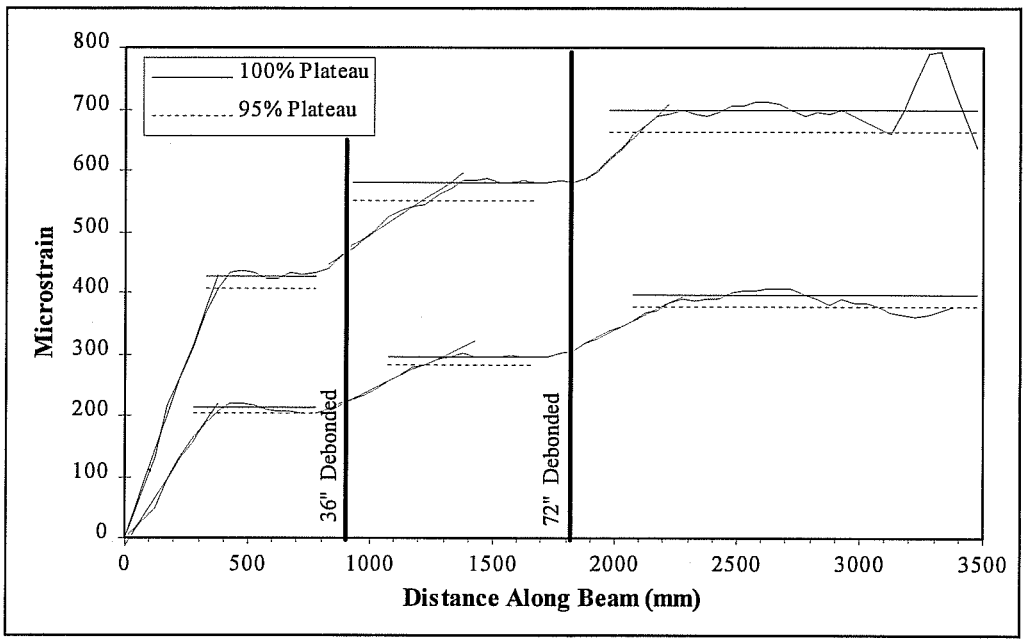

Figure B.19 Transfer Length Data: M4B0 East

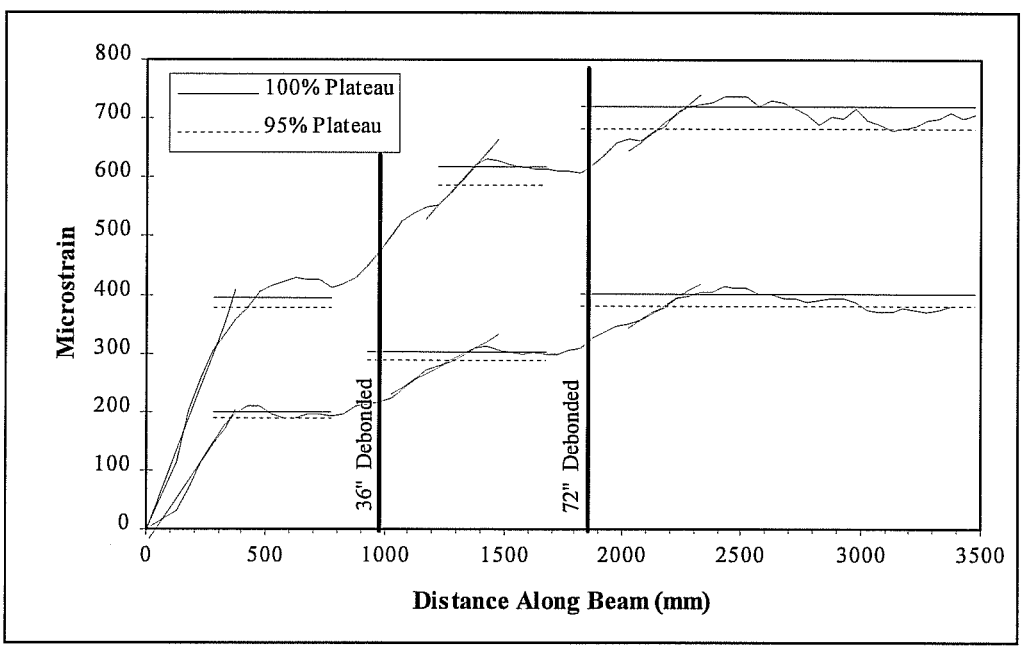

Figure B.20 Transfer Length Data: M4B1 East

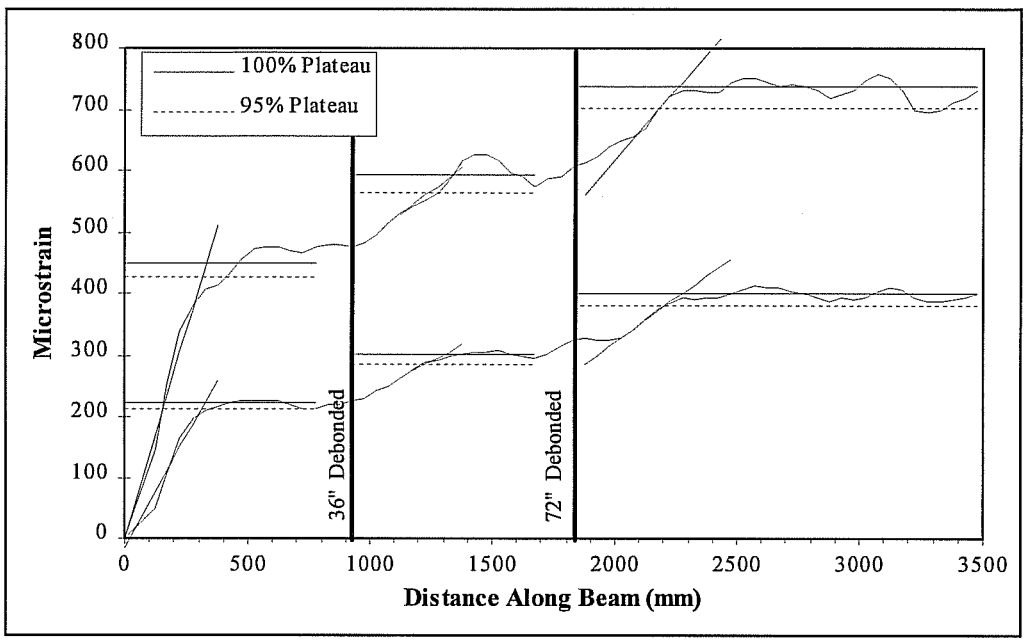

Figure B.21 Transfer Length Data: H4B0 West

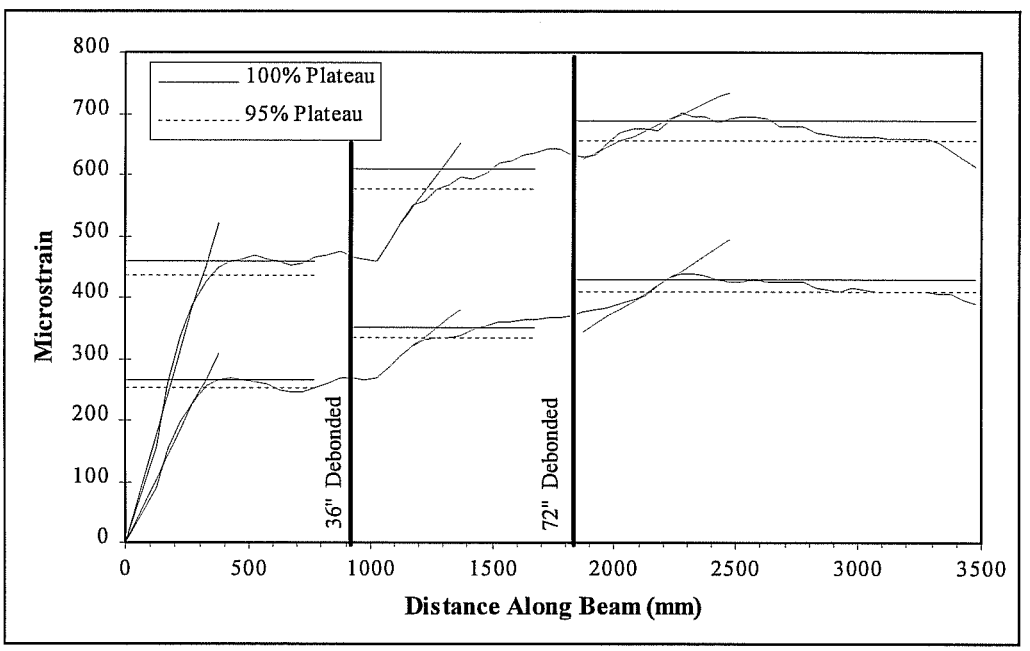

Figure B.22 Transfer Length Data: H4B1 West

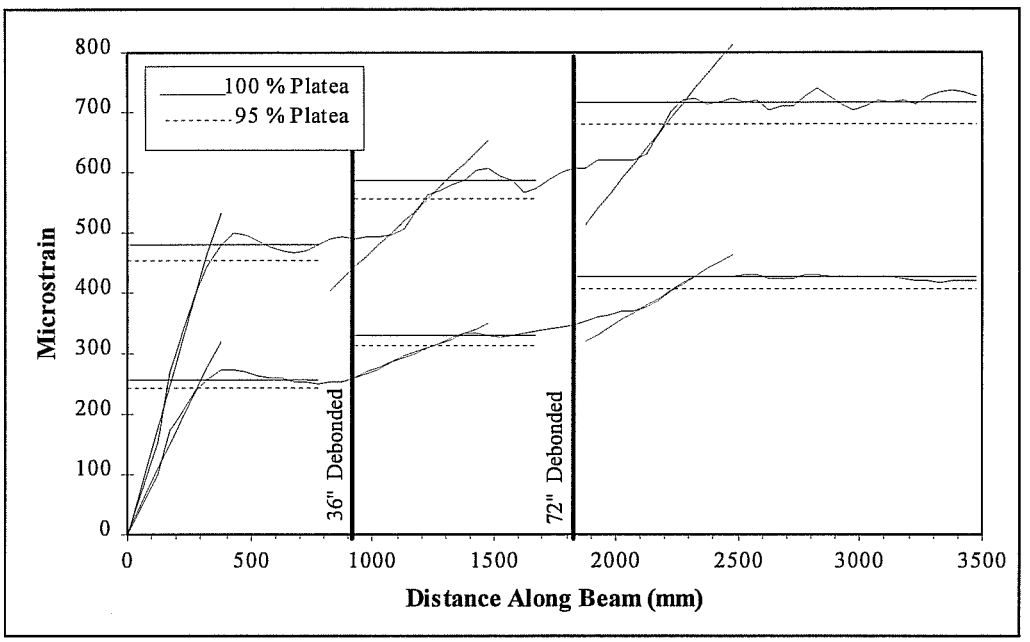

Figure B.23 Transfer Length Data: H4B0 East

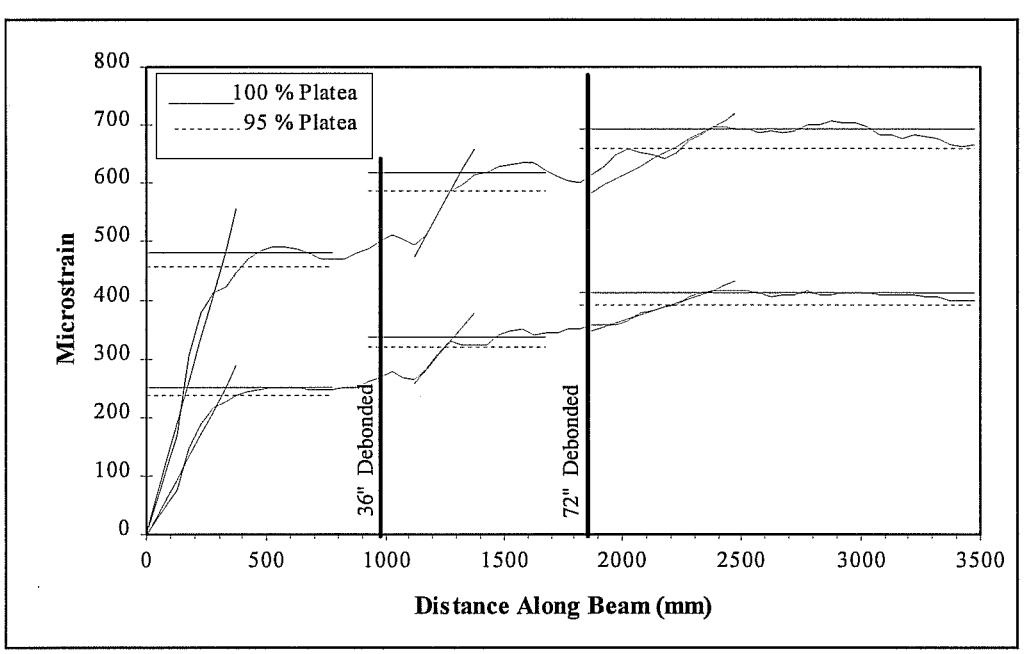

Figure B.24 Transfer Length Data: H4B1 East

APPENDIX C

TEST BEAMS

- **Analysis**
- **Details**

Concrete Compressive Force

Stress Strain Expression:

$$f_c = f'_c \left\{ \frac{2\varepsilon}{\varepsilon_o} - \left(\frac{\varepsilon}{\varepsilon_o} \right)^2 \right\}$$

Compressive Force:

$$F_{conc} = \alpha f'_c c$$

$$\alpha = \frac{\int_{\varepsilon 1}^{\varepsilon 2} f_c d\varepsilon_c}{f'_c \left(\varepsilon_2 - \varepsilon_1 \right)} \qquad \alpha = \frac{\left\{ 3\varepsilon_2^2 \varepsilon_o - \varepsilon_2^3 - 3\varepsilon_1^2 \varepsilon_o + \varepsilon_1^3 \right\}}{3\varepsilon_o^2 \left(\varepsilon_2 - \varepsilon_1 \right)}$$

Centroid of Compressive Force:

$$Centroid = \gamma c$$

$$\gamma = 1 - \frac{\int_{\varepsilon 1}^{\varepsilon 2} \varepsilon f_c d\varepsilon_c}{\varepsilon_2 \int_{\varepsilon 1}^{\varepsilon 2} f_c d\varepsilon_c} \qquad \gamma = \frac{\left\{ 8\varepsilon_2^3 \varepsilon_o - 3\varepsilon_2^4 - 8\varepsilon_1^3 \varepsilon_o + 3\varepsilon_1^4 \right\}}{\varepsilon_2 \left\{ 12\varepsilon_2^2 \varepsilon_o - 4\varepsilon_2^3 - 12\varepsilon_1^2 \varepsilon_o + 4\varepsilon_1^3 \right\}}$$

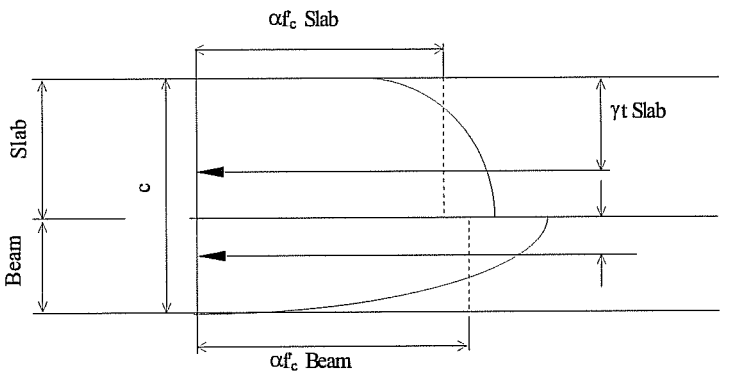

Figure C.1 Concrete Stress Block Over The Slab and Beam

Deflection

Moment Curvature:

$$\Delta = \sum_{n=1}^{n} \left(\frac{\left(\phi_n x_n + \phi_{n+1} x_{n+1}\right)}{2} \right) \left(x_{n+1} - x_n\right)$$

Calculated load-deflection response for test beams is determined using the above theory and calculate by a spreadsheet.

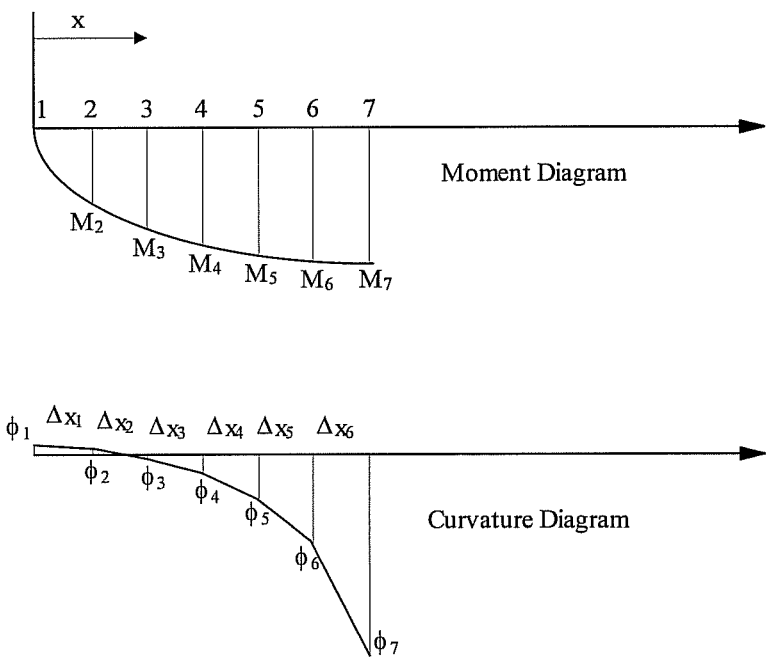

Figure C.2 Moment and Curvature Diagrams

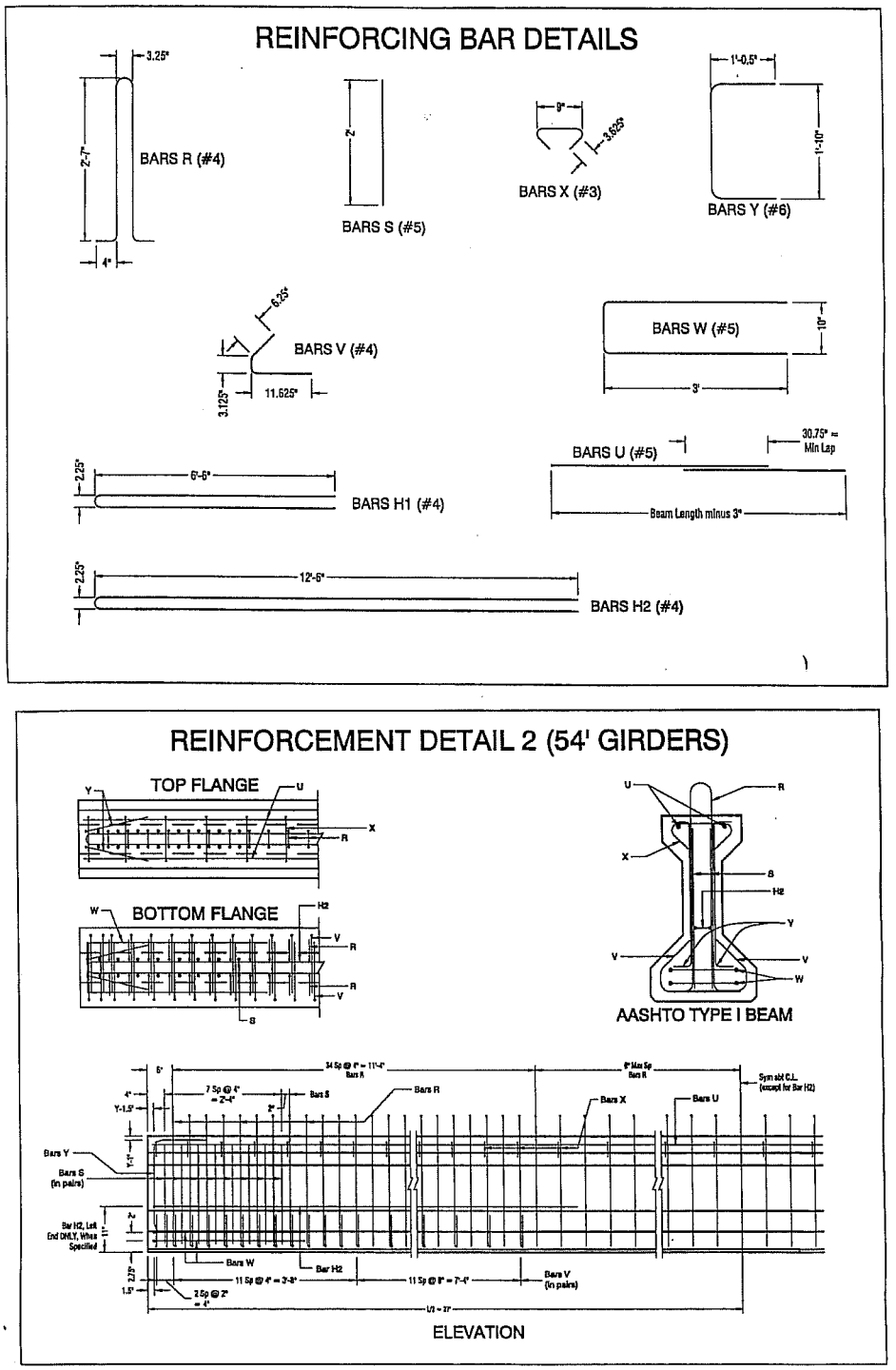

Figure C.3 Details for reinforcement for Test Beams

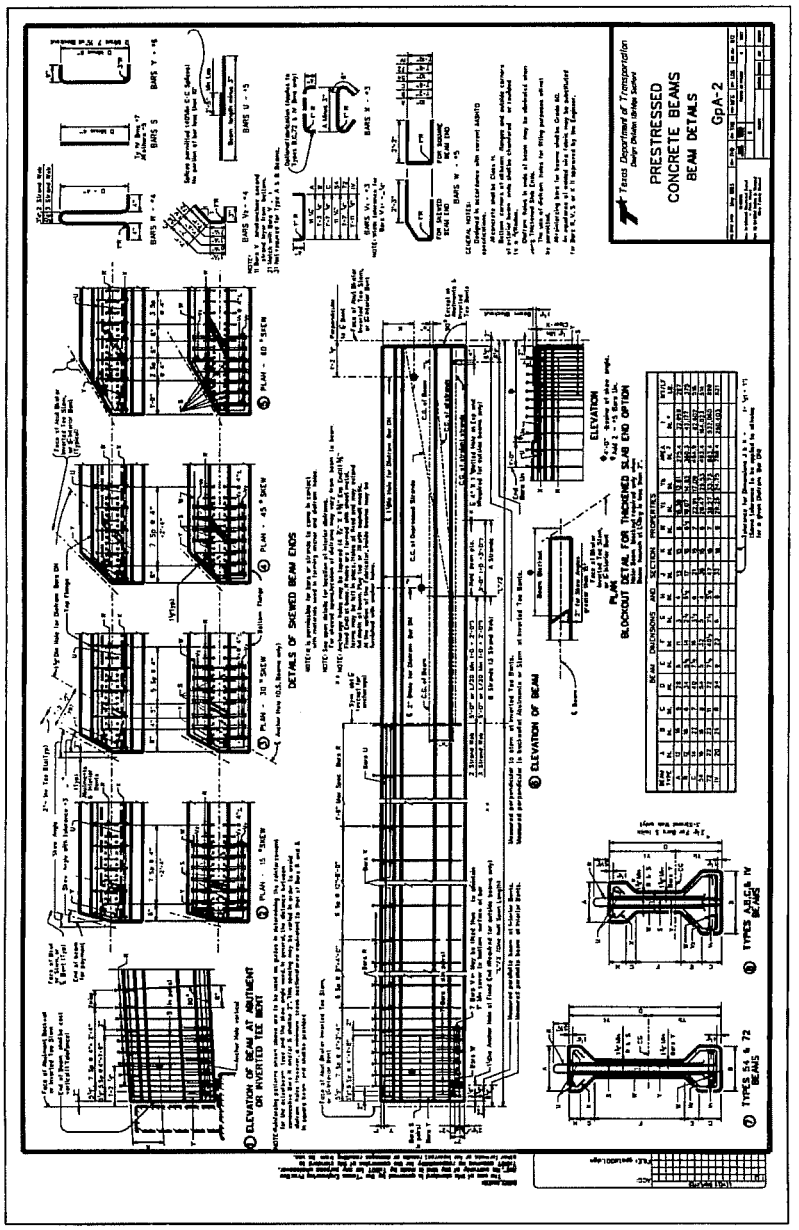

Figure C.4 Texas Department of Transportation Beam Standard

APPENDIX D

DEVELOPMENT LENGTH TEST RESULTS

- **P - Δ Curves**
- **Concrete Strain vs. Applied Load**
- **(f_{su}-f_s) vs. L_{fb}**
- **f_s vs. End Slip**

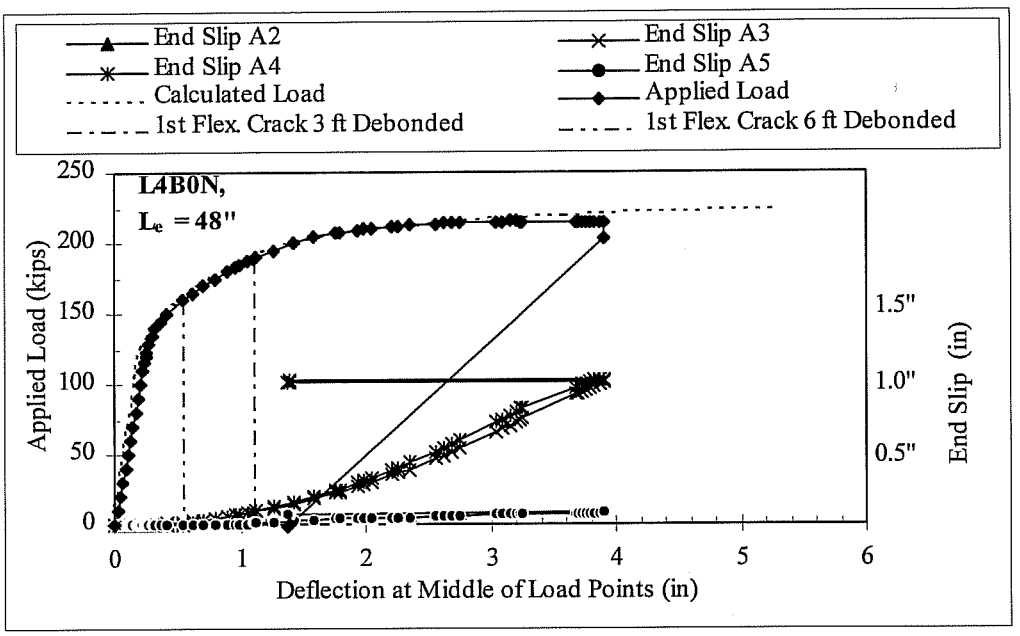

Figure D.1 Load-deflection Curve for Test L4B0N.

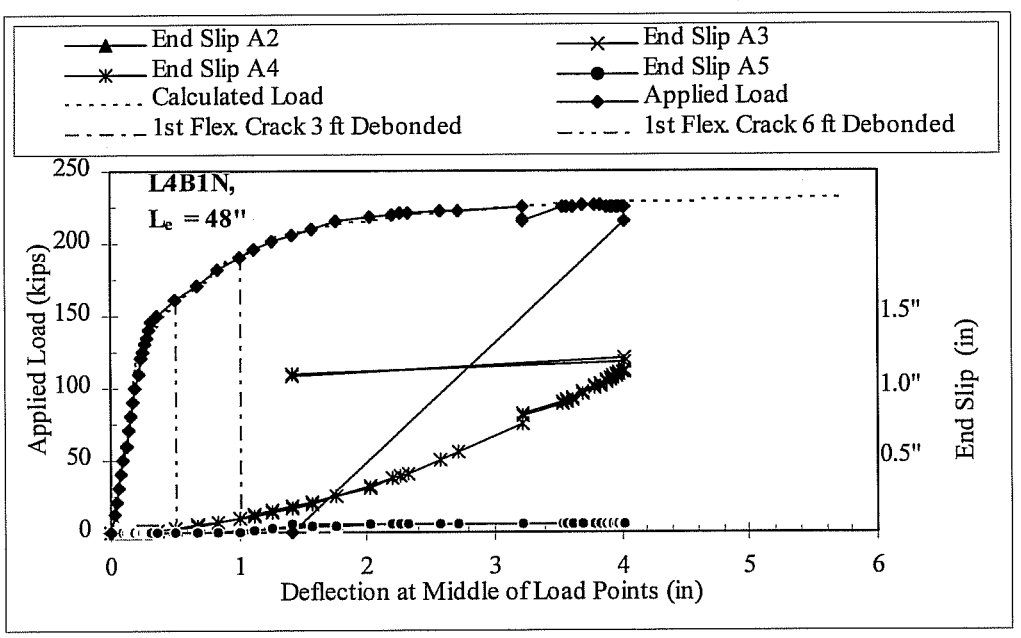

Figure D.2 Load-deflection Curve for Test L4B1N.

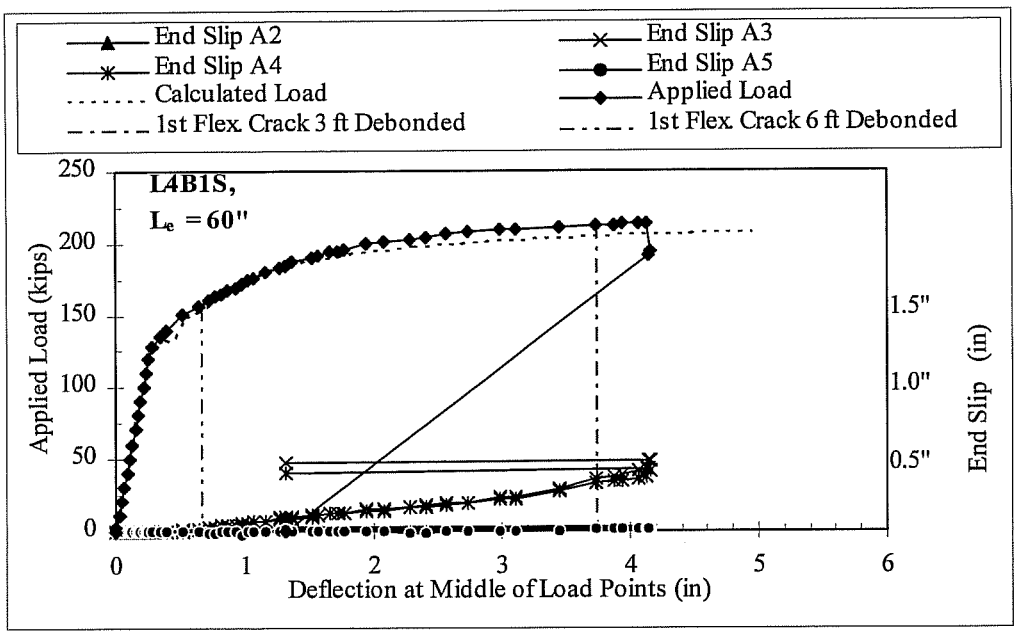

Figure D.3 Load-deflection Curve for Test L4B1S.

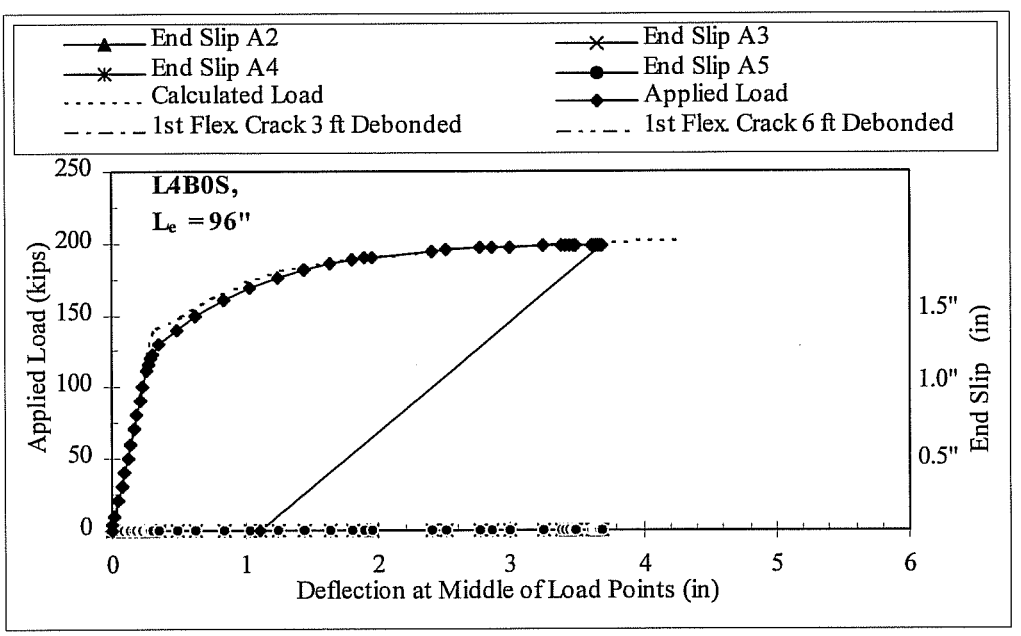

Figure D.4 Load-deflection Curve for Test L4B0S.

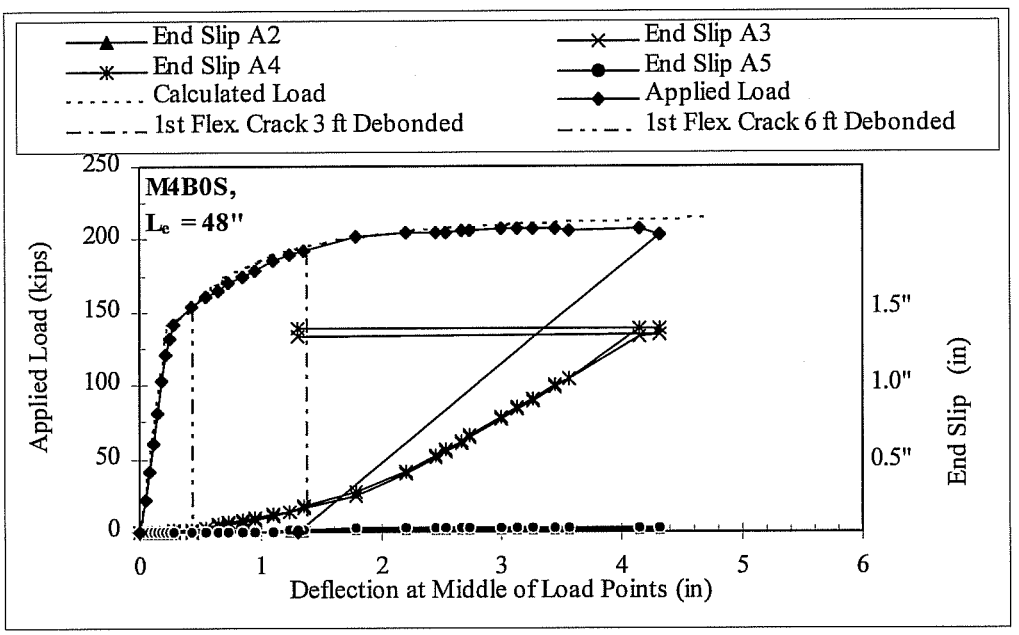

Figure D.5 Load-deflection Curve for Test M4B0S.

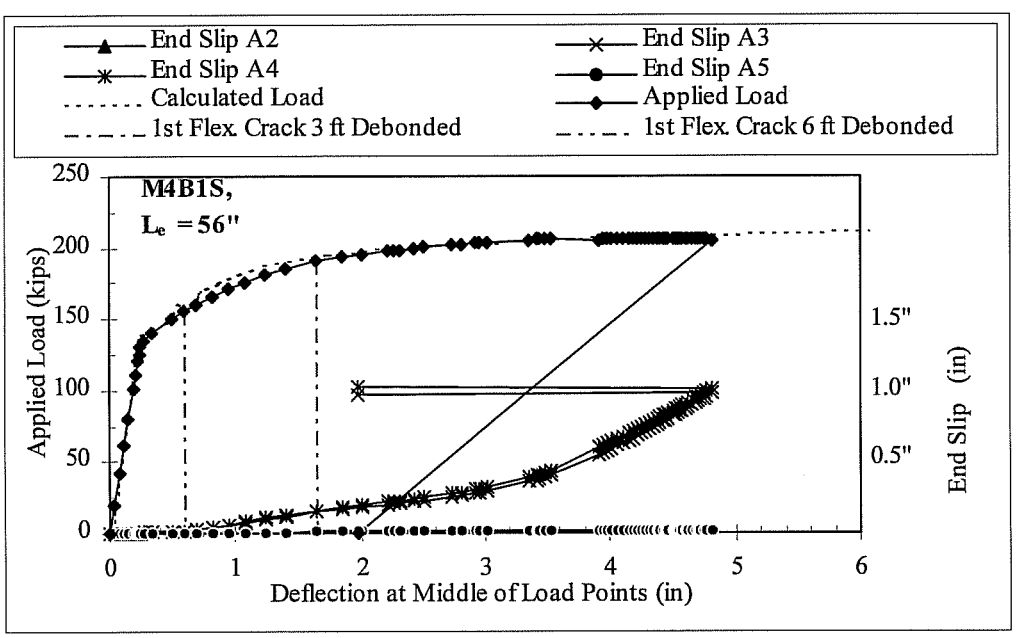

Figure D.6 Load-deflection Curve for Test M4B1S.

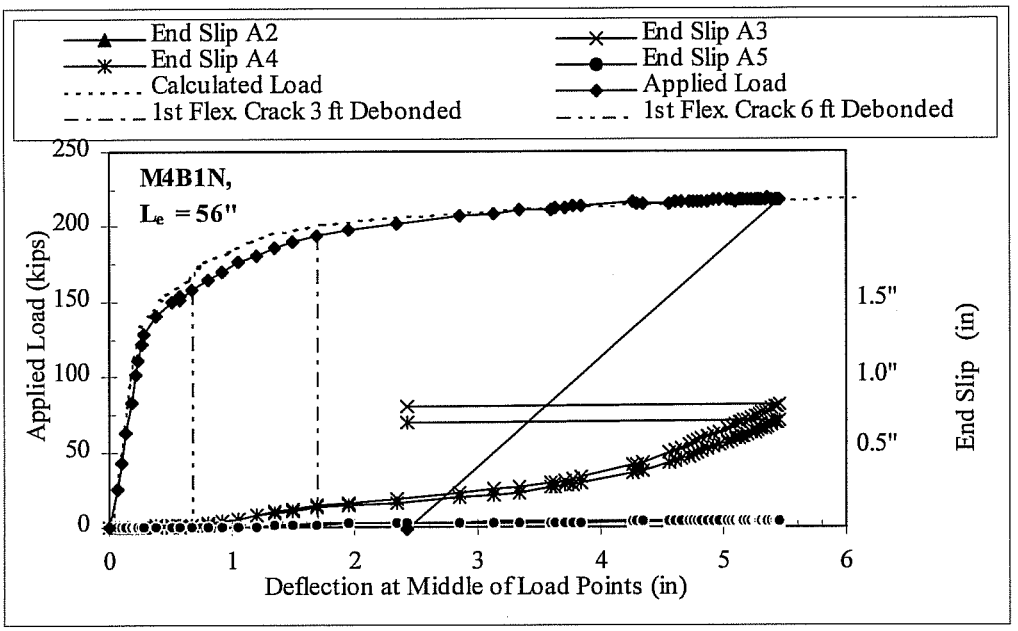

Figure D.7 Load-deflection Curve for Test M4B1N.

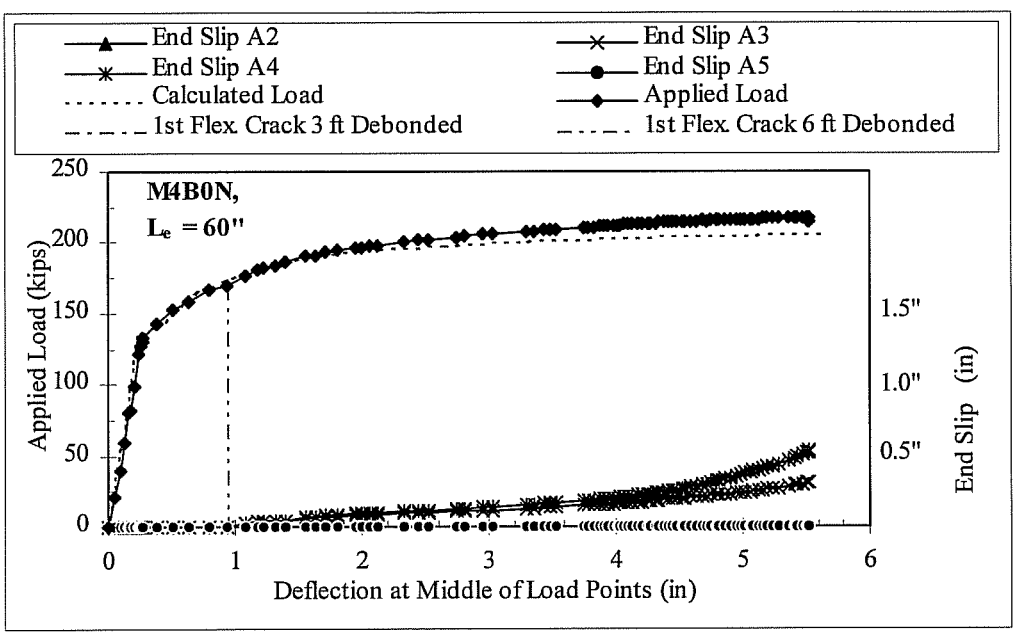

Figure D.8 Load-deflection Curve for Test M4B0N.

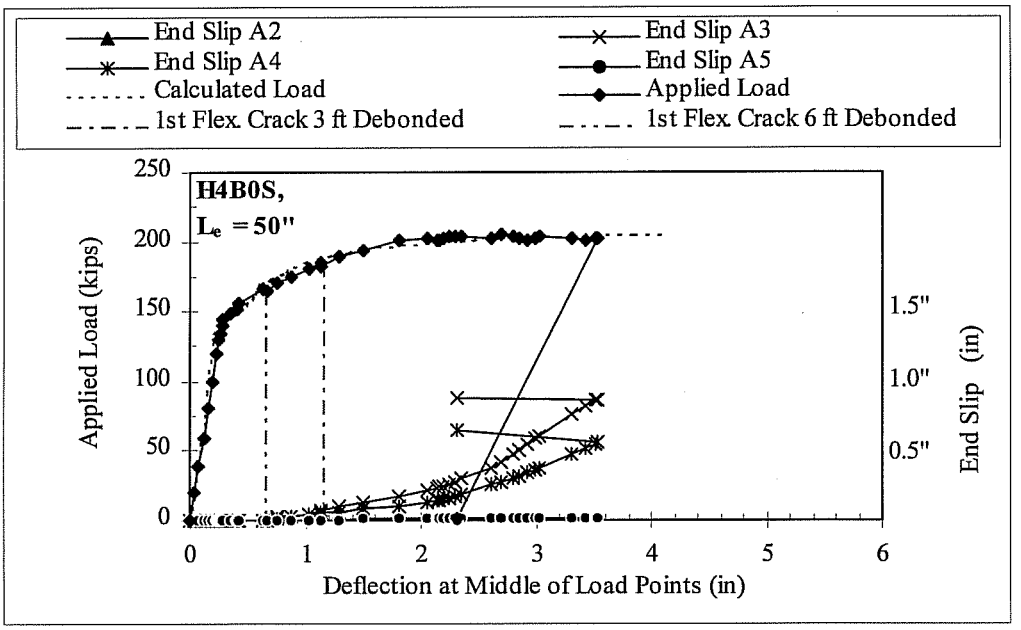

Figure D.9 Load-deflection Curve for Test H4B0S.

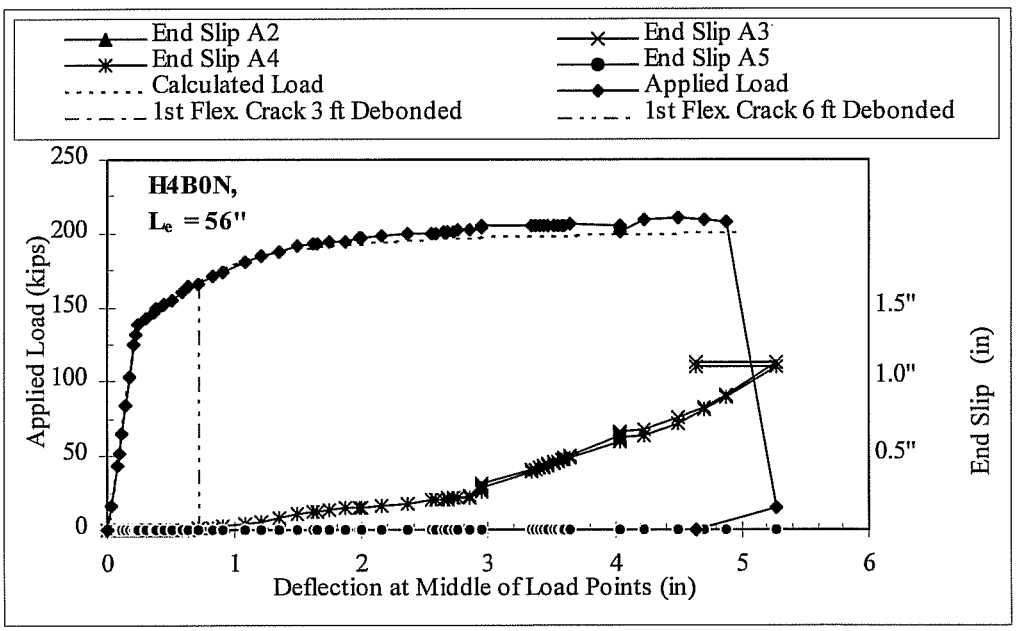

Figure D.10 Load-deflection Curve for Test H4B0N.

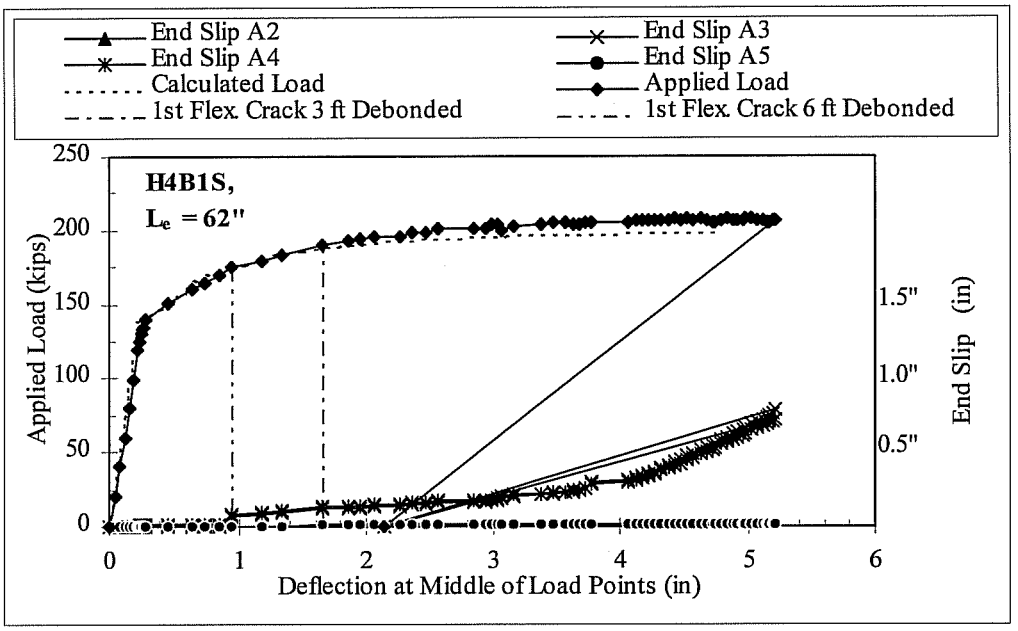

Figure D.11 Load-deflection Curve for Test H4B1S.

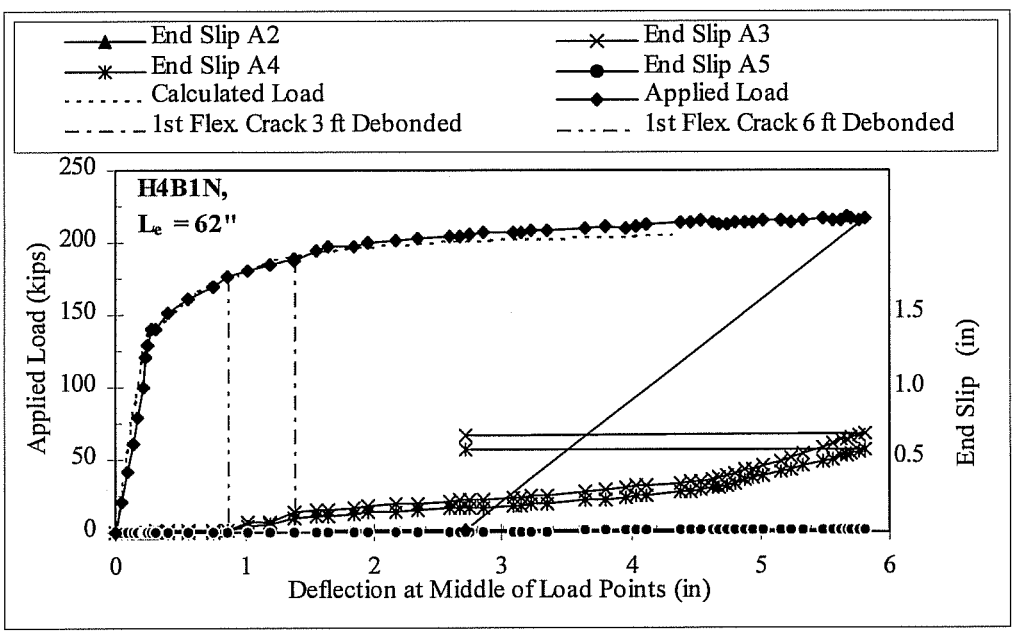

Figure D.12 Load-deflection Curve for Test H4B1N.

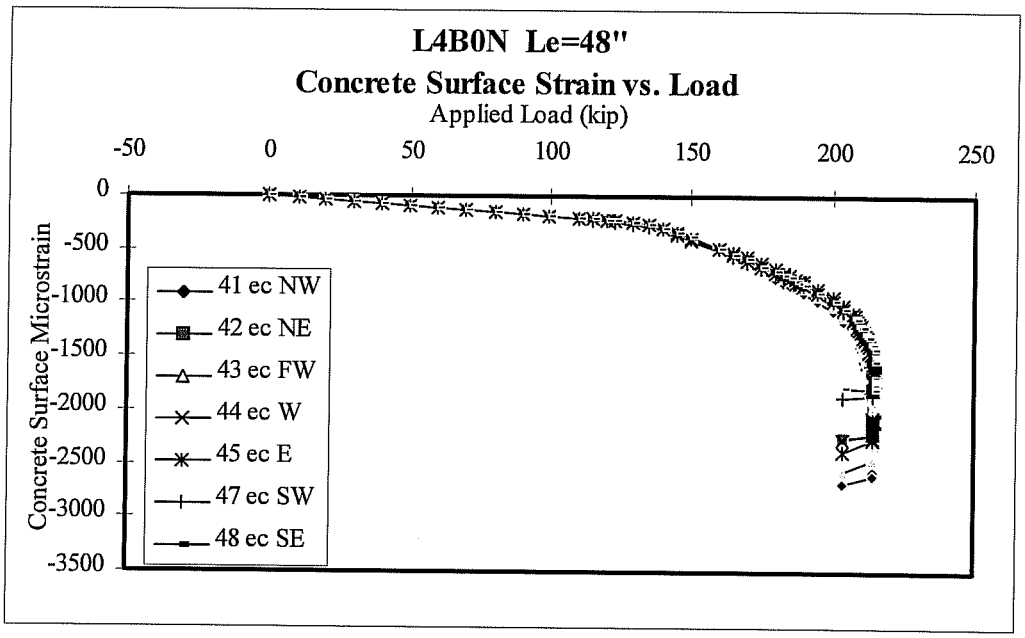

Figure D.13 Concrete Strain vs. Load: Test L4B0N.

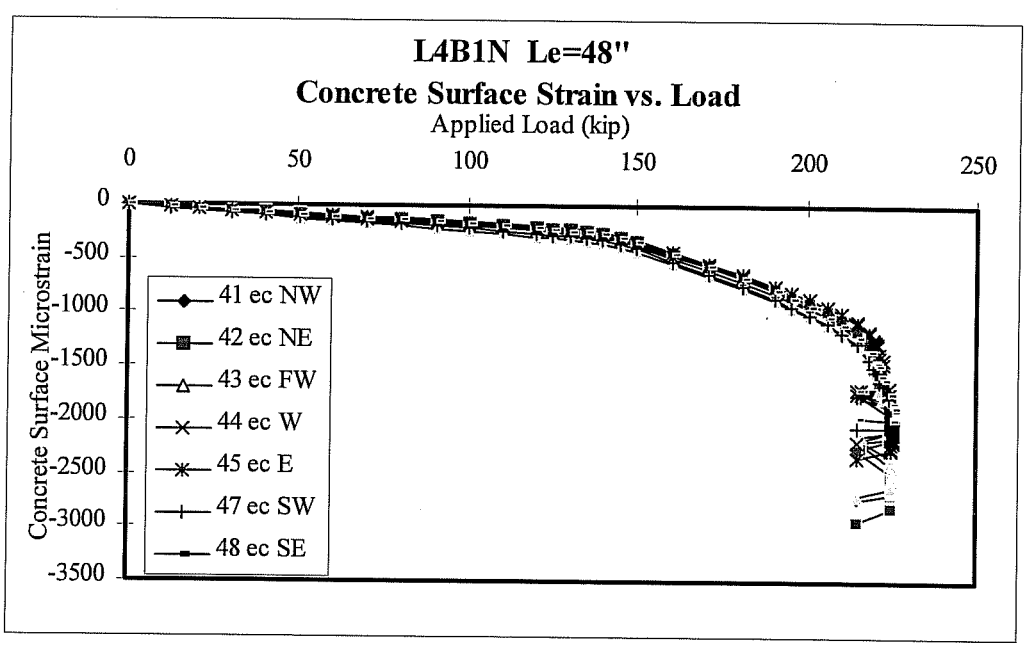

Figure D.14 Concrete Strain vs. Load: Test L4B1N.

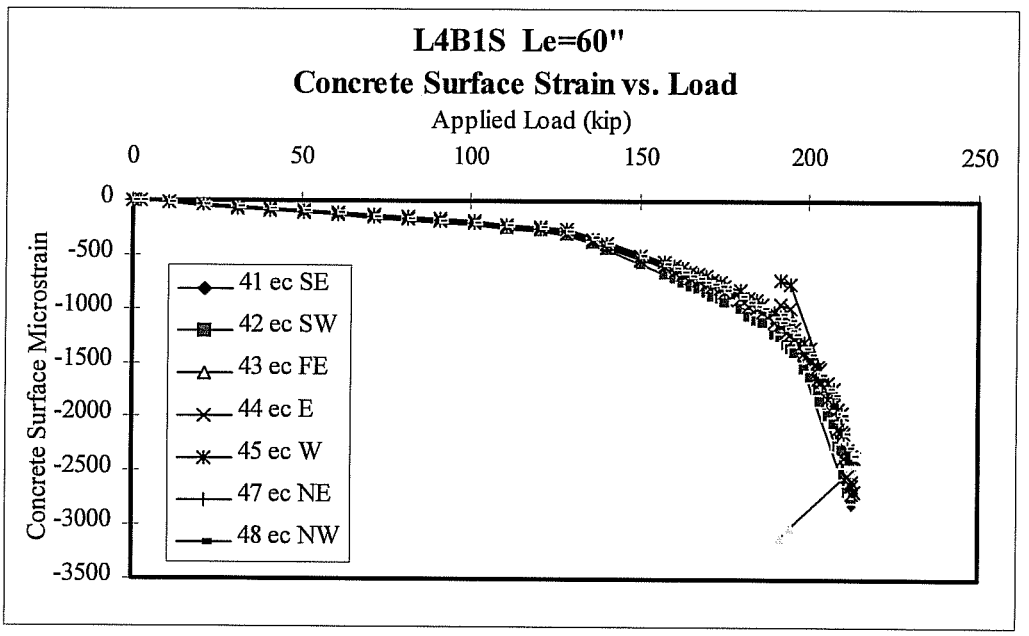

Figure D.15 Concrete Strain vs. Load: Test L4B1S.

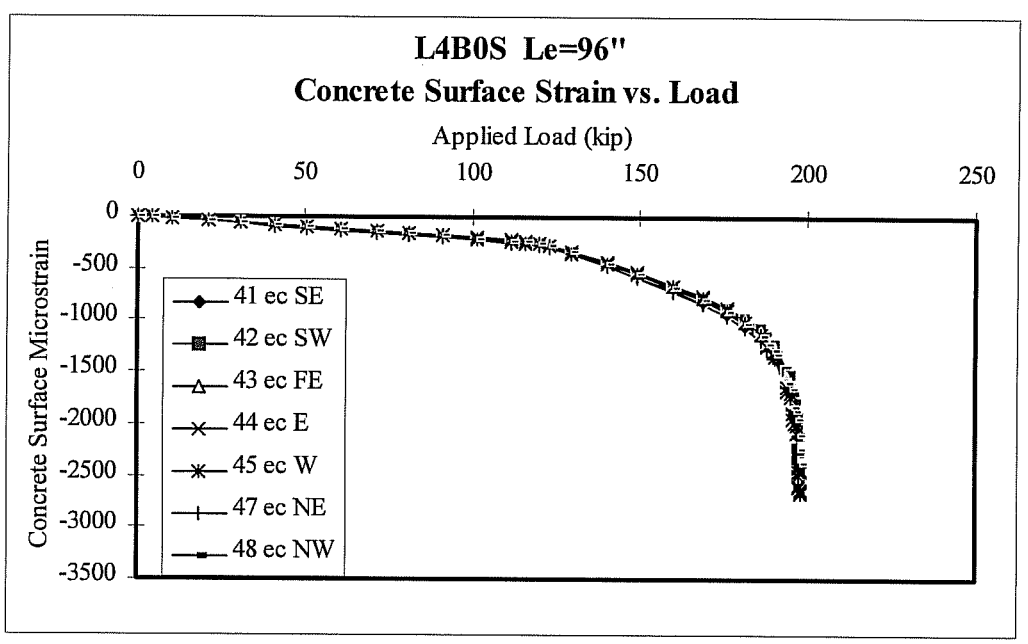

Figure D.16 Concrete Strain vs. Load: Test L4B0S.

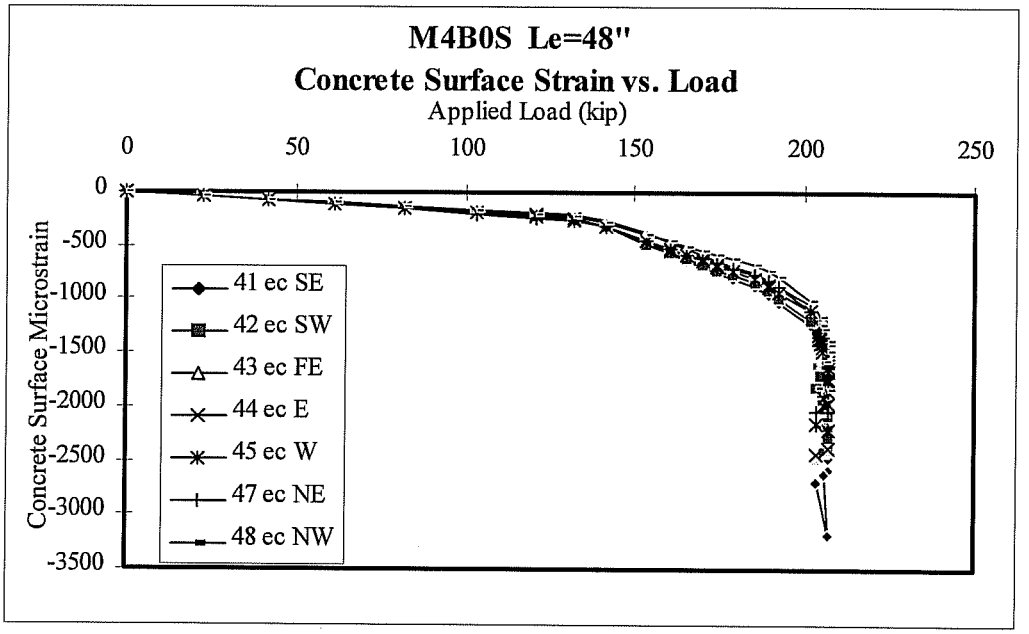

Figure D.17 Concrete Strain vs. Load: Test M4B0S.

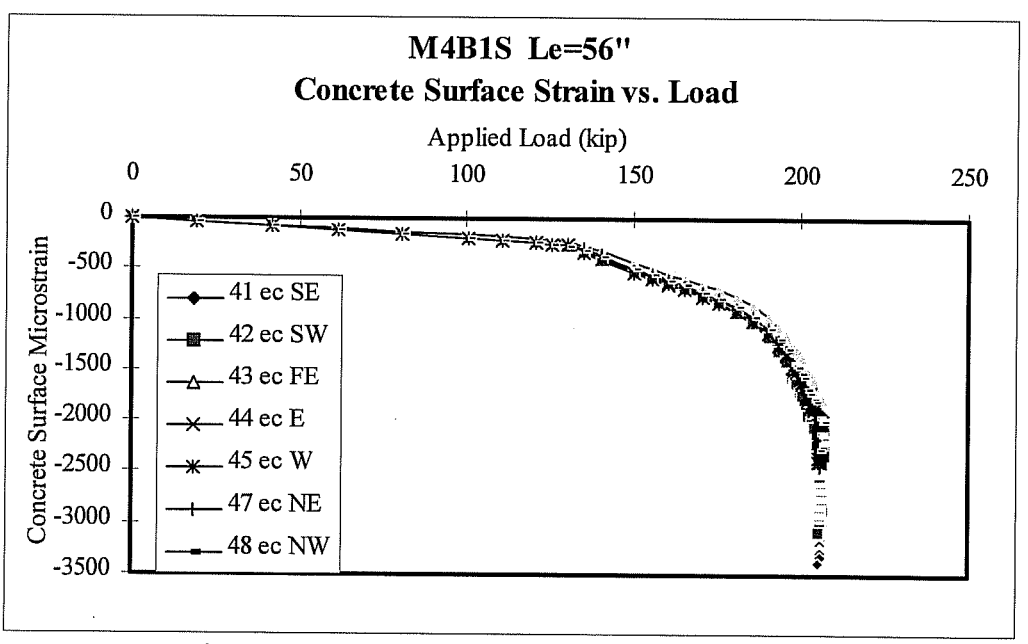

Figure D.18 Concrete Strain vs. Load: Test M4B1S.

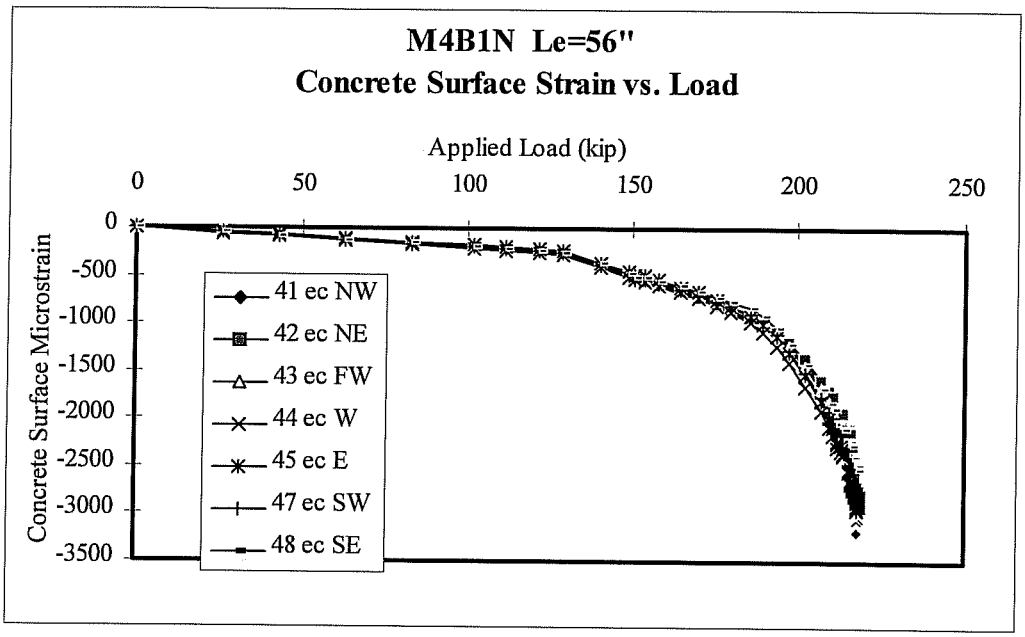

Figure D.19 Concrete Strain vs. Load: Test M4B1N.

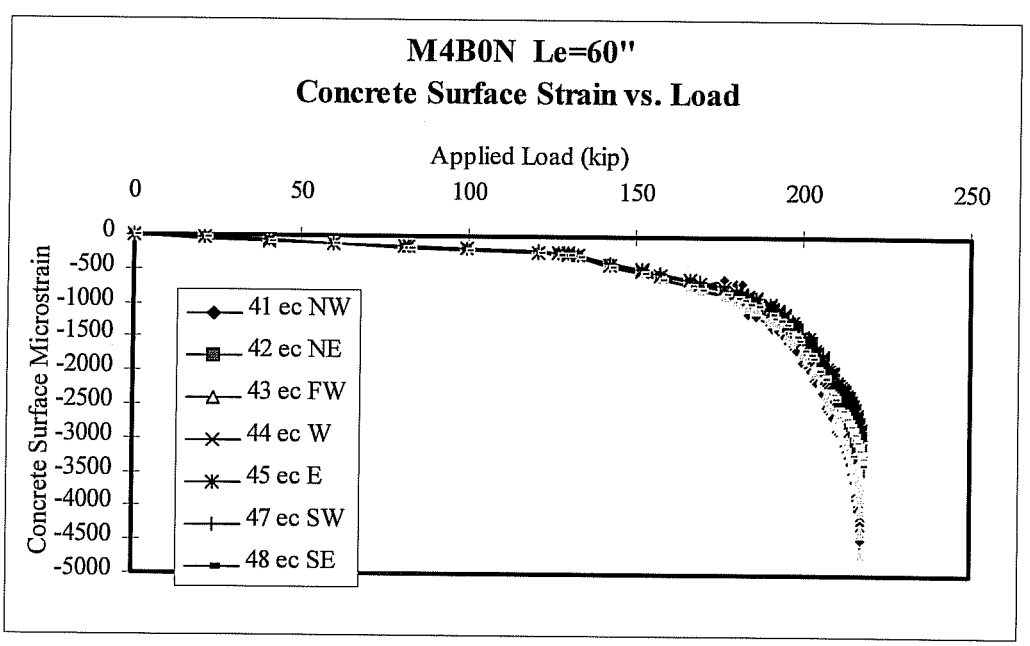

Figure D.20 Concrete Strain vs. Load: Test M4B0N.

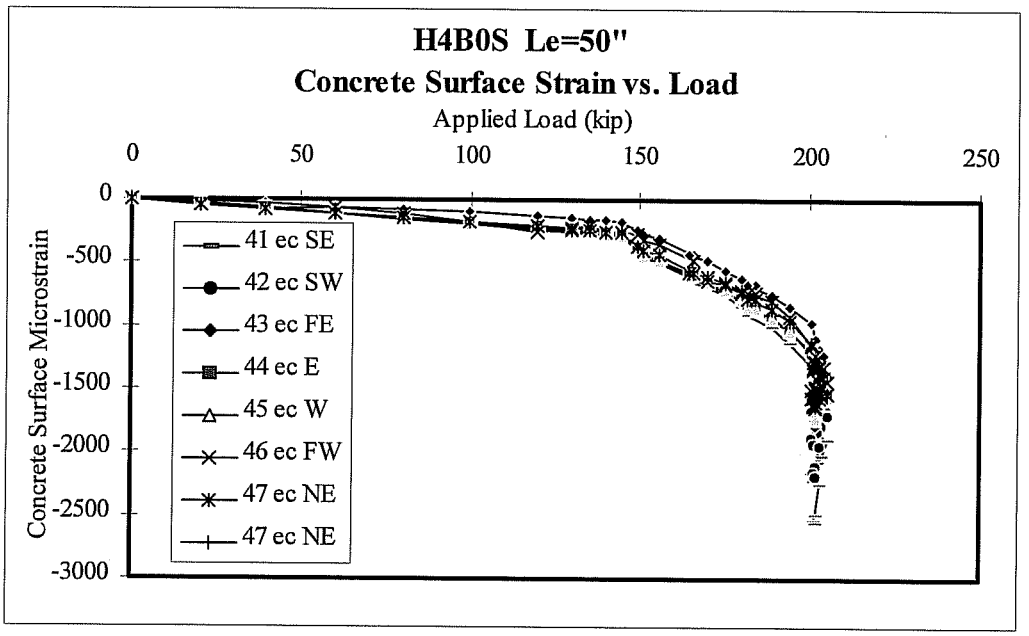

Figure D.21 Concrete Strain vs. Load: Test H4B0S.

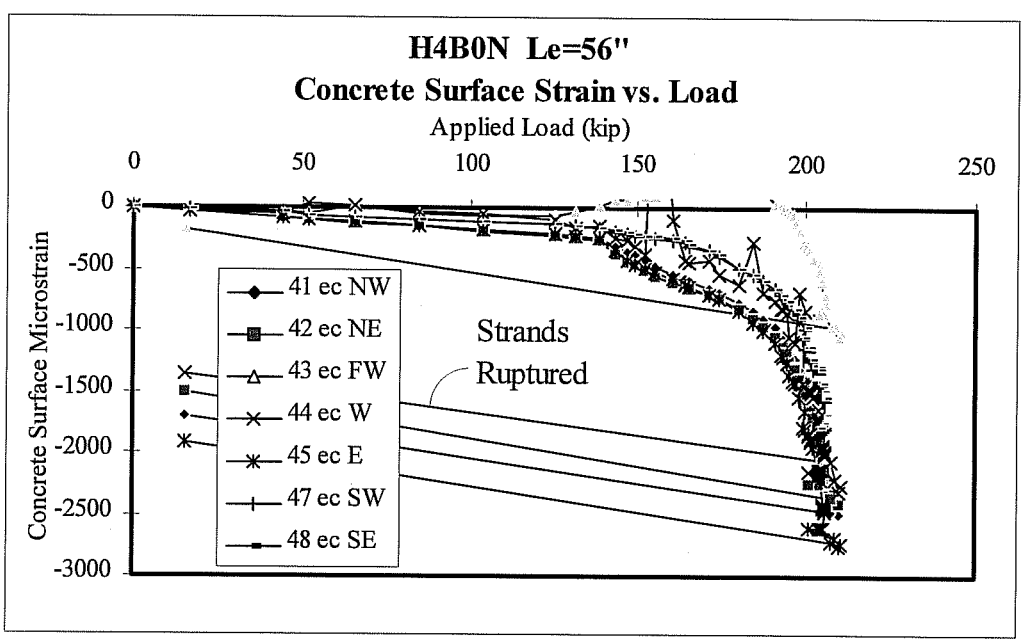

Figure D.22 Concrete Strain vs. Load: Test H4B0N.

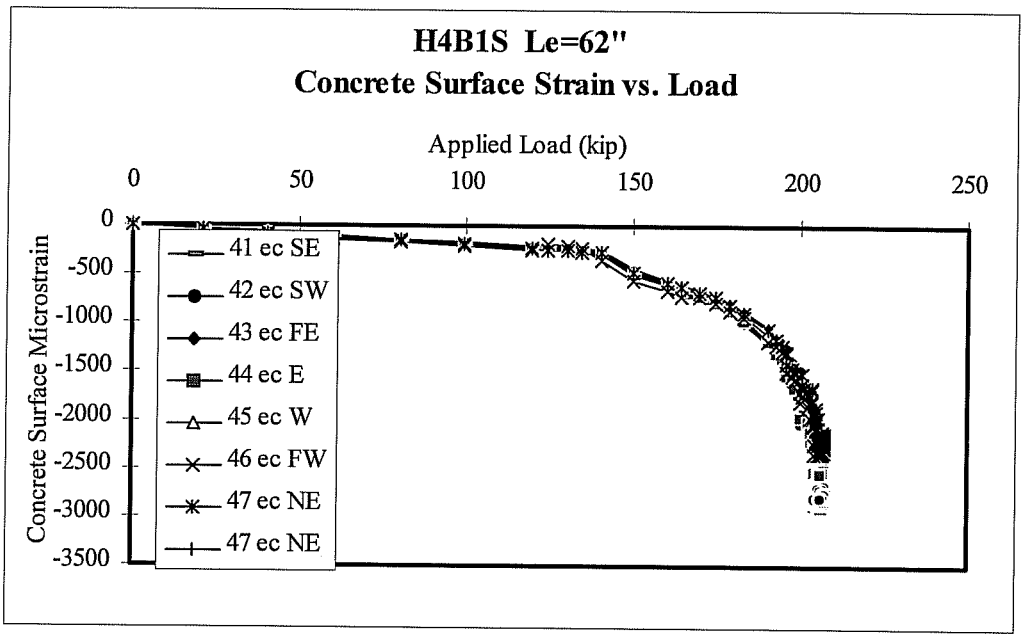

Figure D.23 Concrete Strain vs. Load: Test H4B1S.

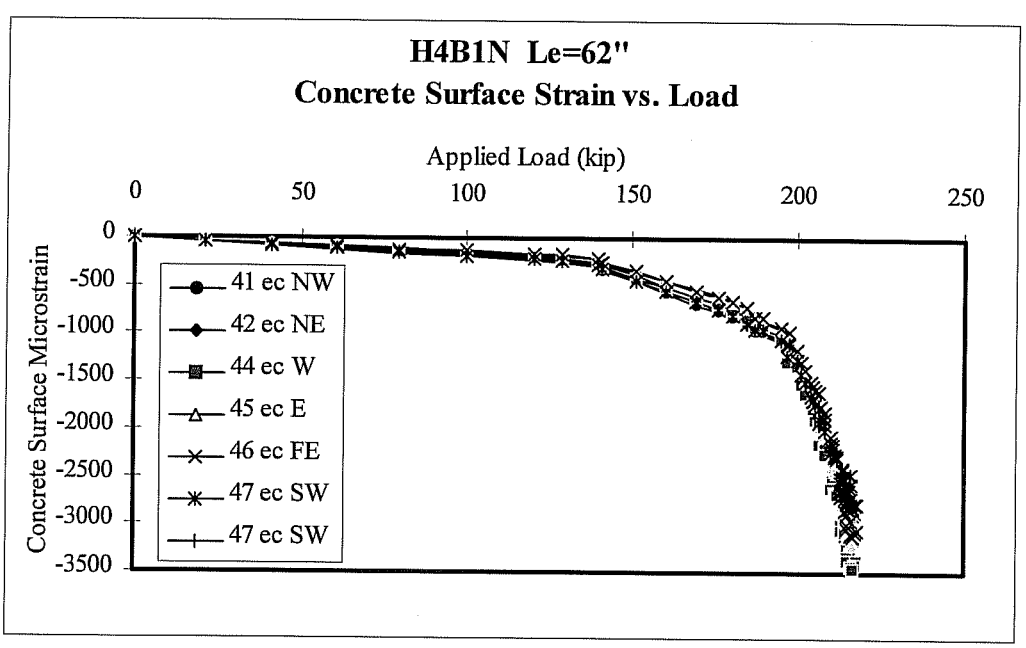

Figure D.24 Concrete Strain vs. Load: Test H4B1N.

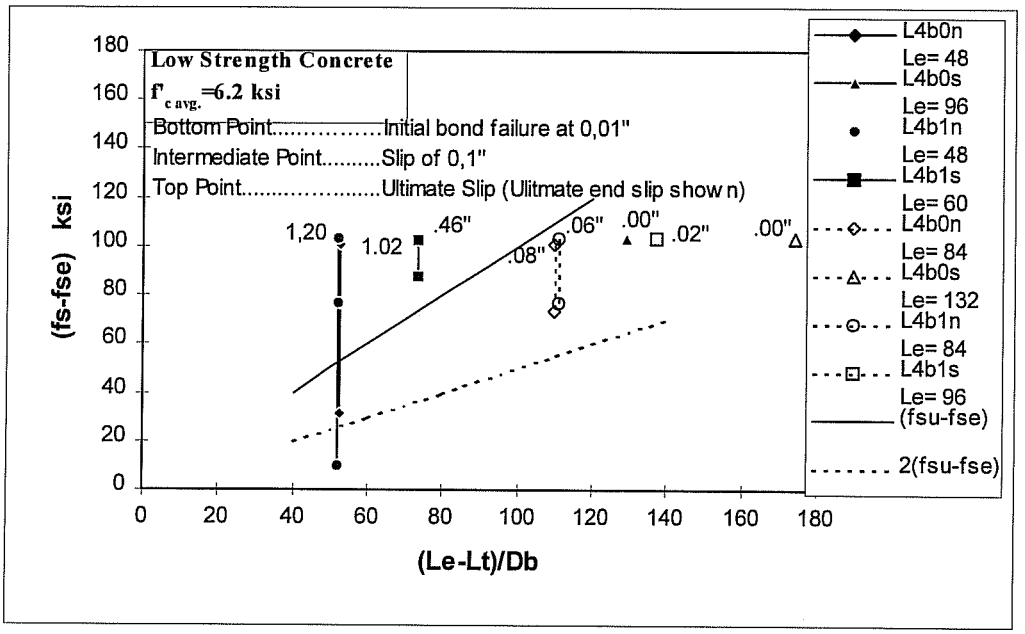

Figure D.25 Flexural Bond vs. Flexural Bond Length (f'c=6.2 ksi).

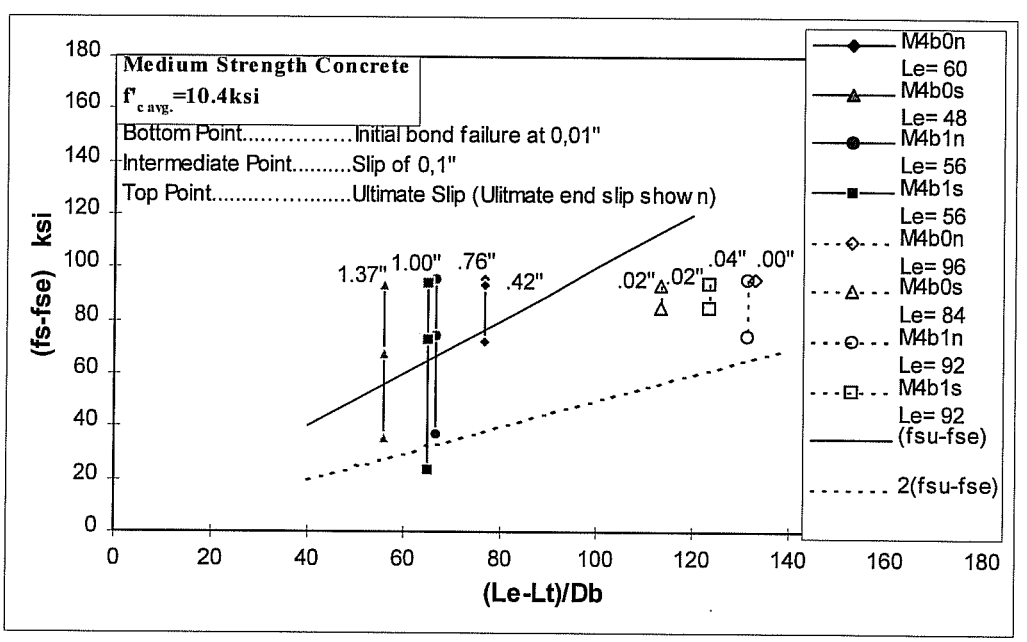

Figure D.26 Flexural Bond vs. Flexural Bond Length (f'c=10.4 ksi).

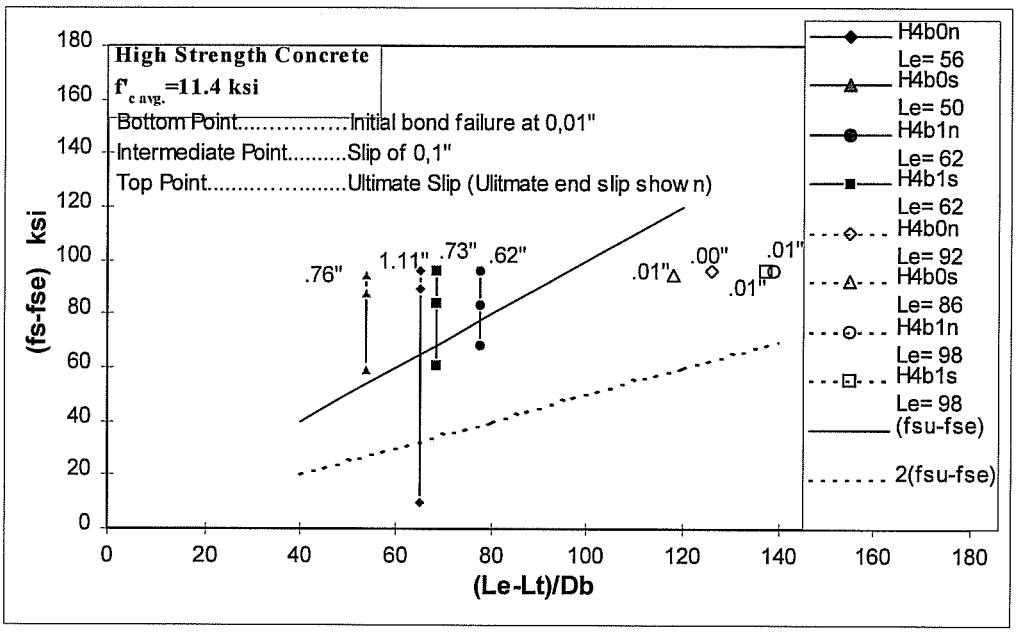

Figure D.27 Flexural Bond vs. Flexural Bond Length (f'c=11.4 ksi).

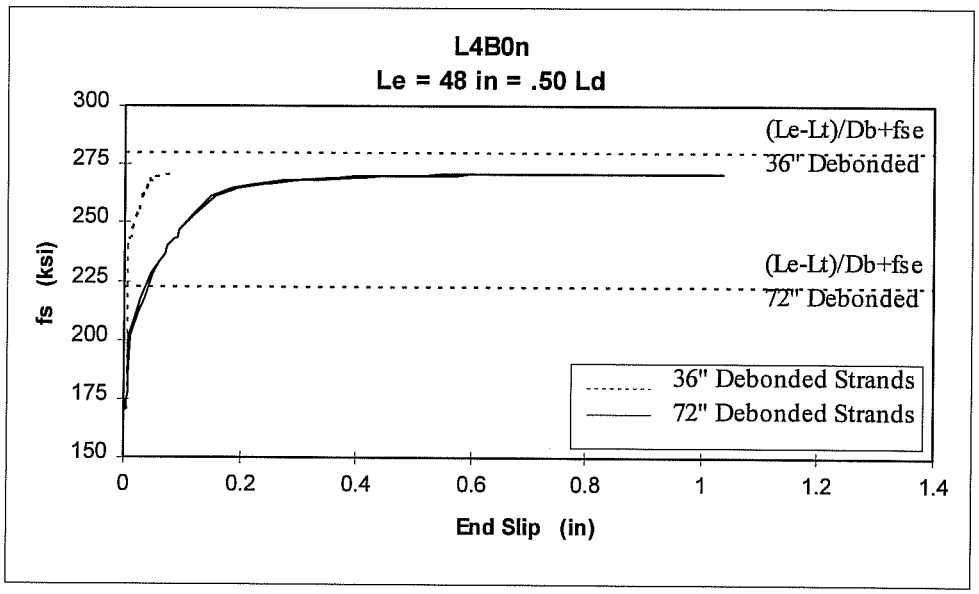

Figure D.28 f_s vs. End Slip: Test L4B0N.

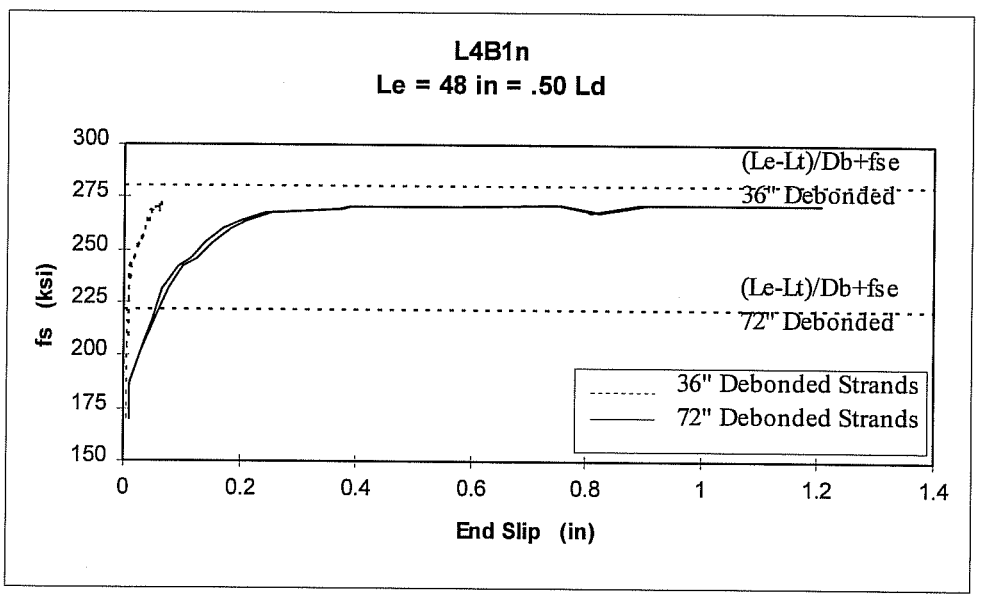

Figure D.29 f_s vs. End Slip: Test L4B1N.

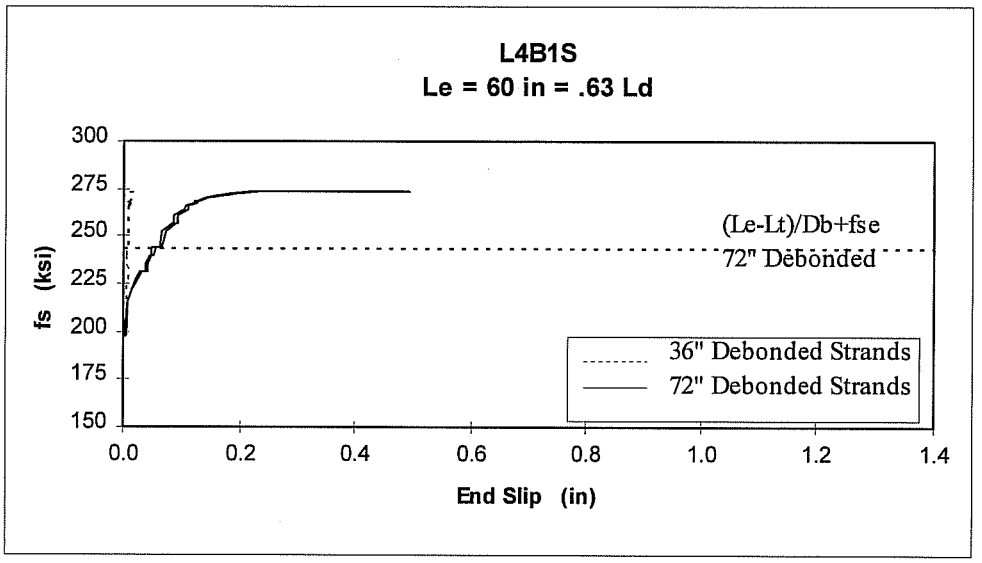

Figure D.30 f_s vs. End Slip: Test L4B1S.

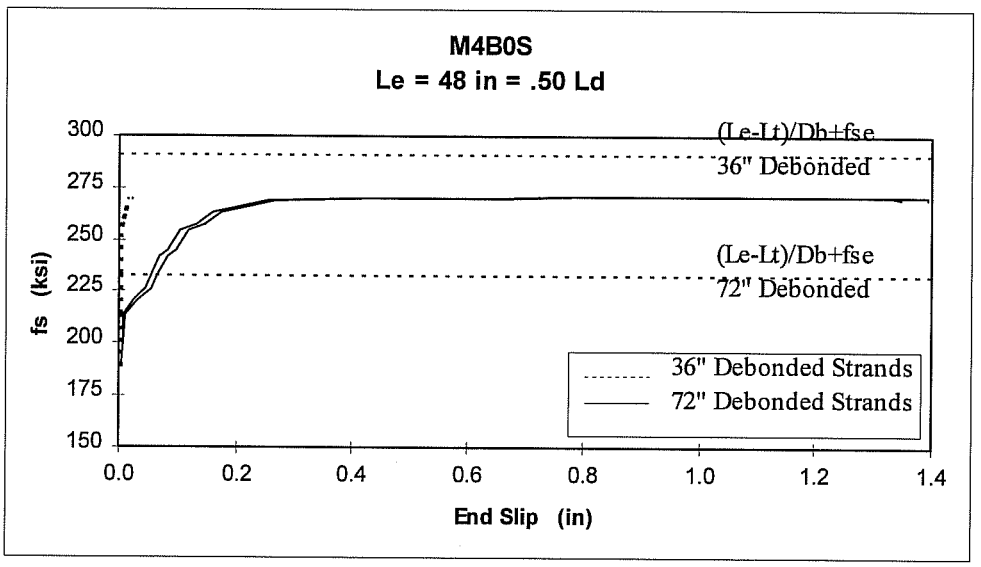

Figure D.31 f_s vs. End Slip: Test M4B0S.

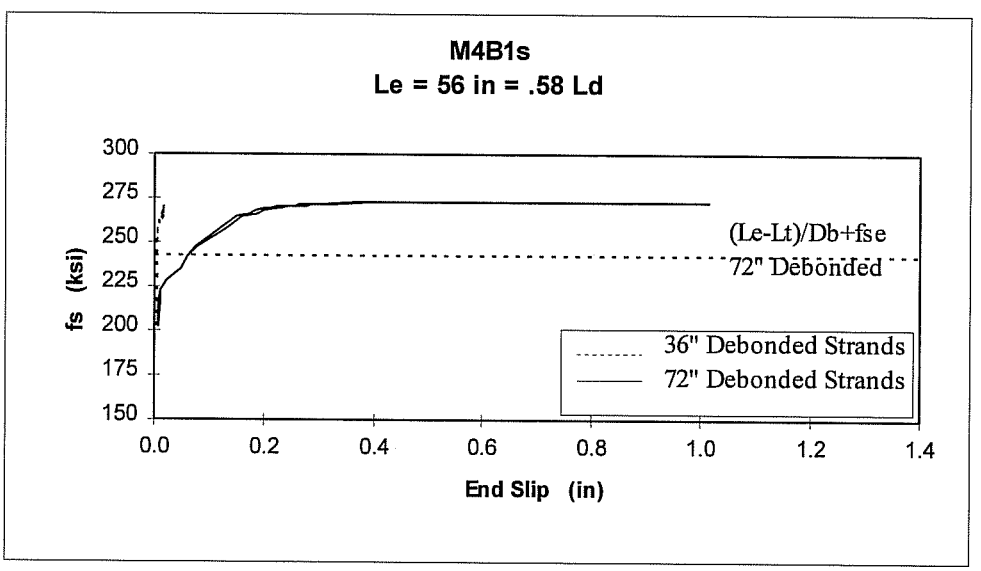

Figure D.32 f_s vs. End Slip: Test M4B1S.

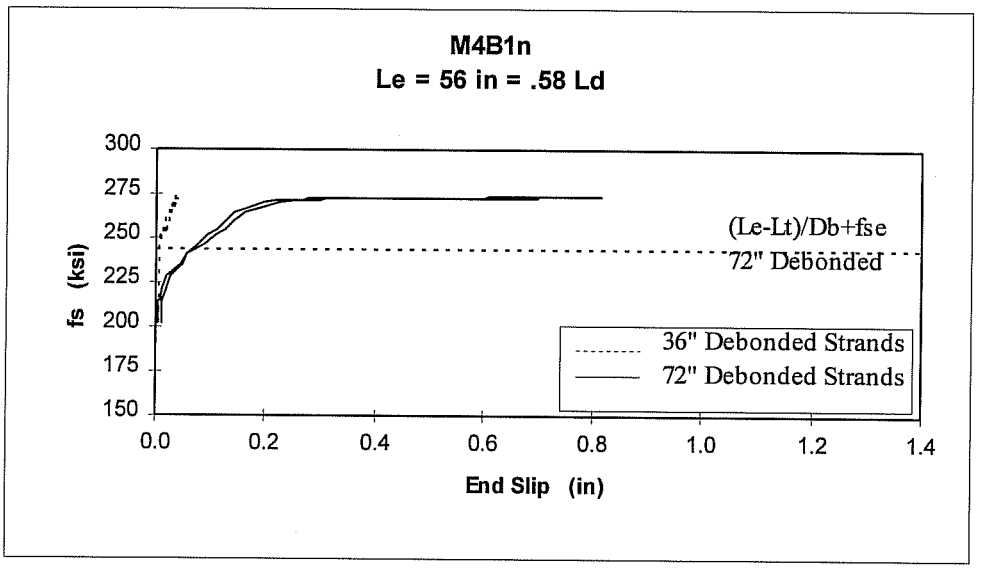

Figure D.33 f_s vs. End Slip: Test M4B1N.

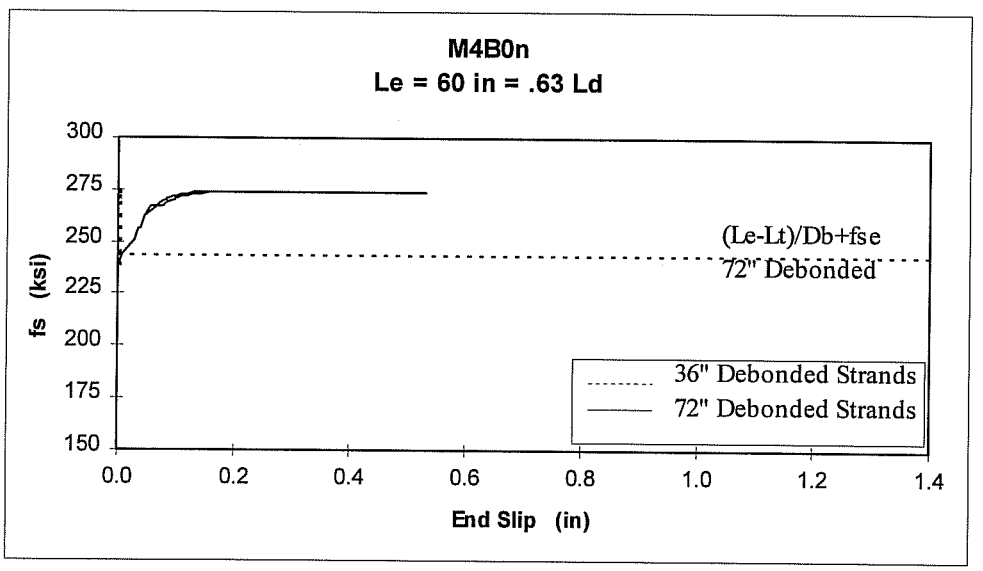

Figure D.34 f_s vs. End Slip: Test M4B0N.

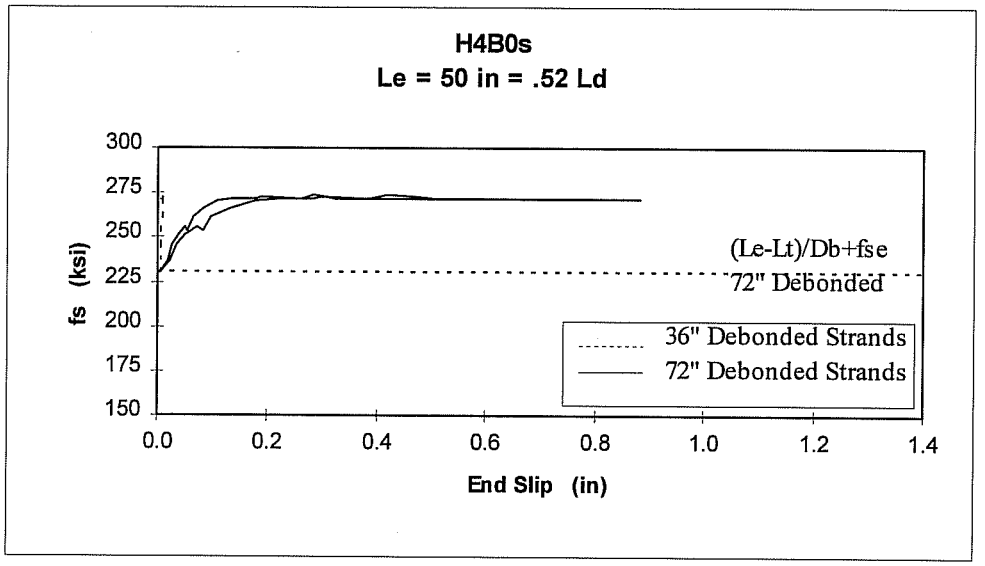

Figure D.35 f_s vs. End Slip: Test H4B0S.

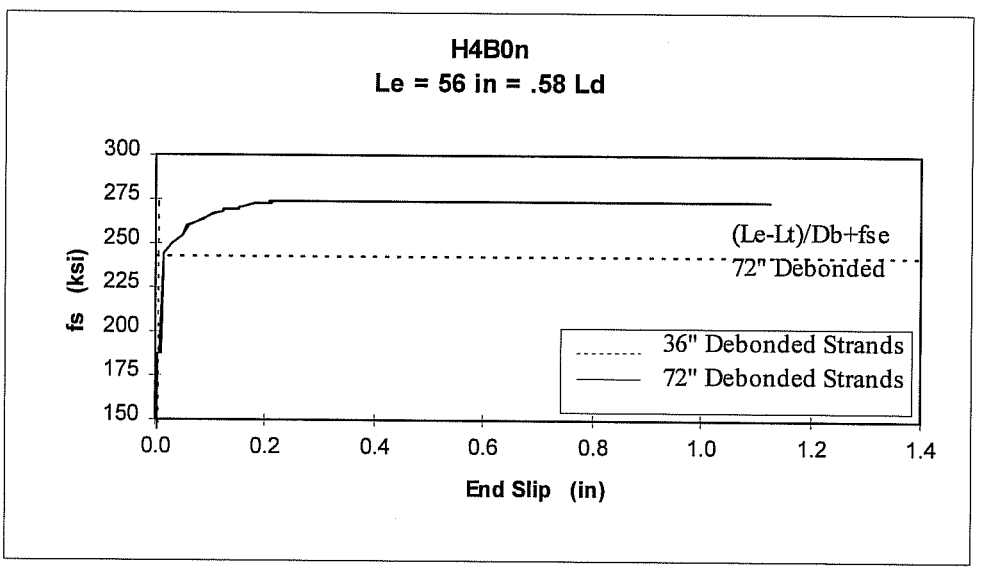

Figure D.36 f_s vs. End Slip: Test H4B0N.

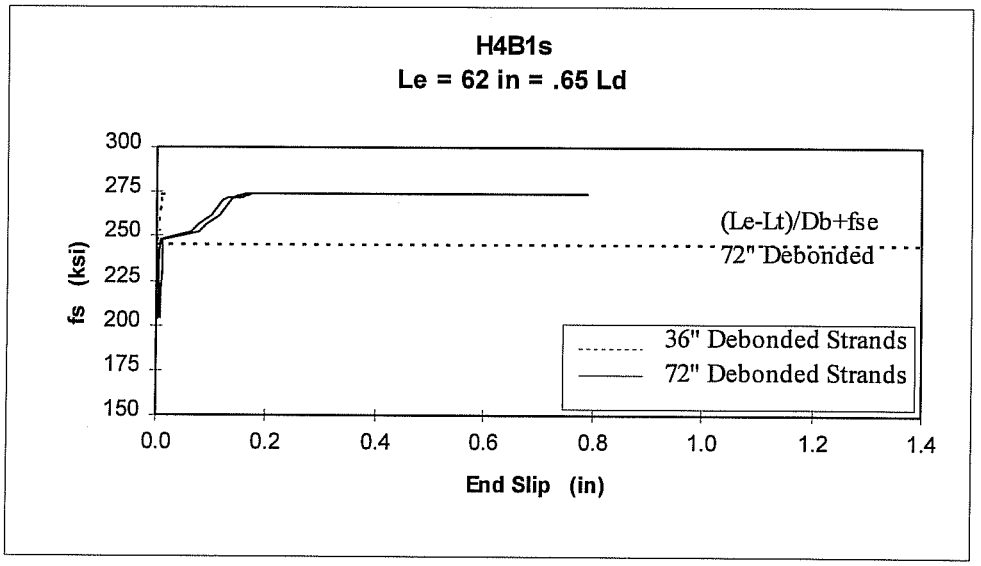

Figure D.37 f_s vs. End Slip: Test H4B1S.

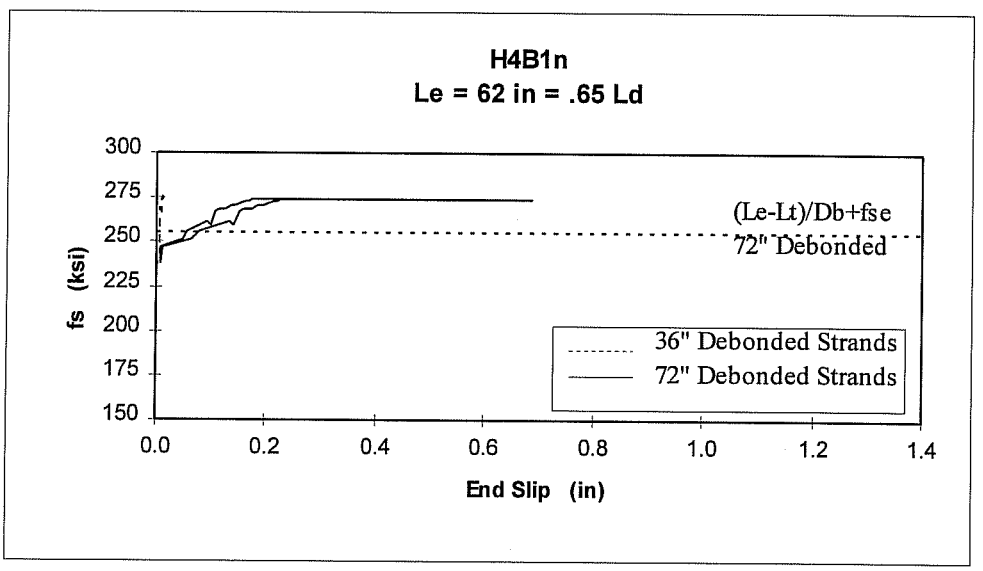

Figure D.38 f_s vs. End Slip: Test H4B1N.

APPENDIX E

PULL-OUT TEST RESULTS
&
END SLIP MEASUREMENTS
AT TRANSFER
(PULL IN)

TABLE E.1 PULL-OUT TEST RESULTS

Test Beam: L4BX

f'c: 5720 ksi (Sure Cure Strength)

Embedment Length in	Peak Load kips	Peak Stress ksi	Pull-out Length in	Failure Type
18	46.1	212	1.15	Pull-out
18	51.0	235	1.15	Pull-out
18	54.1	249	1.25	Pull-out
20	58.7	271	1.25	Pull-out
20	54.1	249	1.15	Pull-out
20	53.9	248	0.75	Pull-out

TABLE E.2 PULL-OUT TEST RESULTS

Test Beam: M4BX

f'c: 9970 ksi (Sure Cure Strength)

Embedment Length in	Peak Load kips	Peak Stress ksi	Pull-out Length in	Failure Type
18	61.8	285	0.50	Fracture
18	62.1	286	0.55	Fracture
18	62.1	286	0.45	Fracture
20	61.8	285	0.65	Fracture

TABLE E.3 PULL-OUT TEST RESULTS

Test Beam: H4BX

f'c: 10740 ksi (Sure Cure Strength)

Embedment Length in	Peak Load kips	Peak Stress ksi	Pull-out Length in	Failure Type
18	43.0	198	2.15	Pull-out
18	38.2	176	1.75	Pull-out
18	30.0	138	1.50	Pull-out
18	33.6	155	1.75	Pull-out
18	39.9	184	2.00	Pull-out
18	49.3	227	1.90	Pull-out

PULL-OUT TEST BLOCK DIMENSIONS

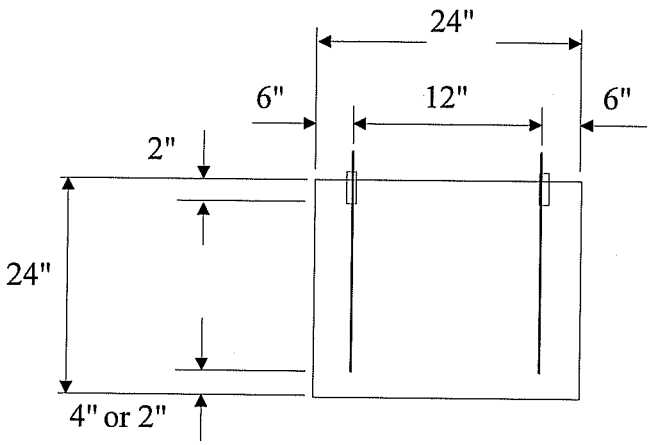

END VIEW

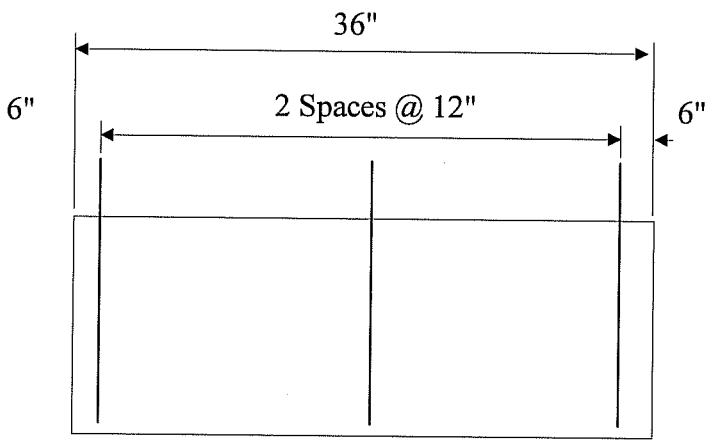

SIDE VIEW

Figure E.1 Pull-out Block Dimensions

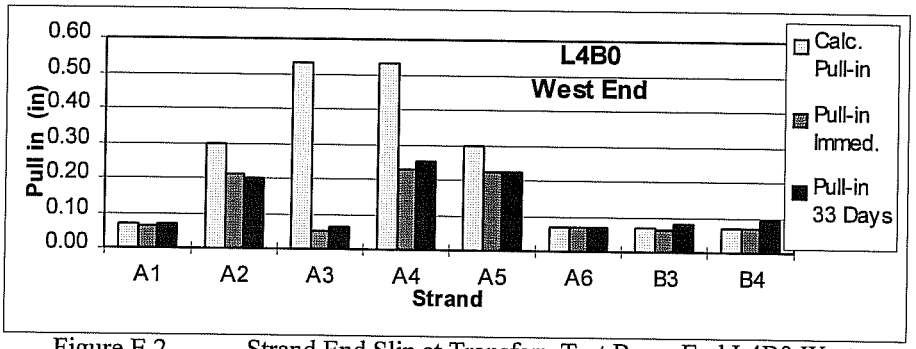

Figure E.2 Strand End Slip at Transfer: Test Beam End L4B0 West

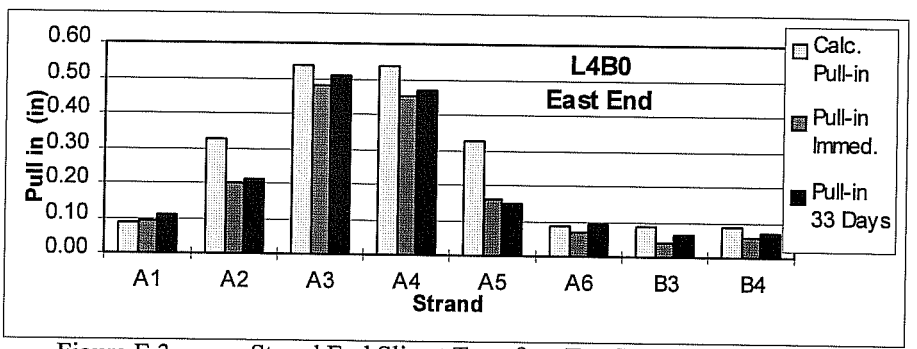

Figure E.3 Strand End Slip at Transfer: Test Beam End L4B0 East

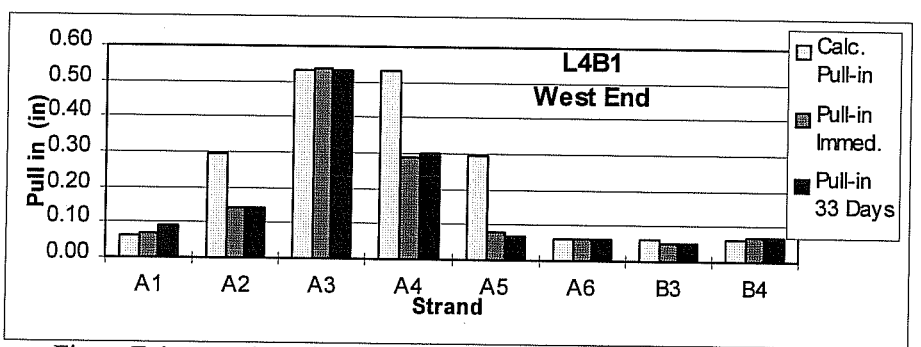

Figure E.4 Strand End Slip at Transfer: Test Beam End L4B1 West

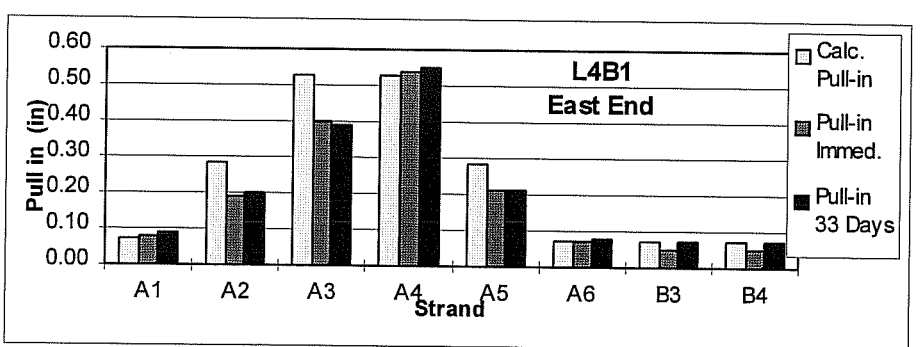

Figure E.5 Strand End Slip at Transfer: Test Beam End L4B1 East

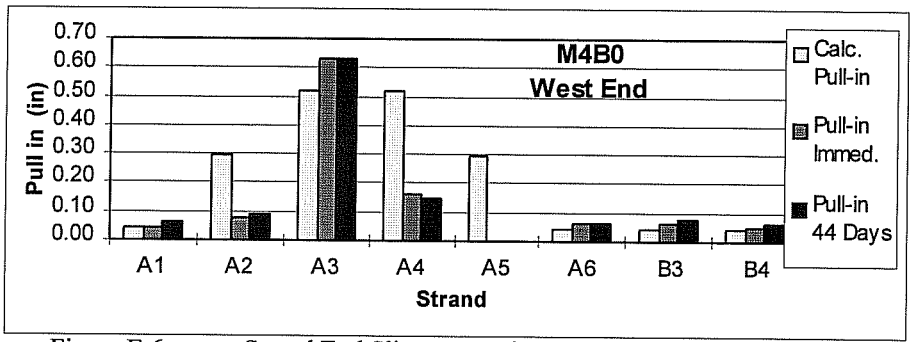

Figure E.6 Strand End Slip at Transfer: Test Beam End M4B0 West

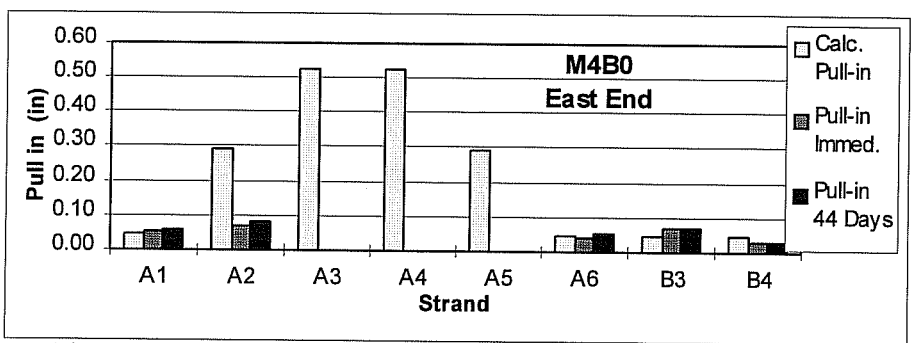

Figure E.7 Strand End Slip at Transfer: Test Beam End M4B0 East

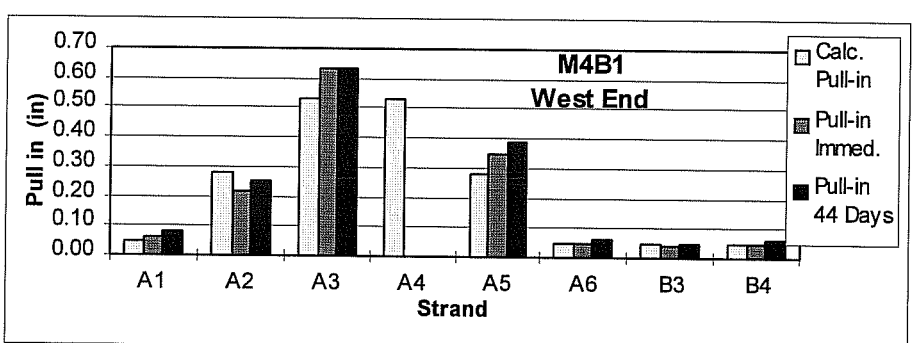

Figure E.8 Strand End Slip at Transfer: Test Beam End M4B1 West

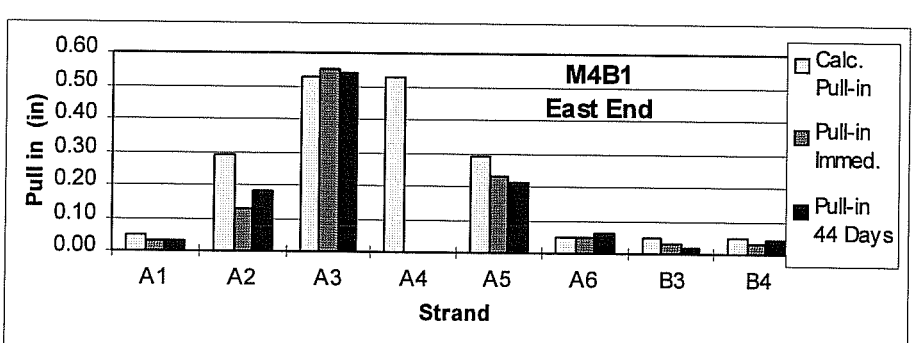

Figure E.9 Strand End Slip at Transfer: Test Beam End M4B1 East

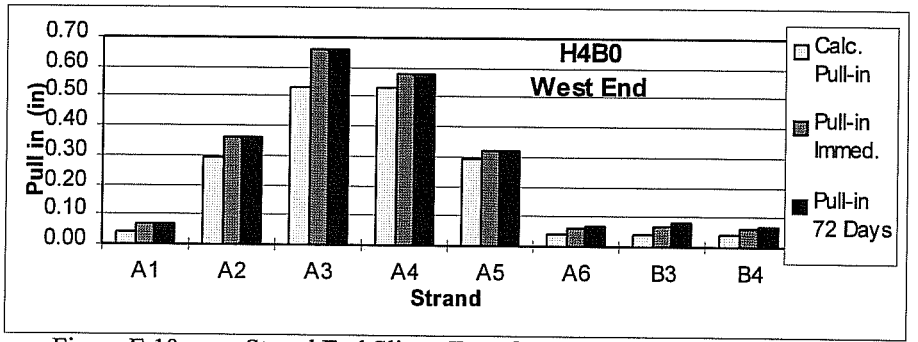

Figure E.10 Strand End Slip at Transfer: Test Beam End H4B0 West

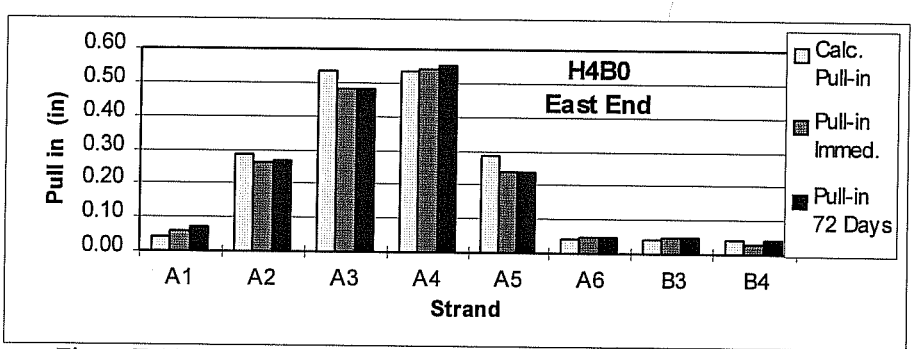

Figure E.11 Strand End Slip at Transfer: Test Beam End H4B0 East

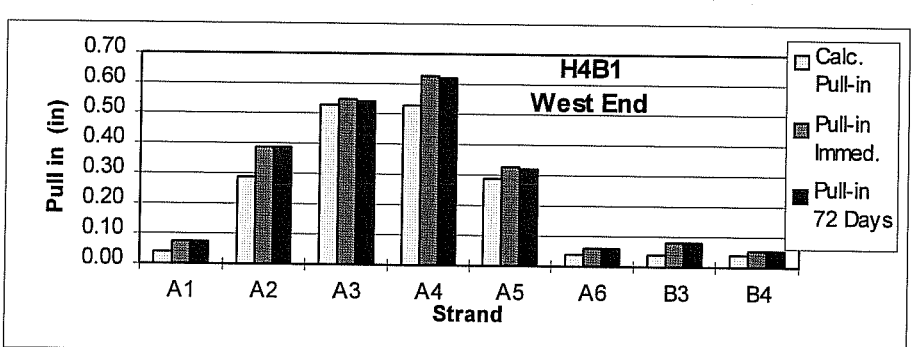

Figure E.12 Strand End Slip at Transfer: Test Beam End H4B1 West

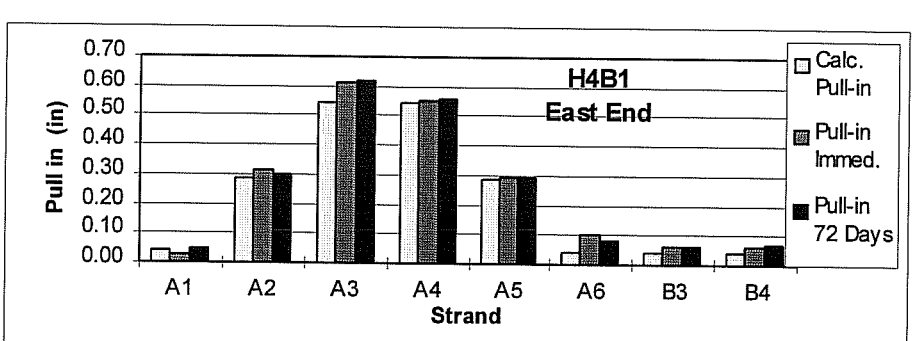

Figure E.13 Strand End Slip at Transfer: Test Beam End H4B1 East

The following equations were used to determine the calculated end slip at transfer (pull in). The measured transfer length for the beam end being considered was used. Strand stress is assumed to vary linearly from zero at the end of the beam to the effective initial prestress (f_{si}) at the end of the transfer zone. This method does not include the confining pressure of the surrounding concrete, but is reasonably accurate and correlated well with data in this study (see Figures E.2 through E.13).

$$\Delta = \int_0^{Lt} \varepsilon_s(x)dx \qquad \varepsilon(x) = \frac{f_{si}x}{E_{ps}L_t}$$

$$\Delta = \frac{f_{si}L_t}{2E_{ps}}$$

TABLE E.4	
L_{db} in	End Slip@ in
36	0.24
72	0.47

@Table E.4 shows the elastic shortening in the debonded portion of strands which is not due to slip in the transfer zone.

Robert Mast in 1980 suggested that factors which affect initial strand slip (Lt) have a proportional effect on the flexural bond length. A discussion of this slip theory is covered in the article by Logan[12]. Mast suggests the following relationship between end slip at transfer and development length:

TABLE E.5	
Magnitude of Slip	$L_{d\ Actual}$ $L_{d\ ACI}$
< .09	< 1
= .09	= 1
> .09	> 1

TABLE E.6							
BEAM :	L4B0	Cast West End			Cast East End		
Strand ID	Length of Debond	Pull-in Immed. in	Pull-in 33 Days in	Lt in	Pull-in Immed. in	Pull-in 33 Days in	Lt in
A1	0	0.06	0.07	20.8	0.09	0.11	26.3
A2	36	0.21	0.2	18.1	0.2	0.21	27.4
A3	72	0.05	0.06	16.4	0.48	0.51	18.5
A4	72	0.23	0.25	16.4	0.45	0.47	18.5
A5	36	0.22	0.22	18.1	0.16	0.15	27.4
A6	0	0.07	0.07	20.8	0.07	0.09	26.3
B3	0	0.06	0.08	20.8	0.04	0.06	26.3
B4	0	0.07	0.09	20.8	0.06	0.07	26.3

TABLE E.7							
BEAM :	L4B1	Cast West End			Cast East End		
Strand ID	Length of Debond	Pull-in Immed. in	Pull-in 33 Days in	Lt in	Pull-in Immed. in	Pull-in 33 Days in	Lt in
A1	0	0.07	0.09	18.9	0.08	0.09	21.8
A2	36	0.14	0.14	17.5	0.19	0.2	13.6
A3	72	0.54	0.53	17.0	0.4	0.39	16.0
A4	72	0.29	0.30	17.0	0.54	0.55	16.0
A5	36	0.08	0.07	17.5	0.21	0.21	13.6
A6	0	0.06	0.06	18.9	0.07	0.08	21.8
B3	0	0.05	0.05	18.9	0.05	0.07	21.8
B4	0	0.07	0.07	18.9	0.05	0.07	21.8

TABLE E.8							
BEAM :	M4B0	Cast West End			Cast East End		
Strand ID	Length of Debond	Pull-in Immed. in	Pull-in 44 Days in	Lt in	Pull-in Immed. in	Pull-in 44 Days in	Lt in
A1	0	0.04	0.06	13.6	0.05	0.06	14.7
A2	36	0.08	0.09	16.3	0.07	0.08	16.1
A3	72	0.63	0.63	14.1	-	-	14.6
A4	72	0.16	0.15	14.1	-	-	14.6
A5	36	-	-	16.3	-	-	16.1
A6	0	0.06	0.06	13.6	0.04	0.05	14.7
B3	0	0.06	0.08	13.6	0.07	0.07	14.7
B4	0	0.05	0.06	13.6	0.03	0.03	14.7

TABLE E.9							
BEAM :	M4B1	Cast West End			Cast East End		
Strand ID	Length of Debond	Pull-in Immed. in	Pull-in 44 Days in	Lt in	Pull-in Immed. in	Pull-in 44 Days in	Lt in
A1	0	0.06	0.08	13.5	0.03	0.03	14.5
A2	36	0.22	0.25	13.3	0.13	0.18	17.1
A3	72	0.63	0.63	16.0	0.55	0.54	16.6
A4	72	-	-	16.0	-	-	16.6
A5	36	0.35	0.39	13.3	0.23	0.21	17.1
A6	0	0.05	0.06	13.5	0.05	0.06	14.5
B3	0	0.04	0.05	13.5	0.03	0.02	14.5
B4	0	0.05	0.06	13.5	0.03	0.04	14.5

TABLE E.10							
BEAM :	H4B0	Cast West End			Cast East End		
Strand ID	Length of Debond	Pull-in Immed. in	Pull-in 72 Days in	Lt in	Pull-in Immed. in	Pull-in 72 Days in	Lt in
A1	0	0.07	0.07	13.0	0.06	0.07	13.3
A2	36	0.36	0.36	16.6	0.26	0.27	15.3
A3	72	0.66	0.66	17.1	0.48	0.48	17.8
A4	72	0.58	0.58	17.1	0.54	0.55	17.8
A5	36	0.32	0.32	16.6	0.24	0.24	15.3
A6	0	0.06	0.07	13.0	0.05	0.05	13.3
B3	0	0.07	0.08	13.0	0.05	0.05	13.3
B4	0	0.06	0.07	13.0	0.03	0.04	13.3

TABLE E.11							
BEAM :	H4B0	Cast West End			Cast East End		
Strand ID	Length of Debond	Pull-in Immed. in	Pull-in 72 Days in	Lt in	Pull-in Immed. in	Pull-in 72 Days in	Lt in
A1	0	0.07	0.07	13.0	0.03	0.05	12.8
A2	36	0.39	0.39	14.7	0.31	0.3	14.7
A3	72	0.55	0.54	15.4	0.61	0.62	20.0
A4	72	0.63	0.62	15.4	0.55	0.56	20.0
A5	36	0.33	0.32	14.7	0.29	0.29	14.7
A6	0	0.06	0.06	13.0	0.10	0.08	12.8
B3	0	0.08	0.08	13.0	0.06	0.06	12.8
B4	0	0.05	0.05	13.0	0.06	0.07	12.8

APPENDIX F

NOTATION

A_{ps}	Area of prestressing strand
c	Neutral axis
d_b	Diameter of prestressing strand
E_c	Modulus of elasticity of concrete
E_c	Modulus of elasticity of concrete at transfer
E_{ci}	Modulus of elasticity of prestressing strand
f_c	Stress in concrete
f_{su}	Stress in strand at failure
f_{pu}	Ultimate tensile strength in strands
f_{se}	Stress in strand after losses
f_{si}	Stress in strand immediately after transfer
f'_c	Concrete compressive strength at 28 days
f'_{ci}	Concrete compressive strength at transfer
f_r	Modulus of rupture of concrete
L_{db}	Length of debonding for debonded strands
L_d	Development length of prestressing strands
L_e	Embedment length of prestressing strands
L_{fb}	Flexural bond length of prestressing strands
L_t	Transfer length of prestressing strands
M_{cr}	Cracking moment for section
M_{ult}	Ultimate moment capacity for section
V_{cw}	Nominal shear strength provided by concrete defined by ACI
α	Factor to find average compressive stress in concrete (Appendix C)
ε_{se}	Strain in strands after all losses
ε_{si}	Strain in strands immediately after transfer
γ	Factor to find centroid of concrete compressive force (Appendix C)

REFERENCES

1) "Building Code Requirements for Reinforced Concrete," (ACI 318-95), American Concrete Institute, Detroit, Michigan, 1995.

2) "Standard Specifications for Highway Bridges," 15th Edition, American Association of State Highway and Transportation Officials (AASHTO), Inc., Washington, DC, 1992.

3) Kaar, Paul H., and Magura, Donald D., "Effect of Strand Blanketing on Performance of Pretensioned Girders," Journal of the Prestressed Concrete Institute, December 1965, pp. 20-34.

4) "PCI Design Handbook, Precast and Prestressed Concrete," 4th Edition, Precast/Prestressed Concrete Institute (PCI), Chicago, Illinois, 1992.

5) Cousins, Thomas E., Johnston, David W., and Zia, Paul, "Transfer and Development Length of Epoxy-Coated Prestressing Strand," PCI Journal, Vol. 35, No. 4, July-August 1990, pp. 92-103.

6) Janney, J. R., "Nature of Bond in Pretensioned, Prestressed Concrete," ACI Journal, Vol. 50, 1954, pp. 717-736.

7) Mattock, Alan. H., "Proposed Redraft of Section 2611 - Bond," letter to W. Burr Bennett, Jr., ACI Committee 323 Correspondence, December 6, 1962.

8) Hanson, N., and Kaar, Paul., "Flexural Bond Tests of Pretensioned Prestressed Beams," Research and Development Bulletin D28, Portland Cement Association, Skokie, IL, January 1959, pp. 783-802.

9) Kaar, P., LaFraugh, R., and Mass, M., "Influence of Concrete Strength on Strand Transfer Length," PCI Journal, Vol. 5, No. 8, October 1963, pp. 47-67.

10) CEB-FIP, "Model Code for Concrete Structures: CEB-FIP International Recommendations," 3rd edition, Comite Euro-International du Beton, Paris, 1978

11) Buckner, C.D., "An Analysis of Transfer and Development Lengths for Pretensioned Concrete Structures," Report No. FHWA-RD-94-049, Federal Highway Administration, Washington, DC, December 1994, 108 pp.

12) Logan, D. L., "Acceptance Criteria for Bond Quality of Strand for Pretensioned Prestressed Concrete Applications," PCI Journal, March-April 1997, pp. 52-90.

13) Russell, Bruce. W., and Burns, Ned. H., "Design Guidelines for Transfer, Development and Bonding of Large Diameter Seven-Wire Strands in Pretensioned Concrete Girders," Research Report No. 1210-5F, Center for Transportation Research, University of Texas at Austin, Austin, Texas, 1993, 286 pp.

14) Cousins, T., Johnston, D. And Zia, P., "Bond of Epoxy Coated Prestressing Strand," Department of Civil Engineering, North Carolina State University at Raleigh, 1986.

15) Burdette, E. G., and Deatherage, J. H., "Development Length and Lateral Spacing Requirements of Prestressing Strand for Prestressed Concrete Bridge Products," The University of Tennessee at Knoxville, 1990.

16) Shahawy, M., and Batchelor, B., "Bond and Shear Behavior of Prestressed AASHTO Type II Beams," Progress Report No. 1, Structural Research Center, Florida Department of Transportation, February 1991.

17) Dane, J., III, and Bruce, R. N., Jr., "Elimination of Draped Strands in Prestressed Concrete Girders," State of Louisiana, Technical Report No. 107, June 1975.

18) Rabbat, B. G., Kaar, P. H., Russell, R. N., Jr., "Fatigue Tests of Pretensioned Girders with Blanketed and Draped Strands," PCI Journal, July-August 1979, pp. 88-112.

19) Tabatabai, H., Dickson, T. J., "The History of the Prestressing Strand Development Length Equation," PCI Journal, November-December 1993, pp. 64-75.

20) Horn, D. G., Preston, H. K., "Use of Debonded Strands in Pretensioned Bridge Members," PCI Journal, July-August 1981, pp. 42-58.

21) Ghosh, S. K., Fintel, M., "Development Length of Prestressing Strands, Including Debonded Strands, and Allowable Concrete Stressed in Pretensioned Members," PCI Journal, September-October 1986, pp. 38-57.

22) Moustafa, Saad, "Pull-Out Strength of Strand and Lifting Loops," Concrete Technology Associates Technical Bulletin, 74-B5, May 1974.

23) Mitchell, D., Cook, W. D., Khan, A. A., Tham, T., "Influence of High Strength Concrete on Transfer and Development Length of Pretensioning Strand," PCI Journal, May-June 1993, pp. 52-66.

24) Martin, L. D., Scott, N. L., "Development of Prestressing Strand in Pretensioned Members," ACI Journal, Vol. 73, No. 8, 1976, pp. 453-456.

25) Zia, P., Mostafa, T., "Development of Prestressing Strands," PCI Journal, Vol. 22, No. 5, 1977, pp. 54-65.

26) Hognestad, Eivind, "A Study of Combined Bending and Axial Load in Reinforced Concrete Members," Bulletin No. 399, University of Illinois Engineering Experiment Station, November 1951, 128 pp.

27) Hognestad, E., Hanson, N. W., and McHenry, D., "Concrete Stress Distribution in Ultimate Strength Design," ACI Journal, Proceedings Vol. 52, December 1955, pp. 455 - 479.

28) Burns, Ned H., "Moment Curvature Relationships for Partially Prestressed Concrete Beams," PCI Journal, Vol. 9, No. 1, February 1964, pp. 52 - 63.

29) Park, R., Paulay, T., "Reinforced Concrete Structures," John Wiley & Sons, New York, 1975, pp. 195 - 203.

30) Jobson, H. L., "Transfer and Development Length of Fully Bonded 15.2 (0.6 in) in Standard AASHTO Type I Concrete Beams," University of Texas, Austin, Texas, 1997.

VITA

Jon Hansen Kilgore was born John Hansen Luckens in Shamokin, Pennsylvania on October 2, 1961, the son of John Saul Luckens and Sherry Jane Luckens. He was later adopted by Ronald W. Kilgore after his mother remarried in 1967. After graduation from Dickson County Senior High School, Dickson Tennessee, in 1980, he entered Texas A & M University in College Station, Texas. While at Texas A & M University he participated in and completed the cooperative education program working with Houston Light and Power for three alternating semesters. He received the degree of Bachelor of Science from Texas A & M University December, 1985 as a member of the Chi Epsilon Civil Engineering Honor Society. During the following ten years, he worked for the Texas Department of Transportation. He began as a designer in an area office working on bridge and freeway projects until he transferred to the San Antonio District Bridge Section in 1992. From January 1993 to January 1996 he supervised structural design for this office. In January 1996 he entered the Graduate School at The University of Texas. He is currently working for the Texas Department of Transportation in Austin, Texas at the Construction and Maintenance Division.

Permanent Address: 115 Timber Lane
New Braunfels, Texas 78130

This thesis was typed by the author.